The Development of a New Orthodontic Appliance Using Non-Conventional Electromechanical Methods

by
Tim Wucher

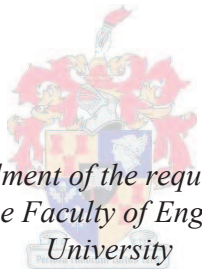

Thesis presented in fulfilment of the requirements for the degree of Master of Science in the Faculty of Engineering at Stellenbosch University

Supervisor: Prof. C. Scheffer

March 2013

Declaration

By submitting this thesis electronically, I declare that the entirety of the work contained therein is my own, original work, that I am the sole author thereof (save to the extent explicitly otherwise stated), that reproduction and publication thereof by Stellenbosch University will not infringe any third party rights and that I have not previously in its entirety or in part submitted it for obtaining any qualification.

Signature: .....
T. Wucher

Date: .....

Abstract

The Development of a New Orthodontic Appliance using Non-Conventional Electromechanical Methods

T. Wucher

Department of Mechanical and Mechatronic Engineering,
University of Stellenbosch,
Private Bag X1, Matieland 7602, South Africa.

Thesis: MScEng (Mechatronic)

March 2013

Orthodontics is the field of dentistry concerned with the treatment of malocclusion and anomalies of the dento-facial complex. This thesis is concerned with studying the underlying biomechanical principles of orthodontic tooth movement. It aims to develop a novel treatment approach and an orthodontic appliance to facilitate said approach by employing advanced technologies. A thorough review of the literature is used to form a comprehensive knowledge base pertaining to the factors affecting orthodontic tooth movement. It is hypothesised that an electromechanical orthodontic appliance could improve treatment by characterising orthodontic cases based on the relationship between the applied mechanical stimulus and the resulting changes to the affected structures, which can then be sensed by the appliance. A prototype is built using electronically controllable linear actuators and a custom built force transducer system for measuring orthodontic forces. Electronic circuits are developed to connect the appliance to a USB port and allow it to be controlled from a graphical user interface (GUI). This further facilitates real-time viewing of important orthodontic parameters. Experiments are carried out to evaluate the appliance functionality with regard to the proposed hypothesis. To conclude, the relevance of the results to the orthodontic field is highlighted and recommendations for further development of an electromechanical orthodontic appliance are provided.

Uittreksel

Afrikaans translation: Die Ontwikkeling van 'n Nuwe Ortodontiese Apparaat deur gebruik te maak van Nie-Konvensionele Elektromeganiese Metodes

T. Wucher

Departement Meganiese en Megatroniese Ingenieurswese,
Universiteit van Stellenbosch,
Privaatsak X1, Matieland 7602, Suid Afrika.

Tesis: MScIng (Megatronies)

Maart 2013

Ortodonsie is die vakgebied in tandheelkunde gemoeid met die behandeling van wanpassing en abnormaliteit van die tand- en gesig-area. Hierdie tesis bestudeer die onderliggende biomeganiese beginsels van ortodontiese tandbeweging om sodoende 'n nuwe benadering sowel as 'n ortodontiese apparaat te ontwikkel om die genoemde benadering te fasiliteer deur gebruik te maak van gevorderde tegnologie. 'n Deeglike oorsig van die literatuur word gebruik om 'n omvattende kennisbasis op te bou rondom die faktore wat ortodontiese tandbeweging affekteer. Die hipotese word gestel dat 'n elektromeganiese ortodontiese apparaat behandeling kan verbeter deur ortodontiese gevalle te identifiseer/-karakteriseer gebaseer op die verhouding tussen die toegepaste meganiese stimulus en die gevolglike veranderinge aan die geaffekteerde strukture wat deur die apparaat aangevoel word. Elektronies-beheerbare lineêre aandrywers en 'n pasgemaakte krag-oordraerstelsel vir die meet van ortodontiese kragte word gebruik om 'n prototipe te vervaardig. Elektroniese stroombane word ontwikkel om die apparaat te koppel aan 'n USB poort sodat dit beheer kan word d.m.v. 'n grafiese gebruikerskoppelvlak. Eksperimente poog om die apparaat funksioneel te evalueer volgens die voorgestelde hipotese. Ter afsluiting: die toepaslikheid van die verwerfde resultate in die ortodontiese vakgebied word beklemtoon en aanbevelings word gemaak vir toekomstige/verdere ontwikkelings m.b.t. 'n elektromeganiese ortodontiese apparaat.

Acknowledgements

I would like to express my sincere appreciation to my supervisor Prof. Cornie Scheffer. Your continued guidance and advice throughout the project have been invaluable. Thank you for entrusting me with the responsibility to realise my ideas.

I would also like to express my utmost gratitude to Dr. Alfred Dippenaar. Your enormous enthusiasm and appreciation for the completed work have been an incredible motivation, without which the success of this project would certainly not have been the same. Thank you too for the generous financial support, the huge responsibility, and most of all the freedom which have enabled me to complete this task to the best of my abilities.

To my father Dr. Martin Wucher, thank you for the financial assistance which has helped realise this project. Thank you for your endless support and valuable advice on matters that at times may have seemed trivial. But most of all, thank you for your unconditional trust in my abilities.

To my friends and family, thank you for the fun and the amazing times that have given me the strength to complete this task. You have always made me return to the world beyond the screen with great excitement.

Dedications

To all you
who have shown me
that regardless of the colours of the ups and downs
the world is always bright.

Contents

List of figures

List of tables

Nomenclature

Abbreviations

ASIC	Application specific integrated circuit
CBCT	Cone beam computed tomography
CRes	Centre of resistance
CRot	Centre of rotation
CT	Computed tomography
FEA	Finite element analysis
FPC	Flexible printed circuit
FTS	Force transducer system
GUI	Graphical user interface
GUIDE	Graphical user interface development environment
IC	Integrated circuit
IDE	Integrated development environment
INL	Integral non-linearity
LED	Light emitting diode
PDL	Periodontal ligament
Rx	Serial receive
RMS	Root mean square
SMT	Surface mount technology
Tx	Serial transmit
USB	Universal serial bus
WEDM	Wire electrical discharge machining

Symbols

a	Air gap	[mm]
B	Magnetic field strength	[T]
E	Young's modulus of elasticity	[GPa]
F	Force	[cN]
H	Hysteresis	[Inherited]
I	Moment of inertia	[mm^4]
k	Force transducer constant	[cN/bit]
L	Length	[m]
M	Moment	[Nmm]
M_f	Moment due to an applied force	[Nmm]
MF	Moment-to-force ratio	[Nmm/N]
O	Encoder output	[bit]
N	Number of elements	[#]
r	Resolution	[Inherited]
S	Sensitivity	[Inherited]
SD	Standard deviation	[Inherited]
X	Range	[Inherited]
x	Displacement	[mm]
α	Magnetic field gradient	[mT/mm]
δ	Stator displacement	[mm]
θ	Angle	[°]
μ	Fitted average value	[Inherited]
σ	Stress	[MPa]
σ_Y	Yield stress	[MPa]
ϕ	Diameter	[mm]

Chapter 1

Introduction

1.1 Background

The field of orthodontics specialises in the treatment of imperfect alignment of the teeth, referred to as malocclusion. Orthodontics came into existence during the last part of the nineteenth century (Asbell, 1990). It is a branch of science and art of dentistry which deals with the development and positional anomalities of the teeth and the jaws as they affect oral health and the physical, aesthetic and mental well-being of the patient (Salzmann, 1950).

Conventionally, either mechanical braces are bonded to the teeth and are used to initiate the desired tooth movement or appliances are used to induce structural changes of the dento-facial complex. Treatment with such purely mechanical systems, however, pose certain constraints. This is due to the complexity of the underlying biomechanical effects initiating bone remodelling and tooth movement which are further case-specific as well as time-dependent.

A novel electromechanical orthodontic appliance is to be developed to address such challenges. Electronically controllable actuators would affect orthodontic forces, while electronic sensors provide feedback. In conjunction with a micro controller specialised algorithms such an appliance could potentially revolutionise the orthodontic treatment approach.

1.2 Motivation

The advancement of digital technology has greatly benefited the medical device industry, yet its use in orthodontics remains limited. The successful introduction thereof into various medical fields offers great benefits to both patients and practitioners. The integration of microprocessors into medical devices such as pacemakers or hearing aids has become the norm. Even though dentistry, and more specifically orthodontics, have also profited from such technological innovations, their use is largely limited to diagnostic or manufacturing procedures.

Specialised computer software, desktop 3-D scanners or CAD/CAM systems are used for improved treatment planning and manufacturing customized orthodontic appliances. The appliances themselves however remain purely mechanical.

Although the advanced diagnostic and manufacturing processes significantly improve the efficiency of conventional treatment methods, the use of purely mechanical systems has several limitations. Such mechanical systems are rather inflexible considering the complexity and time-dependent nature of orthodontic treatment. Once placed, controlled adjustments to the mechanical system can only be made during appointments with the practitioner. This limits their efficiency in inducing the continuous physiological changes facilitating tooth movement. Using electronically controllable components instead of purely mechanical ones could possibly aid in addressing such issues.

This study is motivated by the potential of improving orthodontic treatment by developing an electromechanical appliance to induce tooth movement. The feedback, control and flexibility facilitated by the use of electromechanical components could be equally beneficial to research as well as to practical applications in orthodontics.

1.3 Objectives

A thorough understanding of the current orthodontic approach by studying the available literature needs to be developed. The focus will be to identify advantageous features of current mechanical systems as well as their limitations by reviewing product information, practical case studies and published research in the field.

Additionally, a comprehensive understanding of the tooth anatomy, the biomechanical coupling and the physiological processes governing tooth movement need to be acquired. This knowledge will enable the critical evaluation of existing systems with regard to the underlying biomechanical principles. It will further facilitate a bottom-up approach for developing a novel treatment method. This will take into account a variety of possible factors and their effect on tooth movement, and will make use of non-conventional electromechanical methods to address such factors.

A further objective is to develop and build an electromechanical system based on the proposed treatment method and to provide a proof-of-concept thereof. Using the outcomes of the literature review, the system specifications will need to be formulated and the appliance designed accordingly. A fully functional system suitable for testing the proposed hypothesis is to be manufactured.

Lastly, this study will aim to test the developed system with respect to the proposed treatment approach. Results will be evaluated and their relevance to the current orthodontic research and treatment approach examined. Limita-

tions of this study need to be identified and potential improvements suggested.

The objectives of this study can be summarised as follows:

1. To systematically revise the background of orthodontics, the current orthodontic treatment approach and existing orthodontic systems.
2. To thoroughly study and understand the underlying biomechanical and physiological principles governing orthodontic tooth movement.
3. To critically evaluate existing orthodontic systems with regard to the outcomes of Objective 2 and to identify shortcomings thereof.
4. To formulate a hypothesis for a novel treatment approach which applies advanced technologies to address such shortcomings and characterise an appliance to facilitate the proposed treatment approach.
5. To develop and build a prototype of an electromechanical orthodontic appliance according to the outcomes of Objective 4.
6. To test the prototype of the electromechanical orthodontic appliance with regard to the hypothesis put forth in Objective 4.
7. To evaluate the experimental results and their significance to the field of orthodontics.

1.4 Thesis Outline

Objective 1 and Objective 2 are addressed in Chapter 2. The outcomes of the literature review relevant to this study are presented. A short background to the field of orthodontics is provided followed by a description of the dental anatomy. Conventional systems are listed and new technological developments are discussed. Thereafter, a detailed discussion of factors affecting orthodontic tooth movement along with relevant literature is provided. In the concluding part of the chapter, Objective 3 is fulfilled by critically evaluating existing systems with regard to reviewed research findings and an alternative approach is suggested.

The hypothesis for a new treatment approach is developed in Chapter 3 as per Objective 4. This leads to the formulation of system requirements and the necessary engineering specifications.

Objective 5 is achieved in Chapter 4, which outlines the physical system development. First, the mechanical system design is described, followed by the electronic circuit design and manufacturing. The software development and functionality is also outlined in this chapter.

Appliance evaluation and testing as per Objective 6 is dealt with in Chapter 5. Following appliance evaluation, three individual experiments are performed

to examine the performance of the electromechanical appliance with respect to the proposed treatment approach.

According to Objective 7, the presented results are discussed in Chapter 6. Physical system limitations are discussed and causes thereof presented. The achieved functionality is also outlined and a comparison drawn to existing systems. Furthermore, the relevance of the obtained results to the orthodontic field is described.

A conclusion to this study is presented in Chapter 7. The attainment of each of the objectives is confirmed. Recommendations for future work on the development of an electromechanical orthodontic appliance are made. A conclusion on the proof of concept of an electromechanical orthodontic appliance is finally drawn.

Chapter 2

Literature review

This chapter provides a review of the literature relevant to the development of an orthodontic appliance. A background of orthodontics is provided followed by a review of the current treatment approach and existing technologies. Thereafter, a detailed discussion of the underlying biomechanical principles is provided. Toward the end of the chapter current methods and systems are critically evaluated with regard to the underlying principles. The outcomes of this chapter are in line with the first three objectives.

2.1 Background of orthodontics

2.1.1 Treatment of malocclusion

Conventionally, orthodontic treatment involves the use of mechanical appliances to generate and apply forces to the teeth and the dento-facial complex to initiate movement of the affected structures. Mechanical components such as wires, springs, brackets, elastics and aligners are used in combination and are attached to the misaligned teeth onto which they exert a mechanical force. This force, if applied over a prolonged period of time, induces the desired movement and allows alignment of the teeth. The challenge therefore, is to characterise the most appropriate force and to accurately apply it to the teeth.

Due to the complex anatomy of the teeth and the dento-facial complex it remains difficult to study the effects of a force exerted to a tooth by an orthodontic appliance. The critical portion of the root of a tooth is housed within the bone and changes induced by an applied force are often only noticed after bone remodelling has occurred or adverse effects such as pain are reported by the patient. This anatomical complexity, combined with the constraint of applying the correct forces remains a significant difficulty in orthodontics. Researchers are constantly working toward a better understanding of the underlying biomechanical principles to improve the treatment of malocclusion.

2.1.2 Dental anatomy

Understanding the dental anatomy is essential to orthodontics. The structures and functions of tissues pertaining to the teeth are closely related, and each of these needs to be considered when controlled movement of the teeth is to be achieved. The correct anatomical terms of location are defined in Appendix A. These need to be understood to describe movement within the dento-facial complex and Appendix A should be consulted where necessary. Here the dental anatomy will be explained with reference to Figure 2.1 which illustrates the most important parts of the dental complex.

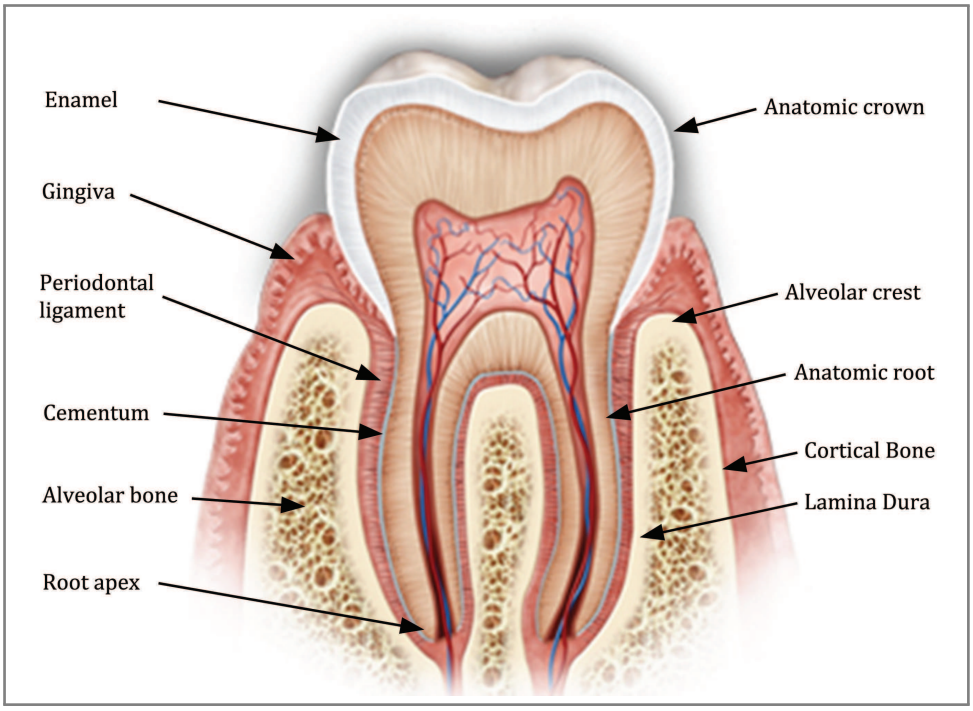

Figure 2.1: Tooth anatomy (IFDEA, 2012)

Firstly, the exterior anatomy of a single tooth will be considered. The tooth consists of two major parts, namely the crown and the root. The crown, which is coated with a layer of enamel, lies above the point at which the gingiva meets the tooth called the gingival margin. It is thus the visible portion of a tooth. The root lies below the gingival margin. It is that part of the tooth which is housed within the osseous cavity called the alveolus. The tip of the root is referred to as the root apex. The root is covered by a thin layer of calcified material called cementum and most importantly, is connected to the periodontal ligament (PDL) which plays an important role in facilitating tooth movement.

The PDL is a thin layer of connective tissue between the root of the tooth and the alveolar bone, consisting mainly of collagen fibres. Its purpose is to provide attachment of the teeth to the osseous alveolus while providing a non-rigid transmission of forces to the bone. The thickness of the PDL ranges from 0.12 mm to 0.24 mm, with the narrowest portion near the middle of the root (0.12 - 0.17 mm) and its thickest part located apically (0.16 - 0.24 mm) (Mueller, 2005). Lastly, the PDL also serves important cellular functions that facilitate tooth movement by bone remodelling.

As illustrated in Figure 2.1 the tooth and the connecting PDL are housed in an osseous structure consisting of the alveolar bone, the cortical bone, and the lamina dura. The alveolar crest is the most coronal portion of the alveolar process and is the point where the lamina dura meets with the hard layer of cortical bone which covers the outer surfaces (Wolf *et al.*, 2005).

2.1.3 Types of tooth movement

Different types of movements are experienced when external forces are applied to teeth over a prolonged period of time. In order to fully describe tooth movement it is necessary to consider translation and rotation in three dimensional space. The anatomical terms of reference in Appendix A are used to describe different types of tooth movements with reference to Figure 2.2.

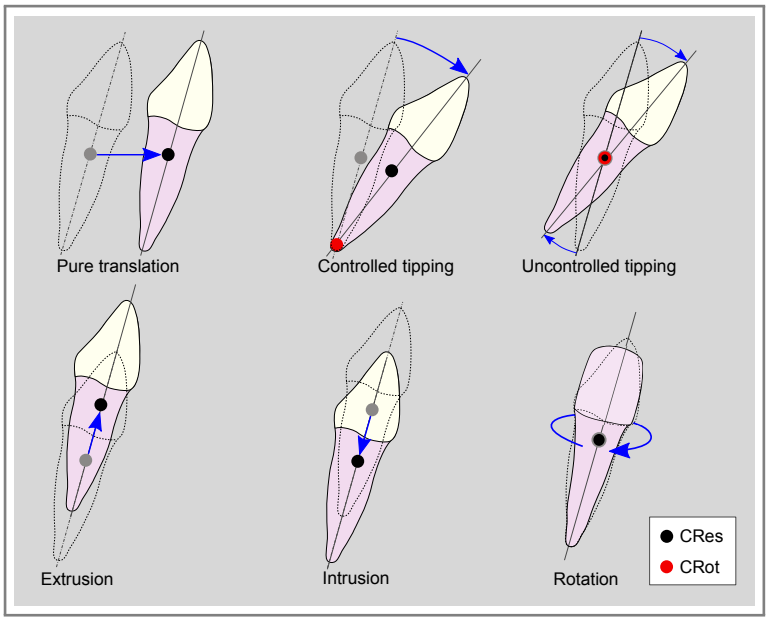

Figure 2.2: Types of tooth movement

Pure translation or bodily translation typically refers to the movement of a tooth parallel to the occlusal plane without it changing its orientation. Mesiodistal translation along the dental arch is most common but labiolingual

or buccolingual movement can also be initiated. To achieve pure translation of a tooth the force must be applied so that its line of action intersects with the center of resistance (CRes) of the tooth which typically lies between one third and one quarter of the tooth length as measured from the alveolar crest (Burstone and Pryputniewicz, 1980; Halazonetis, 1996). Because this point lies within the alveolus and only external forces can be applied to a tooth, it is practically impossible to apply a force through the CRes. Pure translation is therefore hard to achieve by application of a single force.

Translation along a tooth's longitudinal axis is referred to as either extrusion or intrusion. Extrusion occurs when a force is applied in the direction of the occlusal plane and the tooth is extracted from the alveolus. Intrusion is achieved by applying a force in the apical direction, essentially pushing the tooth deeper into the alveolus and thus creating areas of compression in the PDL.

Because the forces necessary for bodily translations are applied at a point that is vertically displaced relative to the CRes, a torque is created giving rise to tipping or rotation of a tooth. A clear distinction must be made between rotation which is the rotation of a tooth around its longitudinal axis, and tipping which is angular displacement of a tooth about an axis parallel to the oclusal plane, as shown in Figure 2.2.

Tipping is further classified as 'controlled' tipping or 'uncontrolled' tipping both of which are illustrated in the above figure. Uncontrolled tipping is often the result of a single force being applied to a tooth at a point vertically displaced from the CRes, which creates a moment and thus rotation about said CRes. In contrast, to achieve the more desirable controlled tipping it is necessary to apply both a force as well as a moment to the bracket. This gives rise to an important orthodontic parameter called the moment-to-force ratio (MF) which is calculated at the bracket as

$$MF = \frac{M}{F} \tag{2.1}$$

Here M is the moment applied to the bracket and F is the magnitude of the applied force. By controlling the MF ratio it is possible to change the position of the centre of rotation (CRot) so that uncontrolled tipping becomes controlled tipping.

Technically speaking the MF should be evaluated at the CRes as $MF = \frac{M+M_f}{F}$ and not at the bracket to better predict tooth movement (Kusy and Tulloch, 1986; Halazonetis, 1998). Here the moment M_f arising due to the force being applied at a vertical displacement to CRes is also taken into account. Clinical orthodontic practice however considers the MF as per equation 2.1 and it will thus be used as such during this study.

2.2 Existing orthodontic systems

2.2.1 Conventional orthodontics

The basis for the majority of existing orthodontic systems is the archwire and bracket combination which dates back to the beginning of the profession. Since then the principles used to induce tooth movement have largely remained the same, but a variety of materials, shapes and sizes have been used to develop new appliances. Two types of conventional braces are shown in Figure 2.3.

(a) *Damon Clear* braces (Ormco, 2011)

(b) *Harmony* lingual braces (Harmony, 2012)

Figure 2.3: Conventional braces

The following list categorizes some of the existing systems and provides information on their functionality:

- **Traditional braces:** Traditional braces use ligatures or small elastic bands to hold the archwire in a special slot on the metal brackets attached to the teeth. Archwires with different shapes, cross-sections and materials are used to produce the desired forces when displaced. They are often less expensive than other systems and are still widely used. However, they have poorer aesthetics when compared to other systems and the friction induced by the rubber bands is also significantly higher (Obaidi, 2009) which limits movement.

- **Self-ligating brackets:** In contrast to conventional braces, self-ligating systems use a passive slide mechanism to maintain the archwire within the bracket instead of ligatures. This reduces the friction on the archwire and allows it to move more freely within the bracket slot. It also enables the use of softer archwires which results in an improved application of the desired forces (Baccetti *et al.*, 2009). This ultimately improves the efficiency of treatment and decreases treatment times (Shivapuja and Berger, 1994). Both the ligature systems as well as the self ligating systems are also made using translucent ceramics to improve aesthetics. Examples of self-ligating systems are the *Damon System*, the *Speed System*, *Clarity SL* and *ODP Agility*.

- **Lingual braces:** Lingual braces make use of brackets which are fitted to the inner surfaces of the teeth instead of attaching them labially as with conventional systems. While being aesthetically more pleasing, these systems are often more expensive and can also be uncomfortable or cause speech difficulties as they come into direct contact with the tongue. Examples include the *Incognito Hidden Braces*, the *STb Light Lingual System* and the *Harmony Lingual Braces* system shown in Figure 2.3(b).

In addition to conventional braces which use the archwire to achieve alignment of the teeth, several other appliances used to induce changes of the oro-facial structures and the jaws exist. These are often used in conjunction with the above systems to correct more severe cases of malocclusion requiring inter-arch movement or maxillary expansion. In some cases they are also used to provide increased anchorage or to prevent movement after treatment.

(a) Distal Jet Appliance (b) Maxillary Retainer (c) Mara Appliance

Figure 2.4: Orthodontic appliances (Dynaflex, 2012)

Orthodontic appliances some of which are shown in Figure 2.4, are categorised as follows:

- **Active appliances:** Active appliances make use of mechanical components such as springs or wires to generate forces and initiate movement. They are used for molar distalization with anterior anchorage, for advancing mandibular incisors and for inducing inter-arch movements. Commonly used active appliances include Rapid Maxillary Expanders, Forsus Appliance, Pendulum Appliance and the Distal Jet Appliance shown in Figure 2.4(a).

- **Passive appliances:** Passive appliances do not produce any active forces, but are used as spacers or retainers to maintain the correct position of the teeth or jaws. Their function is to prevent movement rather than initiate it. Figure 2.4(b) shows an image of a maxillary retainer.

- **Functional appliances:** Functional appliances cause changes of the dento-facial structures, but do not make use of active components. Instead, they employ the muscle actions of a patient to generate orthopaedic forces and are most commonly used for inter-arch movement. Two such functional appliances are the Mandibular Anterior Repositioning Appliance (MARA) in Figure 2.4(c).

2.2.2 Recent technological developments

The advancement of computer technology and digital imaging systems has contributed significantly to the development of new orthodontic systems. The use of 3-D scanners along with CAD/CAM manufacturing processes is well established in restorative dentistry and similar technologies specific to orthodontics are being developed. Advanced imaging techniques enable the construction of accurate 3-D models of a patient's malocclusion which in turn offer a choice of customized orthodontic solutions. Even though newer systems still have certain limitations, they each offer specific advantages such as improved aesthetics, more efficient treatment or decreased treatment duration.

Invisalign (Align technology Inc., San Jose, California, USA) and ClearCorrect (ClearCorrect, Houston, Texas, USA) are two recently commercialised systems which use a series of transparent aligners to achieve the desired movement of teeth. Images of a patient's malocclusion are obtained using a hand-held 3-D iTero (Align technology Inc., San Jose, California, USA) optical scanner and a virtual 3-D model thereof is constructed using specialised software. Using the same software the dental model is modified to represent the desired treatment outcome, which can then be discussed with the patient. Thereafter, a series of steps necessary for the teeth to reach their final position are determined and a clear plastic aligner is manufactured for each of the steps. By wearing the series of aligners, the teeth can systematically be repositioned.

Another new technology called SureSmile (OraMetrix, Inc., Richardson, Texas, USA) uses similar imaging and simulation techniques combined with a robotic manipulator to produce robotically bent archwires (SureSmile, 2012). As with the previously described technology, a virtual dental model is constructed using cone beam computed tomography (CBCT) after which it can be manipulated using specialised computer software. The exact positions and angles of the teeth can be modified on the virtual models to simulate the desired treatment outcome and specialised software is used to calculate the concurrent tooth movements. Finally, the robotic system pictured in Figure 2.5(a) is used for bending customized archwires to generate the prescribed tooth movement. The pre-bent wires feature high accuracy and thus achieve more efficient and more accurate movement of the teeth (Saxe *et al.*, 2010; Alford *et al.*, 2011).

The most recently commercialised technology is used in conjunction with other systems and aims to reduce treatment times by applying increased me-

(a) SureSmile robotic system (SureSmile, 2012)

(b) AcceleDent appliance (AcceleDent, 2012)

Figure 2.5: Advanced orthodontic systems

chanical stimulation to the dentition. The AcceleDent device (OrthoAccel Technologies, Bellaire, Texas, USA) is based on recent research findings (Wang and Mao, 2002; Kopher and Mao, 2003) and is the first commercially available orthodontic device which makes use of non-static forces to speed up orthodontic tooth movement (Kau *et al.*, 2011). The device consists of an external activator and a rubber mouthpiece as displayed in Figure 2.5(b). During orthodontic treatment the AcceleDent device is worn for approximately twenty minutes per day during which a vibrating force is applied to the teeth via the rubber bite plate. The increased stimulation is believed to facilitate higher rates of tooth movement (Kau *et al.*, 2011) and by so doing shorten treatment times.

2.3 Factors affecting orthodontic tooth movement

2.3.1 The importance of an applied force

Over the past decades, numerous studies have been conducted on the factors affecting orthodontic tooth movement and their significance to treatment outcomes. Of these, many have focused on quantitatively analysing the relationship between an applied force and the effects thereof on tooth movement (Quinn and Yoshikawa, 1985; Pilon *et al.*, 1996; Ren *et al.*, 2003; Ren, 2004).

A frequently cited study is that of Quinn and Yoshikawa (1985) who developed four hypotheses for the relationship between the stress generated in the PDL by an applied force and the rate of tooth movement. Each of the four hypotheses was evaluated by comparing it to the experimental database. They found that the clinical data best supported their hypothesis that the relationship between the stress magnitude and the resulting rate of tooth movement is linear up to a certain point. At this point a maximum rate is reached and an increase in the force magnitude does not further increase the rate of tooth movement.

A decade later, Pilon *et al.* (1996) conducted a study in which the rate of tooth movement was measured on 25 young male beagle dogs over a period of 16 weeks. It was found that large individual variations existed for the mean rate of tooth movement even though the same forces were used. An explanation put forth was that each individual could possibly have its own optimal force that would produce the maximum rate of tooth movement.

Ren *et al.* (2003) conducted a systematic literature review of 17 articles on animal studies and 12 articles on human studies conducted between 1966 and 2001. They concluded that the reviewed experimental results were affected by the inability to accurately calculate stresses in the periodontal ligament, the inability to control the type of tooth movement, the different phases of tooth movement and large inter-individual variations or even variations within individuals, and that as a result no exact force magnitude could be recommended.

In a later study, Ren (2004) attempted to develop a mathematical model that describes the relationship between the magnitude of an applied force and the rate of orthodontic tooth movement. They found that their model best supported a hypothesis for which the rate of tooth movement increases proportionally with the PDL stress until a certain level at which a plateau is reached (Quinn and Yoshikawa, 1985). It was however concluded that no optimal force can be calculated and that the force magnitude might not be the major decisive factor for the rate of tooth movement.

In a study by Melsen *et al.* (2007) the importance of force levels in relation to tooth movement is examined by using Finite Element Analysis (FEA) methods. In the light of more recent research findings various traditional views and theories are questioned. Melsen *et al.* (2007) acknowledge that a universally accepted standard for the force threshold or an optimal force does not exist.

Taking into consideration the outcomes of the above mentioned studies it becomes clear that despite great research efforts in this direction, it does not seem possible to quantitatively characterize a general optimal orthodontic force. Instead, the majority of these study outcomes indicate that the force is not the decisive factor in relation to tooth movement.

While accepting the above findings, the applied force however is considered to be the only externally controllable parameter and will thus remain a central part of this study. Instead of being directly related to the rate of tooth movement, the force is considered to initiate various secondary factors and

biomechanical responses, which in turn can be linked to the resulting tooth movement. There are various factors that affect the load transfer mechanism from the tooth to the affected tissues, known as mechanotransduction. These are intrinsic to the force and the physiology of the patient. Relevant factors identified in the literature were classified to produce an overview presented in Figure 2.6. Factors are separated into primary and secondary factors both of which will be discussed in more detail in the following paragraphs.

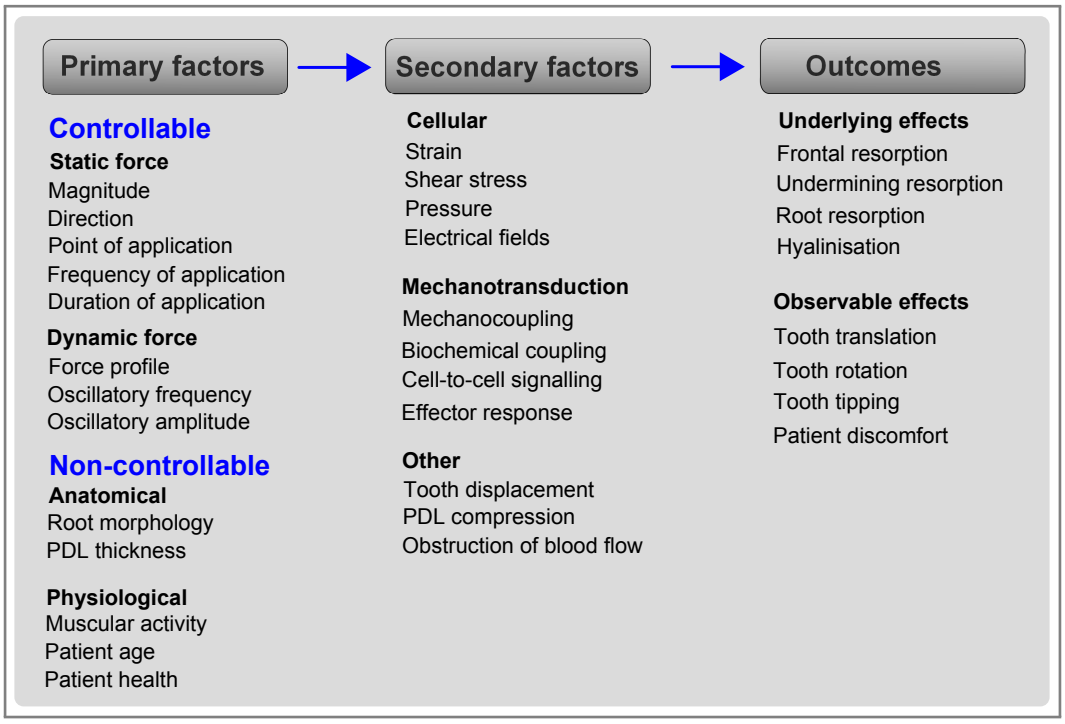

Figure 2.6: Factors affecting tooth movement

2.3.2 Primary factors

Primary factors are considered those attributes that can be identified irrelevant of whether a force is being applied to a tooth or not. These are further separable into controllable factors, which relate to the applied force and non-controllable factors, which include the anatomical characteristics of the dento-facial structures.

Controllable primary factors

The controllable primary factors are intrinsic to the applied force and can be changed independently of the body to which the force is being applied. The line of action, magnitude and point of application, for example, are variables of a constant force vector. If the force is time dependent, further variables

may include the oscillatory frequency, oscillating amplitude as well as the force profile over time. Of importance is that all of the mentioned factors represent controllable parameters of a force, regardless of whether the force is being applied to a tooth or another object. Furthermore, even though not all of these factors have been proven to affect tooth movement, they will be discussed and their potential benefits considered.

Firstly, the magnitude of an applied force has a considerable effect on tooth movement (Pilon *et al.*, 1996) by creating a pressure in the PDL, even if the exact relation between these factors cannot be determined. Studies have shown that even small forces can induce tooth movement and that there exists a very small or practically no minimum threshold that is required to activate tooth movement (Ren, 2004; Schwarz, 1932; Weinstein *et al.*, 1963). None the less, current orthodontic systems can generate and apply significant force levels to a tooth causing excessive pressure in the PDL. This in turn can lead to negative effects such as root resorption, hyalinization or tissue degeneration (Reitan, 1974) and thus needs to be controlled.

Two further externally controllable parameters for which the effects are more apparent are the point of application and the direction or line of action of a force vector. The point of application and direction are important as they largely govern the resulting type of tooth movement.

The duration and frequency of application of a static force also affect the tooth movement. That is, the longer a certain force is applied to a tooth, the greater the movement of said tooth is expected to be. Application times can range from very short periods of time, which can cause immediate changes in the PDL (Jónsdóttir *et al.*, 2006; Qian *et al.*, 2009) to several months or even years, resulting in continuous, more gradual changes of tissue structures.

Considering the possibility of superimposing an oscillatory component onto a static force, the oscillatory frequency and amplitude are further variable parameters. Recent research in this field has shown that non-static forces are an important factor in bone-remodelling and ultimately tooth movement (Darendeliler *et al.*, 2007; Peptan *et al.*, 2008; Nishimura *et al.*, 2008). With vibratory stimulation being identified as an important factor, the need arises to manipulate and control this vibration to further optimise treatment. Thus, both the oscillatory amplitude and frequency are considered important factors relating to orthodontic tooth movement.

Lastly, the profile of an oscillatory force may also affect biomechanical processes relating to tooth movement. Studies show that the application of different mechanical forces to osseous bone cause micro-currents to flow in the affected tissue. The electrical field within the biological tissues arise due to piezoelectric effects, which depend on the rate of application and thus the profile of the applied force (Bassett, 1968; Shapiro *et al.*, 1979; Williams and Breger, 1975). Moreover, these electrical fields have been shown to stimulate the formation of bone (Cochran, 1972) and could thus be a further factor affecting tooth movement.

Non-controllable primary factors

The non-controllable category, in contrast to the characteristics of the applied force, includes intrinsic features of the dental anatomy. These can typically not be changed by the practitioner, but nevertheless greatly influence the resulting tooth movement. All of these factors relate to a mechanism called mechanotransduction, which is the conversion of mechanical forces into local mechanical signals and further effects occurring at a cellular level (Turner and Pavalko, 1998).

One of the most important non-controllable factors is likely to be the anatomical properties of the alveolar structures. Over 50 years ago Reitan (1957) showed that different root lengths influenced the amount of bone resorption and thus the type of tooth movement. Quinn and Yoshikawa (1985) also proposed increasing the total root surface area by using multiple molars for anchorage and by so doing slowing tooth movement.

The physiological and physical properties have also been shown to affect tooth movement. The tissue and the morphology of the periodontium influence the load transfer mechanisms to the alveolar support structures (Cattaneo *et al.*, 2005). Such differences could lead to changes in the localised stress experienced by the PDL for the application of the same force. Similarly, the physiological processes have an influence on the rate of tissue turnover and as such even the patient age or health could play a significant a role.

This argument is supported by findings that there are certain ages at which tooth movement is facilitated more readily (Graber, 1954). Various age dependent factors, such as individual differences in bone density and bone metabolism or PDL thickness can also lead to variations in tooth movement (Pilon *et al.*, 1996). The cellular metabolisms differ for each age group and thus further variations in response can be expected (Reitan, 1967). The best results are experienced in periods of pubertal growth (Graber, 1954).

Furthermore, it has been shown that even light physiological forces within the dento-facial complex are sufficient to affect tooth movement. The resting forces of the lips and the tongue to the labial and lingual surfaces of the teeth contribute to the dental equilibrium (Proffit, 1978). Significant variations of the pressure exerted to the teeth during mastication and swallowing also affect tooth movement and may even be responsible for some types of malocclusion (Ruan *et al.*, 2005).

2.3.3 Secondary factors

In contrast to primary factors, secondary factors are defined in that they are only present when a mechanical force is applied to a tooth. The secondary factors represent both mechanical changes as well as changes on a cellular level, which cause a disturbance of the biomechanical state of equilibrium of the tissues prior to force application. Their temporal nature allows for

rapid changes during initial application as well as ongoing changes during the remodelling process.

Four distinct parameters caused by a mechanical stimulus can be identified at cellular level immediately after the application of a force (Rubin *et al.*, 2006). The four parameters that have been shown to affect bone remodelling are strain, shear stress, pressure and dynamic electrical fields experienced by the tissue cells. Furthermore, research has shown that there exists a relationship between the magnitude of the applied stimulus and the change in mass of bone tissue (Rubin and Lanyon, 1985), the number of cycles and the increase of bone mass (Rubin and Lanyon, 1984), and the loading distribution and new bone formation (Lanyon *et al.*, 1982).

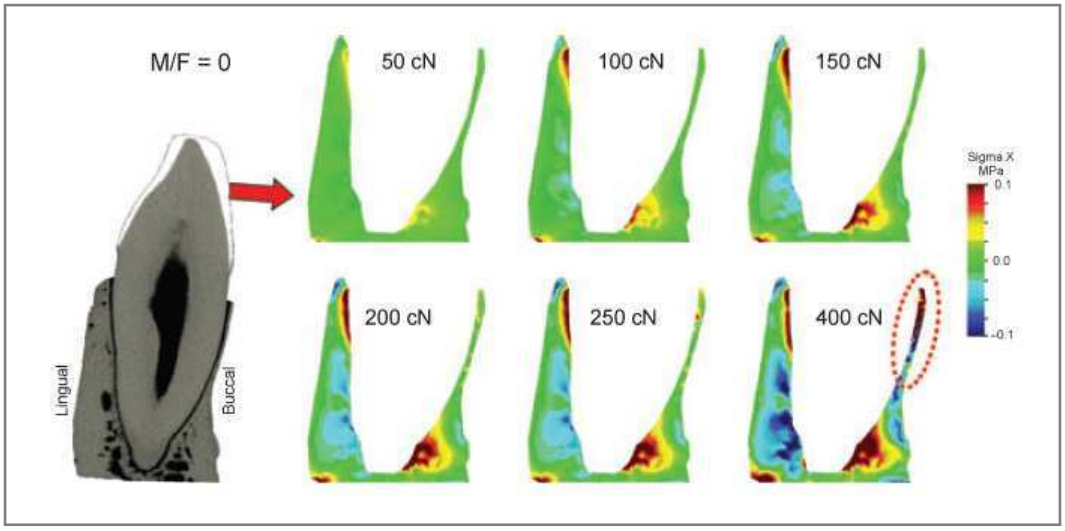

Figure 2.7: Lingual-buccal stress in alveolar bone due to varying levels of an applied force (Cattaneo *et al.*, 2009)

In contrast to the primary factors, a dose-response relationship has also been shown to exist between secondary factors and the resulting bone remodelling (Rubin and Lanyon, 1985). This is important in that it allows an approximation of the resulting tooth movement based on the secondary parameters. Therefore, giving more significance to measuring and controlling the secondary factors during orthodontic treatment planning could be advantageous over considering the force magnitude alone. The problem that arises is that with current technologies it is near to impossible to repeatedly measure the strain or pressure in the PDL for every single tooth, which makes the use of these factors impractical for feedback.

One research approach is to use FEA to simulate the behaviour of the PDL and the alveolar support structures when a force is applied to a tooth. Results obtained by FEA showed that the areas of stresses in the PDL and alveolar bone are not symmetrical and depend on the bone morphology (Cattaneo

et al., 2009). Furthermore, forces as small as 50 cN were sufficient to induce stresses in the alveolar bone as shown in Figure 2.7 by Cattaneo *et al.* (2009). The forces causing these stresses in the alveolar bone are transferable from the tooth to the bone only by means of the PDL, which means that a stress of equal magnitude is likely experienced in the PDL. Because of its low modulus of elasticity, this stress could lead to a complete compression of the PDL, obstructing blood flow and inhibiting the physiological remodelling process (von Boehl and Kuijpers-Jagtman, 2009).

This idea is supported by a second study using FEA by Melsen *et al.* (2007) who found that the amount of deflection experienced by a tooth is not linearly related to the magnitude of the force. Their results, which are reproduced in Figure 2.8 show that a large displacement is experienced for forces up to 12 cN but that the slope of the force-displacement curve decreases for larger force levels. These values seem to correlate with the previously cited study by Ren (2004), in which it was concluded that minute forces leading to very small changes in PDL pressure could be sufficient to induce tooth movement. In contrast, higher forces "might overload the periodontal tissues and cause negative effects that will hinder tooth movement".

The force-displacement relationship has thus been shown to be a vital component of orthodontic tooth movement. Most importantly, this relationship in contrast to the other secondary factors, is measurable using relatively simple external parameters. A force with known parameters can be applied to a tooth, the coronal displacement can be measured using an external appliance and their relationship calculated to produce a curve such as that determined by Melsen *et al.* (2007). This important relationship will be elaborated on in Chapter 3 and represents a central part of this thesis.

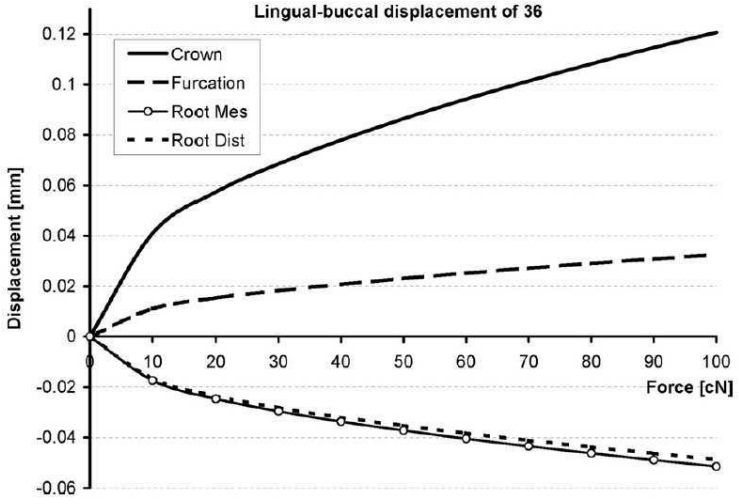

Figure 2.8: Lingual-buccal displacement due to varying levels of an applied force (Melsen *et al.*, 2007)

2.3.4 The concept of an optimal orthodontic force

The concept of an optimal orthodontic force was first defined in 1932 by Schwarz (1932) as "the force leading to a change in pressure that approximates the capillary vessels' blood pressure, thus preventing their occlusion in the compressed periodontal ligament." Oppenheim (1942) considered the optimal force to be very light forces applied over a longer period of time rather than applying larger forces over a short period of time. Another definition was put forth by Storey and Smith (1952) who proposed that there exists a range of force or pressure which results in the maximum rate of tooth movement.

The most recent concept of an optimal orthodontic force also takes into consideration minimal tissue damage and discomfort as well as temporal characteristics. The mechanical stimulus that leads to a maximum rate of tooth movement with minimal irreversible damage to the root, PDL and alveolar bone, is considered to be an optimal orthodontic force (Daskalogiannakis, 2000). The maximum rate of tooth movement must be achieved without applying excessive forces to the alveolar tissues to minimize any adverse effects (Proffit *et al.*, 2007; Ren, 2004).

Since the early definitions of an optimal orthodontic force, considerable effort has been put toward research to substantiate the existence of a generally applicable optimal force. Even recently, many attempts have been made to investigate the relationship between the force magnitude and the resulting rate of tooth movement. Most have failed however, to accurately describe the tooth movement resulting from a certain stimulus or have only been partially successful in proving the theory of an optimal orthodontic force (Ren *et al.*, 2003; Ren, 2004; Cattaneo *et al.*, 2005; Melsen *et al.*, 2007).

It is believed that the failure to characterize an optimal orthodontic force is not due to the hypothesis being incorrect, but rather due to the insufficiency of methods and technology which are used to test said hypothesis. In the previous section, the many factors affecting the rate of orthodontic tooth movement were presented and their complex interdependency was highlighted. Previous attempts to characterize an optimal orthodontic force have largely disregarded this complexity, while considering only a few specific parameters. Such a simplified approach is frequent and no model which incorporates a range of possible factors affecting tooth movement could be found.

Lastly, the availability of technology suitable for characterizing a complex optimal orthodontic force is extremely limited. Advanced models describing the relationship between a stimulus and the resulting tooth movement rely on the availability of improved measurements of both primary and secondary factors. This in turn requires the ability to accurately control the mechanical stimulus and receive reliable feedback from the orthodontic appliance. Current systems rely largely on purely mechanical principles and thus are not suitable for evaluating the hypotheses that have been proposed for an optimal orthodontic force.

2.4 The need for a paradigm shift

Even in the light of the described complexity of the underlying processes of orthodontic treatment, it is generally accepted that an optimal orthodontic force does exist and that if applied to a tooth such a force could significantly increase the rate of tooth movement. But despite great research effort it has not yet been possible to characterise an optimal force or to prove the hypothesis.

The failure to ascertain the optimal force hypothesis can be contributed to several reasons. The inability to accurately control the desired types of tooth movement, the different methods for measuring data, the problems in setting up repeatable experiments in-vivo and the resulting limited sample sizes are just some of the challenges. More significant is the disregard of the complexity arising due to varying anatomical and physiological properties, which make the characterisation of a generally applicable rule near to impossible. Even more noteworthy, however, is the approach of trying to model a highly time-dependent system using only discrete results.

While FEAs offers an improved understanding of the immediate changes, they are not able to account for the ongoing structural changes of the remodelling progress (Brown *et al.*, 1990). Furthermore, the results obtained from the FEA method are limited by the accuracy of the model itself, which requires various anatomical properties to be known.

Even if the means existed to characterize a time-varying optimal orthodontic force, no orthodontic appliance that can effectively use this knowledge to treat malocclusion exists. As shown, most of the existing orthodontic appliances make use of purely mechanical components. The recently commercialised AcceleDent system is the first orthodontic appliance to make use of non-static forces to speed up tooth movement. However, even the vibratory stimulus produced by the device is constant and can thus not be adjusted to suit a time-varying optimal force. This constraint represents the first shortcoming of all existing orthodontic systems.

A further important limitation is the lack of feedback during any orthodontic treatment. Current orthodontic systems do not incorporate any means of feedback, resulting in a rather inefficient open-loop approach. The extent to which the actual tooth movement corresponds to the treatment plan can only be evaluated during appointments with the practitioner, usually scheduled at four to six week intervals.

This open-loop approach relies on some fundamental assumptions regarding the application of orthodontic forces. Firstly, it requires the scientific knowledge describing the best suitable forces to be correct. Yet, the inconsistencies of evidence relating to the optimal orthodontic force indicate that this is not always the case. Secondly, it is based on the assumption that the practitioner is familiar with such knowledge, is able to plan orthodontic treatment accordingly and is able to implement it. Due to human error it is unlikely, however, that even a skilled practitioner would be able to apply forces which are within

the optimal range by manually bending the archwires.

The majority of the presented literature indicates that the means currently available in the orthodontic field are insufficient to address the complexity of characterising an optimal force. To successfully approach this challenge a paradigm shift is required.

It is the view of the author, that instead of simplifying experiments to quantify a generally applicable optimal force, the complexity of the problem should be acknowledged. Methods and advanced technologies to address this complexity should be developed. As an alternative to defining all-encompassing rules, orthodontic systems should be patient-specific and case-specific. The movement of teeth is such and orthodontic appliances should be designed accordingly.

An orthodontic appliance which can apply dynamic mechanical stimuli, can accurately control such stimuli, and can adapt to the ongoing processes of bone remodelling, would be ideal. By incorporating feedback systems into an orthodontic appliance it would be possible to monitor the effect of a certain mechanical stimulus on the surrounding tissues in real-time. The integration of a microprocessor into the appliance could further enable advanced algorithms to monitor tooth position, rate of tooth movement, periods of immobility due to tissue damage, and could make intelligent decisions to adjust the applied stimulus according to such data.

Ultimately, this could improve orthodontic treatment by reducing treatment times, reducing patient discomfort and increasing the control over the type of tooth movement. Furthermore, such an appliance would be less susceptible to human errors and hence could assist in avoiding adverse effects. Finally, the continuous feedback system would enable considerable amounts of data to be collected, which would contribute significantly to research in the orthodontic field and benefit the understanding of the underlying biomechanical principles.

Chapter 3

Conceptual design

As per Objective 4, the following chapter presents a hypothesis for a novel treatment approach and an electromechanical orthodontic appliance to facilitate such an approach is conceptualised. The appliance concept is based on the force magnitude and the immediate tooth displacement which can be measured. System requirements and relevant engineering specifications are summarised in Tables 3.1 and 3.2.

3.1 Hypothesis development

The following hypothesis is based on the previously described idea of an optimal orthodontic force that if applied to a tooth would result in the maximum rate of tooth movement without any adverse effects occurring. As mentioned, the failure to prove the optimal force hypothesis is thought to be a consequence of the approach that is used to analyse the problem rather than the hypothesis being incorrect. Researchers have tried analysing a hugely complex system involving the accurate control of orthodontic forces, time-dependant physiological processes inherent to mechanocoupling and interactions at a cellular level, with orthodontic systems that in comparison seem rather crude. It is believed by the author of this thesis, that by developing advanced technologies suitable for addressing the complexity of the problem rather than simplifying the problem itself, significant advancements could be made in this field.

Firstly, the characterisation of an optimal orthodontic force should be based on the correct secondary factors rather than the primary ones. Even though the primary factors play an important role during tooth movement, these should be treated as input parameters rather than used to describe the optimal condition. Thus, rather than quantifying a force in terms of magnitude, the secondary factors resulting from the applied magnitude should be kept paramount. The force vs. displacement relationship is one such factor which could aid in successfully characterising an optimal force.

Secondly, advanced technologies which incorporate better feedback sys-

tems are required to successfully improve orthodontic treatment. An appliance which incorporates a means for receiving feedback could be used to determine the important relationship between the primary and secondary factors. Thus, instead of controlling the force magnitude as such, a closed-loop feedback system is used to control the secondary factors by varying the controllable primary ones. A possible embodiment of such a system is illustrated in Figure 3.1.

Most importantly however, by making the described feedback continuous, an appliance could repeatedly re-assess the relationship between the primary and secondary factors and make intelligent decisions based on the outcome thereof. This would enable the immediate effects to be examined as done by Melsen *et al.* (2007), the short-term effects as studied by Jónsdóttir *et al.* (2006), and also the long-term results as used by Ren (2004).

The hypothesis put forth in this thesis is summarised as follows:

> It is assumed that for each type of treatment there exists a case-specific and time-specific optimal force which is most effective in achieving the desired treatment outcome, without any adverse side effects. It is possible to develop an appliance that is capable of applying a time-varying mechanical stimulus to a tooth and which, to a limited extent, can receive feedback on the resulting secondary factors. By calculating the relationship between the primary and secondary factors such an appliance will be capable of describing specific orthodontic cases. This case characterisation which can be immediate, short-term or long-term, could aid in defining and applying an optimal orthodontic force which would ultimately lead to improved orthodontic treatment.

3.2 System characterization

Specific parameters relating to the optimal force are identified and used to formulate a simplified version of the above hypothesis. The selected control parameters are equivalent to those used in many previous studies to examine the immediate effects of an applied force (Melsen *et al.*, 2007; Qian *et al.*, 2009). The developed system must however be capable of significantly increasing the amount of collected data by acquiring such information on regular intervals during tooth movement.

The proposed approach is illustrated in Figure 3.1, which shows the relationship between the orthodontic appliance, the tooth to which a mechanical stimulus is applied, the immediate secondary factors and the long-term resulting tooth movement. As can be seen, feedback of both the secondary factors and the resulting tooth movement is supplied to the appliance, which uses this information to correct the mechanical stimulus and by doing so is able to apply a stimulus which more closely resembles an optimal orthodontic force.

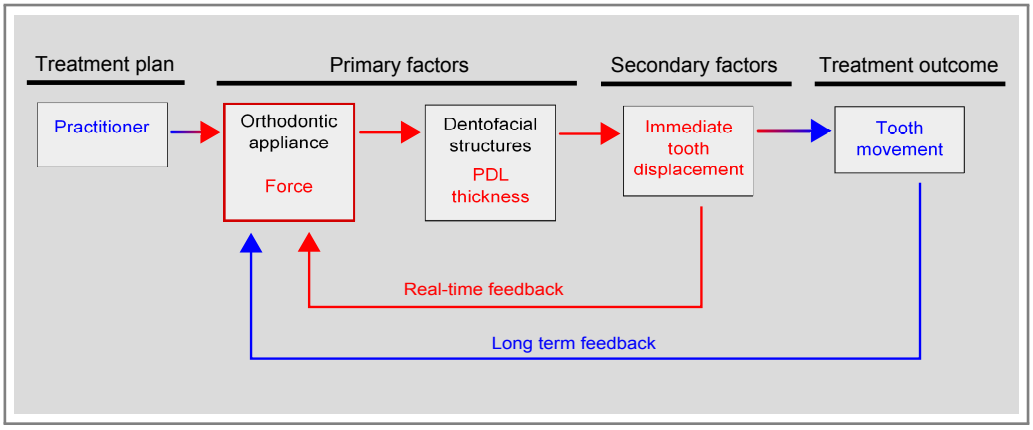

Figure 3.1: System overview

The two parameters under investigation are the force magnitude and its relationship to the immediate coronal tooth displacement, as illustrated in Figure 3.2. For the scope of this project the force magnitude will be taken to represent the controllable primary factors, while the immediate coronal tooth movement will represent the resulting secondary factors. The appliance must be able to produce a force F suitable for orthodontic tooth movement and must apply such a force to a single tooth. Furthermore, the appliance must be capable of measuring the coronal tooth displacement x resulting from the application of the orthodontic force F. It is generally accepted that if the force F has zero magnitude the coronal tooth displacement will also be zero. As the force magnitude increases however, the properties of the PDL will facilitate a slight displacement of the tooth. By using this approach the appliance aims to determine a relationship between the primary and secondary factors. The coronal tooth displacement for a specific case as a function of the applied force F is

$$x_{case1} = f_{case1}(F) \tag{3.1}$$

for which the magnitude of F can also vary so that

$$F_{large} > F_{light} \tag{3.2}$$

and thus

$$x_{case1}(F_{large}) > x_{case1}(F_{light}) \tag{3.3}$$

Furthermore, because x is a function of not only the applied force but also other primary factors such as the PDL thickness, the function f will differ for each case. Thus, if f_{case1} is a function describing the tooth displacement as a function of an applied force for a tooth with a thick PDL and f_{case2} is the equivalent for a tooth with a thin PDL, then for the same force

$$f_{case1}(F) \neq f_{case2}(F) \tag{3.4}$$

and thus the results of the above equation is

$$x_{case1}(F) \neq x_{case2}(F) \tag{3.5}$$

In order to characterise the above formulae and distinguish between different orthodontic cases the appliance will incorporate a feedback system such as that illustrated in Figure 3.1. As shown, the appliance gives rise to specific primary factors which represent input parameters to the control loop and applies a stimulus to the dental structures, which constitute the non-controllable primary factors of the system. The combination thereof gives rise to immediate secondary factors, which are fed back to the appliance. This part of the system shown in red is time-independent and the feedback can either be in real-time or can be generated at intervals. If maintained over a prolonged period of time, the output from the inner loop becomes the input parameter to the outer time-dependant control loop.

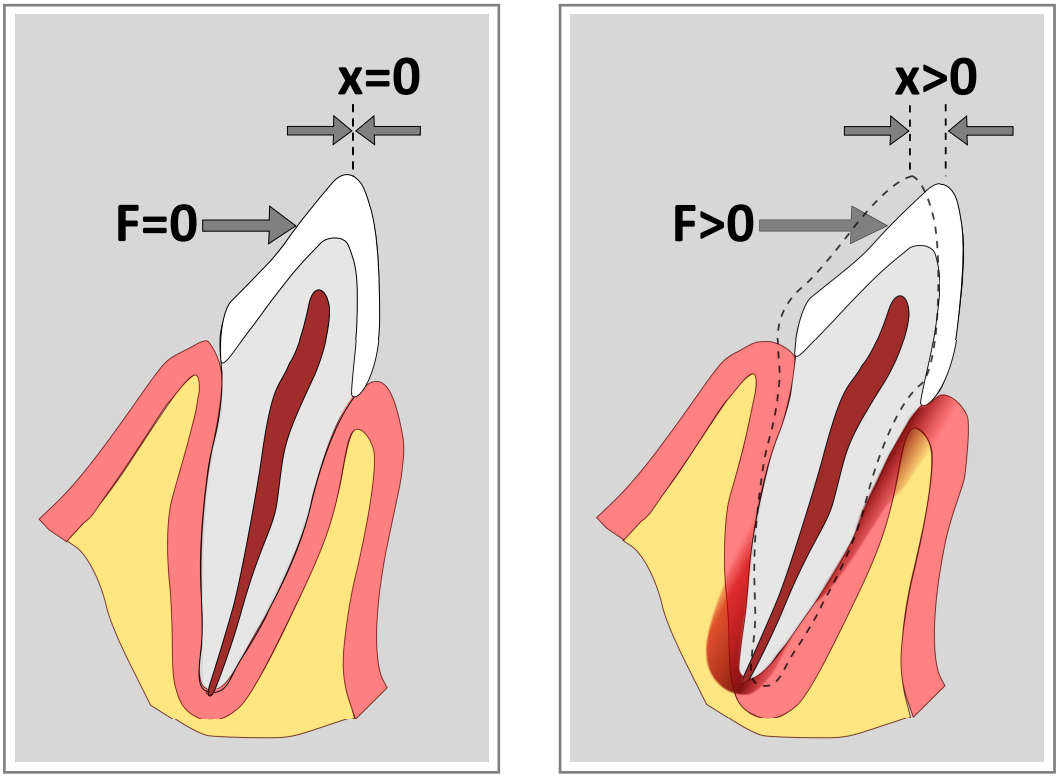

(a) State of equilibrium (b) Force applied to tooth

Figure 3.2: Force vs. displacement relationship

The outer feedback loop is facilitated by successful mechanocoupling of which the effects only become visible after a certain period of time and as such, is time-dependant. A maintained mechanical stimulus to the affected tissues will induce biomechanical changes that facilitate bone remodelling and

tooth movement. The appliance must also be able to receive feedback on such time-dependant factors and should be able to incorporate these for modelling purposes.

To complete the control loop, the orthodontic appliance must be able to communicate with the user or practitioner in order to receive and execute commands and return relevant data for viewing and processing. This should be done via a computer interface and more specifically via the USB port of a computer. Furthermore, the data exchange should be fast enough to allow for real-time control of the device as well as real-time viewing of acquired data.

While ensuring the functional features described above, the device should also allow for convenient testing and should be small enough to enable intra-oral tests to be performed. The appliance miniaturisation is considered one of the primary requirements during its development. Yet another requirement is the support of a stand-alone mode during which the appliance is battery operated and can apply and control a prescribed stimulus to a tooth. This mode would be essential if such an appliance was to be worn by a patient during the treatment process.

At this stage, limitations of the current study should be mentioned. Even though the design should take into account the physical considerations of the intra-oral environment as best as possible, the prototype developed during the scope of this project will not be required to function intra-orally. Constraints set by the micro-manufacturing capabilities do not allow for a physical system to be produced which is water and corrosion resistant. Furthermore, the use of medical grade components such as the batteries for the prototype development is not viable. The purpose of the developed prototype is to provide a proof-of-concept and no in-vivo experiments are required therefore. The prototype will thus not be required to adhere to safety standards regulating commercially used orthodontic appliances

The system requirements characterizing the device are summarised in Table 3.1. The listed functions form the basis for the orthodontic appliance design according to which the final development outcomes will be evaluated.

Table 3.1: System requirements

No.	Description
	Functional requirements
1	Must be able to apply a mechanical stimulus similar to that applied by conventional orthodontic systems, but also including advanced non-static force parameters, to at least one tooth.
2	Must be able to control the mechanical stimulus and make changes thereto without the need for physical system changes.
3	Must be able to measure, record and transmit data describing the mechanical stimulus to the user.
4	Must be able to control the mesio-distal position and tipping of a tooth as specified by the user.
5	Must be able to measure, record and transmit to the user data describing the relative tooth position and orientation within the mesio-distal plane.
6	Must be able to measure, record and transmit to the user data describing at least one secondary parameter, in this case immediate coronal tooth displacement due to loading of the PDL.
7	Must be able to receive and execute commands from a user.
8	Must be able to function in battery mode during which a predefined mechanical stimulus is produced without a connection to a computer.
	Interfacing requirements
9	Must be controllable via a USB port.
10	Must be able to return acquired data of system parameters via the USB port at high speed.
11	Must provide basic feedback on the state of the appliance, independent to the USB connection.
	Dimensional requirements
12	Must be suitable for intra-oral use for short periods of time.

3.3 Engineering specifications

The engineering specifications are based on the previously formulated system requirements. For each of the functional requirements, numerical values were extracted from the literature to form the engineering specifications.

The requirements for the mechanical stimulus were selected according to

previous research done on the relationship between the stimulus and the immediate resulting tooth displacement. Melsen *et al.* (2007) examined forces ranging from 0 cN to 100 cN and found that the most significant results were observed for forces well within this range. No minimum value was specified for the magnitude of the force moment, as this is a function of both the force magnitude and the mechanical system design.

The minimum operating range for the orthodontic appliance should be similar to that necessary for basic orthodontic treatment. The minimum distance for tooth displacement was thus chosen to be 2 mm, while the minimum angle for mesio-distal tipping should be at least 5 °.

The desired closed-loop feedback requires the force sensor range and the position sensor range to be greater or equal to the corresponding ranges of the stimulus. Thus, the position sensor must be able to accurately determine the orthodontic bracket position over the entire operating range of 2 mm and the force sensor must be able to measure forces ranging from 0 cN to 100 cN. Also, the force sensor must operate across the entire range of movement and not just at one position.

Table 3.2: Engineering specifications

Property	**Value**	**Units**
Stimulus specifications		
Orthodontic force magnitude	≥ 60	cN
Movement specifications		
Movement range	≥ 2	mm
Tipping range	≥ 5	°
Sensor specifications		
Position sensor range	≥ 2	mm
Position sensor resolution	≤ 5	µm
Force sensor range	≥ 100	cN
Force sensor resolution	≤ 2	cN

Finally, the sensor resolution for both the position and force sensor should provide at least 100 data points across the measurement range required for the force-displacement. For a force range of ±100 cN the resolution is thus required to be 2 cN. The maximum expected displacement of a tooth is ±0.5 mm, which translates into a resolution of 5 µm.

Chapter 4

System development

The following chapter describes physical prototyping and development of the electromechanical orthodontic appliance. Three subsections describe the mechanical system, the electronic components and the software development, respectively. Each section begins with an overview of the corresponding subsystem which is followed by a detailed description of its components. The current chapter illustrates the development process described by Objective 5.

4.1 Mechanical subsystem

4.1.1 Overview

The following section discusses the mechanical design and manufacturing procedures of the project. Each part of the physical system is discussed individually, illustrating design considerations with respect to the functional requirements set forth in the previous chapter. An overview of the mechanical system components is provided in Figure 4.1.

The mechanical design process was in no way an isolated process and was influenced by the interdependency of the mechanical and the electronic subsystems. This interdependency arises mainly due to the need for excellent physical interfacing of all system components to minimize the overall appliance size. Thus, some of the mechanical features such as the force sensing mechanism, were designed according to electronic component selection.

The material choice was also influenced by the choice of sensors. For instance hall sensors measure the magnetic field lines and based thereon, obtain a reading. To minimize the magnetic interference therefore, all larger mechanical components were made using non-ferrous titanium.

Due to the small-scale nature of the appliance, the availability of manufacturing capabilities and associated costs played an important role. Early concepts were designed for flexibility, using small screws and other similarly complex features to enable repeated system assembly and disassembly. The

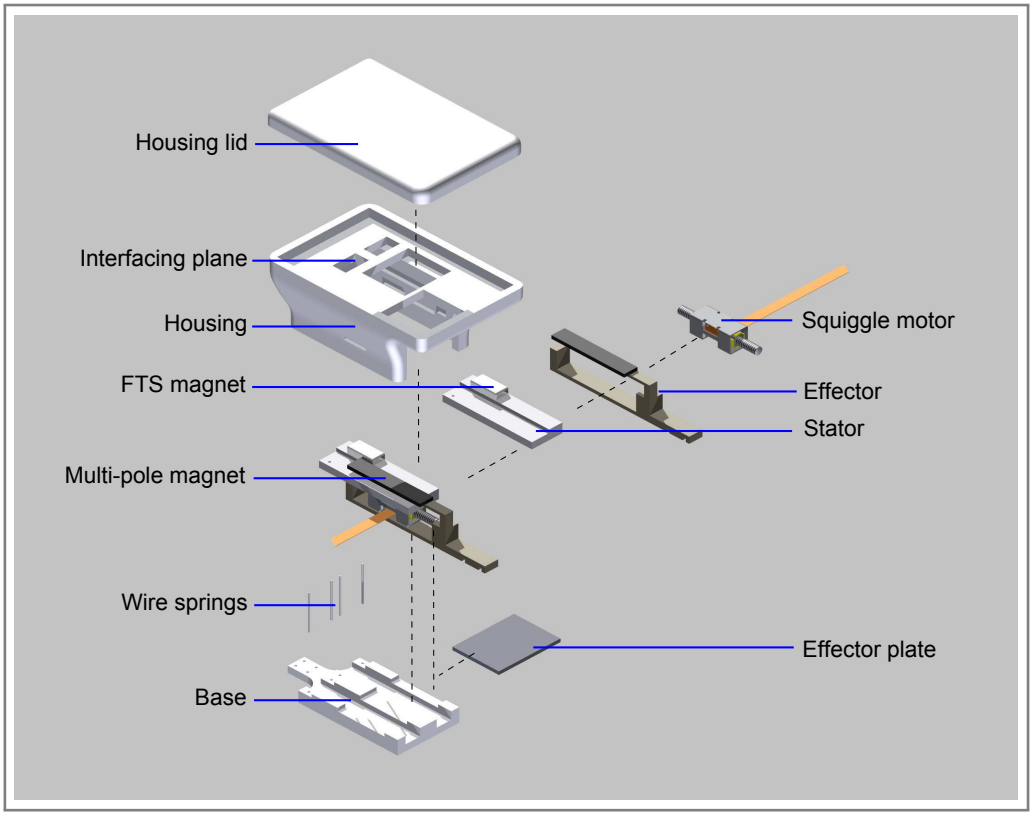

Figure 4.1: Mechanical system overview

high cost of micro-manufacturing capabilities required for such features led, however, to a revised design approach.

For the final mechanical component design, simplicity and the ease of manufacturing were kept paramount. The number of machine set-ups was also reduced by omitting certain features and no means for disassembly were incorporated into the design. The design was further optimized according to the micro-manufacturing capabilities of the manufacturer. Jan Hugo Precision Engineering (Pretoria, South Africa) manufactured the mechanical components and specialises in the development and production of biomedical components.

The mechanical assembly consists of the actuating mechanism comprising the stator, the effector and the Squiggle motor, the force transducer mechanism consisting of the stator and the straight-wire spring mechanism, and finally the housing design.

4.1.2 Actuating system

Two linear piezoelectric Squiggle micro-motors (New Scale Technologies, New York, USA) were selected as actuators due to their small size and superior performance compared to other commercially available micro-motors. A common challenge for micro-motor design is minimizing both the motor size as

well as that of the required control and driver circuit. Also, relatively large forces should be produced using low-voltages. The Squiggle motor is the only commercially available actuator that was found to fulfil these requirements and showed far superior performance to comparable micro-motors.

The 2.7x2.7x6 mm Squiggle motor features a simple design consisting of only two major components. When the motor is activated, short pulses of electrical potential are applied to the piezoelectric actuators, which are mounted on the four sides of the stator. These create ultrasonic vibrations and cause a threaded nut on the inside of the stator to vibrate in an orbit, which in turn leads to a linear motion of a lead screw. This mechanism has several advantages that make it ideal for use in orthodontic appliances such as zero backlash, nanometre resolution, high force of up to 50 cN and power-off hold (NewScaleTechnologies, 2012).

Two linear actuator Squiggle motors are arranged in parallel and integrated into a cylinder-piston type assembly to achieve control of the two desired degrees of freedom. The effectors are connected to the orthodontic bracket using the interfacing features described in Section 4.1.5 which enable both the translation and tipping of a tooth to be controlled. Translation, which represents the first degree of freedom, is achieved by moving both effectors in either a forward or backward direction by exactly the same amount. Tipping, which represents the second degree of freedom is achieved by moving the two motors in opposite directions.

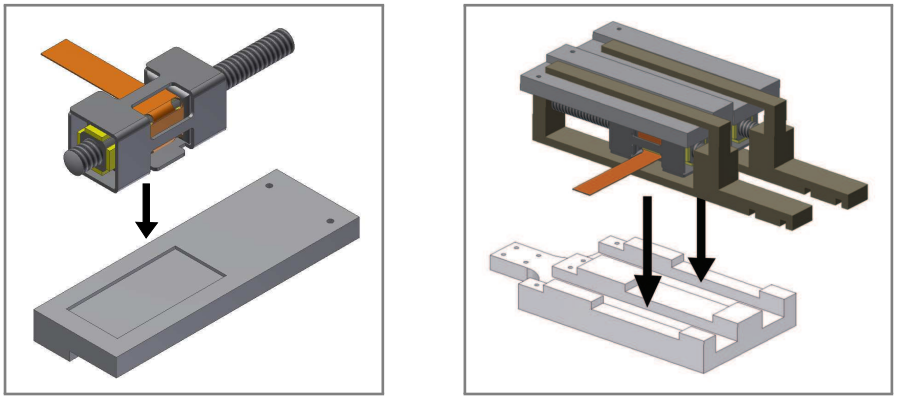

(a) Squiggle motor mounting on stator component

(b) Effector and base assembly

Figure 4.2: Actuator assembly

The described configuration requires the motors to transmit both a pushing and a pulling force to the bracket via the effectors. The linear movement of the Squiggle motor, however, is enabled by the lead screw being able to rotate freely and forces are transferred purely by it pushing against a flat, ideally polished, surface. Thus, the effectors are designed so that the lead screw of the Squiggle motor is enclosed between two opposing surfaces.

A multi-pole magnetic strip is mounted onto the effector in such a way that it coincides with the interfacing plane indicated in Figure 4.1. The magnetic strip, which is used in conjunction with the magnetic linear position encoder, is mounted on the upper surface of the effector extension. Because this extension is not required to withstand any force, it was designed with the minimum dimensions allowed by the manufacturing processes and the material properties. Manufacturing of the effectors was done using wire electrical discharge machining (WEDM).

The motor housing, with which the lead screw engages, is mounted to a second component called the stator to enable relative movement between the two. Of the several motor mounting options suggested by the supplier, the one requiring the least parts and thus the smallest space was achieved by using adhesive. A 0.15 mm deep intrusion was machined into the bottom surface of the stator to accommodate the base of the motor housing as shown in Figure 4.2.

Finally, the base features two longitudinal slots within which the effectors are guided to achieve relative movement. At its rear end, the the base is rigidly connected to an orthodontic bracket, relative to which movement should be achieved. The stators, which make up part of the force transducer system (FTS) are mounted to the base, and the motor and effector assembly in turn is connected to the stator as described above. When activating the Squiggle motors, the effectors are caused to slide within the slots in the base similar to a piston within a cylinder.

4.1.3 Force transducer system

A custom force transducer was developed due to the lack of suitable commercially available force sensors. No suitable sensor which incorporates the force measurement requirements into a sufficiently small system without the need for complex external amplification and control circuitry could be sourced.

As a result, a straight-wire spring mechanism was designed which allows externally applied forces to the effector to be transformed into small displacements of the stator. Two straight-wire springs arranged in parallel were connected to the base at one end and to the stator at the other. When a force is applied to the effector, the wires are subjected to bending forces and the stator is displaced relative to the base, as shown in Figure 4.3. These small changes in relative stator position are sensed by an AS5510 (Austria Micro Systems, Unterpremstaetten, Austria) magnetic position encoder. The transducer thus includes the design of the straight-wire spring mechanism as well as the magnet-encoder interface.

The magnetic interface depends on the type of magnet, the distance between the encoder and the magnet, and the encoder sensitivity, which is adjustable. A square two-pole NdFeB sintered Nickel-coated magnet with 1.21 T remanence was mounted on each of the stators, in such a way that they coin-

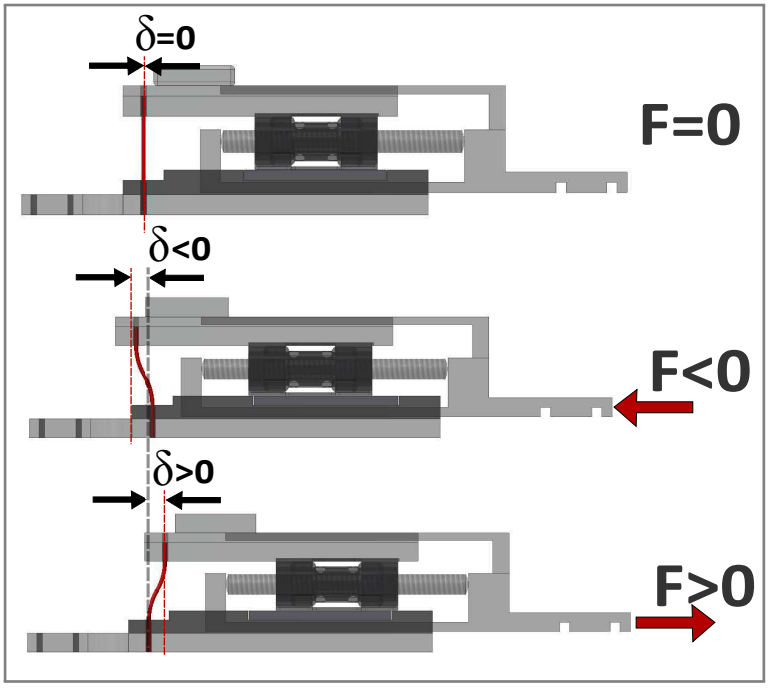

Figure 4.3: Force sensor mechanism

cide with the interface plane. The air gap between the magnet and the AS5510 encoder on the sensor board is approximately 0.75 mm. The magnet is centred along the line of movement relative to the encoder so that the pole interface coincides with the zero position of the encoder. Upon stator movement the encoder senses a change in the magnetic field and outputs a 10 bit resolution position measurement via the I2C interface.

The encoder resolution r_{Enc} is a function of the magnetic field gradient α and the encoder sensitivity S_{Enc}. The magnetic field strength depends on the air gap between the magnet and the encoder and cannot be changed after assembly, but S_{Enc} can still be adjusted via the I2C interface. By doing so, the encoder resolution r_{Enc} and the sensor range can be controlled. The resolution as a function of S_{Enc} and α is calculated by

$$r_{Enc} = \frac{1}{\alpha S_{Enc}} \tag{4.1}$$

The magnetic field strength, as measured by the encoder, is described by the function

$$B = \alpha\delta \tag{4.2}$$

where B denotes the magnetic field strength in mT and δ is the stator displacement from the equilibrium position due to an applied force.

Using the above equations, the encoder output O_{Enc} as a function of δ can be described by

$$\begin{aligned} O_{Enc} &= S_{Enc}B \\ &= S_{Enc}\left(\alpha\delta\right) \end{aligned} \tag{4.3}$$

Lastly, in order to be able to obtain the value of an applied force from the encoder output, the relationship between the force magnitude and the relative stator displacement needs to be described. For the current configuration $\delta(F)$ is described by

$$\delta = \frac{\mathrm{L}^3}{24EI}F \tag{4.4}$$

where L is the wire length, I is the moment of inertia and E is the Modulus of Elasticity of the material. Rearranging Equation 4.3 and 4.4 and substituting δ allows the calculation of $F(O_{Enc})$, where

$$\begin{aligned} F &= \frac{24EI}{\mathrm{L}^3}\delta \\ &= \frac{24EI}{\mathrm{L}^3}\left(\frac{O_{Enc}}{\alpha S_{Enc}}\right) \\ &= \frac{24EI}{\alpha S_{Enc}\mathrm{L}^3}O_{Enc} \end{aligned} \tag{4.5}$$

Because all variables except the decoder output O_F remain constant, these can be combined into a single variable k defined as

$$k = \frac{24EI}{\alpha S_{Enc}\mathrm{L}^3} \tag{4.6}$$

and thus Equation 4.5 simply becomes

$$F = kO_{Enc} \tag{4.7}$$

The variables in Equation 4.5 represent the design variables, which were optimized to meet the engineering requirements set forth in Section 3.3. The main objective of the design was to allow for the measurements of small forces ranging from 0 cN to 60 cN for each of the two effectors. The wire length was maximized to 3.25 mm, while not increasing appliance dimensions and a small diameter of 0.25 mm was calculated to be suitable. Furthermore, the air gap between the magnet and the encoder was minimized to 0.75 mm. The value of the magnetic field constant at a distance of 0.75 mm was determined from supplier specifications as $\alpha = 31.58\,\mathrm{mT/mm}$.

According to the previously developed equations, two different FTS were designed and tested. The first transducer design maximizes the resolution of the force transducer by using soft nickel-titanium (NiTi) wires. NiTi wires

feature a very low Young's Modulus of 32 GPa (Zadno, 1989) and thus give rise to significant displacements, even when subject to very light forces. Table 4.1 lists physical transducer parameters and technical specifications for the NiTi FTS.

Table 4.1: NiTi force transducer system

Property	Symbol	Value	Units
Wire specifications			
Material	-	Nickel-Titanium	-
Young's Modulus	E	32	GPa
Length	L	3.25	mm
Diameter	ϕ	0.23	mm
Moment of inertia	I	1.38×10^{-4}	mm^4
Flexural rigidity	EI	4.40	Nmm^2
Magnet specifications			
Air gap	a	0.75	mm
Magnetic constant	α	31.58	mT/mm
Encoder specifications			
Sensitivity	S_{Enc}	36.62	µT/bit
Encoder range	X_{Enc}	±18.75	mT
Force sensor specifications			
Force range	X_{FTS}	±257	cN
Resolution	r_{FTS}	0.36	cN/bit
Relation to encoder value	$F(O_{NiTi})$	$F = 0.36O_{NiTi}$	-

The use of NiTi wires allows for force measurements with a high resolution of 0.36 cN/bit, but could possibly introduce non-linear behaviour of the FTS. The mechanical properties of the NiTi wires are sensitive to changes in temperature and yielding of the material due to excessive external forces could cause non-linear behaviour of the NiTi wires (Zadno, 1989). During initial appliance development, the actuator forces were used to determine the maximum stresses, which for the straight wire spring configuration are calculated by

$$\sigma_{max} = \frac{FL\phi}{8I} \tag{4.8}$$

When evaluated, this results in a maximum stress of $\sigma_{max} = 264.83$MPa. Comparing the yield stress σ_Y found in the literature of approximately 450 MPa,

this indicates that yielding will not occur. The value found in literature differs significantly however (Huang and Liu, 2001; Liu *et al.*, 1998), and thus this outcome cannot be guaranteed.

Due to the uncertainties regarding the NiTi FTS a second FTS was designed using steel wires. The steel wires resulted in a reduced sensor resolution but yielding thereof would not occur. The Young's Modulus of the wires provided in Table 4.2 was determined experimentally due to uncertainties regarding the material properties. Beam bending tests were performed, and the average result thereof used for the FTS design. It should be noted that the approximate Young's Modulus of 87 MPa was used during the design only, and that the FTS was calibrated as described in Chapter 5.

To compensate for the reduced resolution, the encoder sensitivity S_{Enc} of the AS5510 encoder was adjusted to 24.41 µT/bit resulting in a force resolution of $r_{FTS} = 1.24$ cN. Further specifications for the steel wire FTS design are provided in Table 4.2.

Table 4.2: Steel force transducer system

Property	**Symbol**	**Value**	**Units**
Wire specifications			
Material	-	Steel	-
Young's Modulus	E	87	GPa
Length	L	3.25	mm
Diameter	ϕ	0.27	mm
Moment of inertia	I	2.61×10^{-4}	mm^4
Flexural rigidity	EI	22.70	Nmm^2
Magnet specifications			
Air gap	a	0.75	mm
Magnetic constant	α	31.58	mT/mm
Encoder specifications			
Sensitivity	S_{Enc}	24.41	µT/bit
Encoder range	X_{Enc}	±12.5	mT
Force sensor specifications			
Force range	X_{FTS}	±634	cN
Resolution	r_{FTS}	1.24	cN/bit
Relation to encoder value	$F(O_{Steel})$	$F = 1.24O_{Steel}$	-

4.1.4 Housing design

The previously described mechanical system was integrated into a housing to provide a compact appliance design. To reduce the number of components required for assembly, the housing also includes features to assemble the sensing circuit with the mechanical assembly. Additional functions of the housing are to protect the fragile mechanical system during handling and to prevent contamination of the moving components.

The housing, which includes complex internal features, was manufactured by means of 3-D printing. Using the CAD model shown in Figure 4.4(a), the final component was printed on an EOS P380 machine with polyamide PA 2200. The final product of which a photograph is shown in Figure 4.4(b) offered a practical and robust means for integrating the sensing circuit with the mechanical system.

A second housing was designed to accommodate the adaptor board circuit, which will be described in Section 4.2.4. Designing and manufacturing it using 3-D printing again offered a robust packaging solution for housing the circuit components.

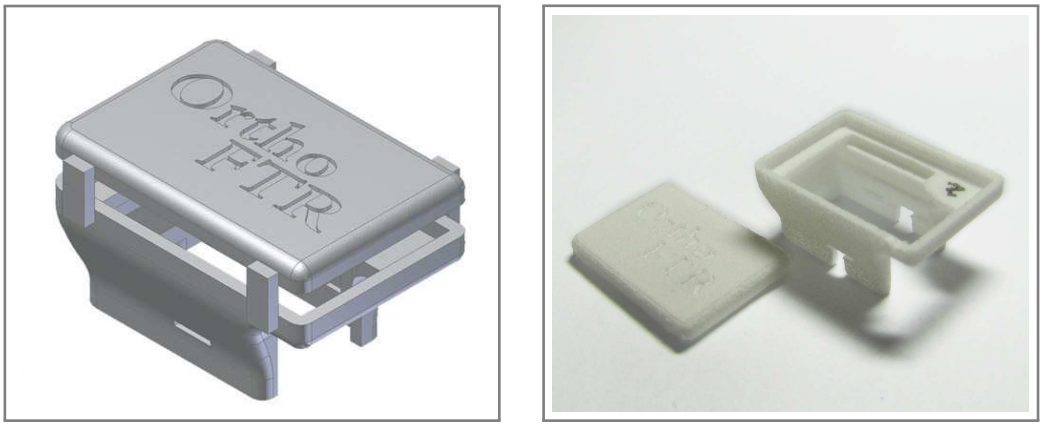

(a) Virtual CAD model of appliance housing

(b) Appliance housing manufactured by 3-D printing

Figure 4.4: Appliance housing

4.1.5 Dental interface

An interfacing method for conveniently attaching the appliance to the teeth was required. The interface needed to be such that the appliance could easily be attached and detached to orthodontic brackets fixed to the teeth. To reduce manufacturing costs, however, the required features were not included in the initial mechanical design, but were machined into the components manually. A 0.5 mm thick aluminium oxide cutting disc driven by a Dentalfarm micro

motor (Torino, Italy) was used to machine the features into the effectors and the base.

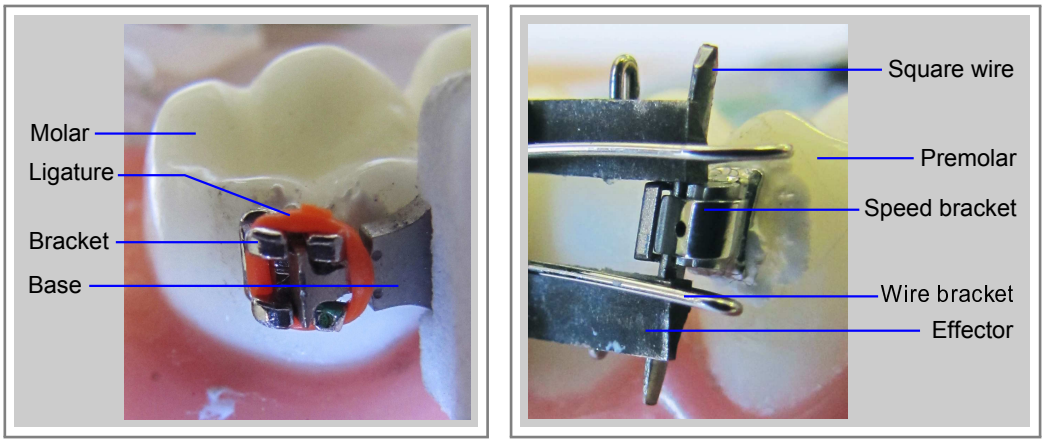

(a) Base attached to a vertical slot bracket using an elastic ligature

(b) Effectors connected to Speed bracket using a square steel wire

Figure 4.5: Dental interface features

Two V-shaped slots were cut into the underside of the effector to accommodate a square stainless steel wire. A wire bracket was bent for each effector to keep the square within the V-shaped slots. With the straight wire in place, the two V-shaped slots allow rotation of the square wire relative to each of the effectors, but limit translation. If used in combination, the effectors can thus control both the translation as well as the angle of the square wire. To connect the effectors to a tooth, the centre of the square wire is inserted into the slot of a Speed bracket (Strite Industries, Cambridge, Ontario, Canada).

The interfacing features on the base allow it to be mounted onto any orthodontic bracket featuring a vertical slot. As shown in Figure 4.5(a) the base feature is inserted and maintained in the bracket using an elastic ligature. Because the base sits tightly within the bracket slots, this method provides a rigid connection in the plane of movement.

4.2 Electronic subsystem

4.2.1 Overview

The electronic subsystem design comprises three separate circuit boards, which are referred to as the CPU board, the sensor board and the adaptor board. Firstly, the CPU board is responsible for central processing of appliance data and coordinating the functions of all other electronic components. It is further used for communicating with the computer via the adaptor board, receiving

commands from the user and executing these. Secondly, the sensor board represents the interface between the mechanical and the electronic subsystems and is thus integrated into the appliance assembly. It features two magnetic encoders for the FTS, two position encoders for determining the effector position, and two motor driver ASICS to control the Squiggle motors. Thirdly, the adaptor board is designed to provide a convenient interface to the USB port of a computer and also functions as a lithium-ion battery charger. The following sections provide an overview of the electronic subsystem shown in Figure 4.6. A more detailed description of the electronic subsystem is provided in Appendix C. The appendix provides technical specifications for the electronic components, board interfacing, circuit board layouts, and circuit diagrams.

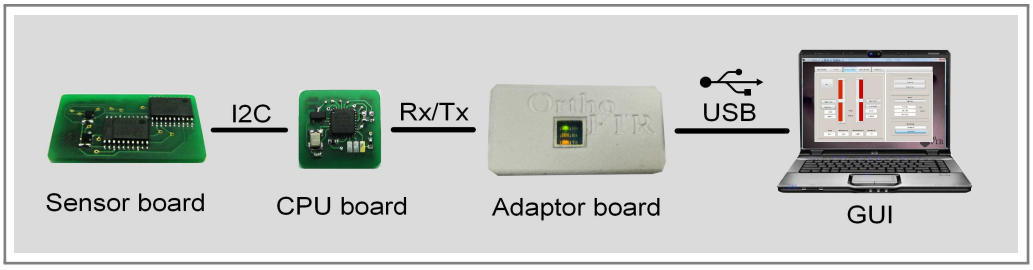

Figure 4.6: Electronic subsystem overview

During the iterative development of the three circuits, the reduction of the overall circuit dimensions was kept paramount. Substantial effort was put toward component selection to minimize the overall footprint and interfacing sizes. Further important considerations for the electronic component selection included low voltage operating modes at 3.3 V, compatibility with two-wire communication protocols, and low power consumption to allow for battery operation. A description of each of the three individual circuits follows.

4.2.2 CPU board

During the development of the CPU board, three prototypes were designed and built. The electronic design was based largely on that of the Arduino UNO board (Ivrea, Italy) as this combined the desired functionality with a simple programming interface. For the development of Prototype 1, a breadboard circuit was designed to test the interfacing of electronic components, whilst discarding unused hardware from the Arduino UNO. Prototype 1 additionally provided a platform to begin the software development. Prototye 2 was designed using surface mount technology (SMT) components and was manufactured using in-house manufacturing facilities. The use of SMT components improved interfacing and greatly reduced the overall circuit size. Finally, Prototype 3 further reduced the appliance size by using advanced manufacturing

processes, which allowed for smaller tolerances and multilayer circuits to be produced.

The final CPU board makes use of the ATmega328P chipset (Atmel, San Jose, California) to achieve its processing requirements. The ATmega328P offers a suitable solution as it is compatible with the Arduino integrated development environment (IDE) and is thus easily programmable. It features an I2C interface, serial port communication, and 8 MHz operation at a supply voltage of 3.3 V, which make the appliance suitable for battery operation. Also incorporated into the CPU board are a 16 MHz clock and a voltage regulator for power management. Three differently coloured light emitting diodes (LED) are used to provide user feedback on the state of the CPU board independently of the graphical user interface (GUI). The final dimensions of the CPU board, shown in Figure 4.7 are 15x18x2 mm.

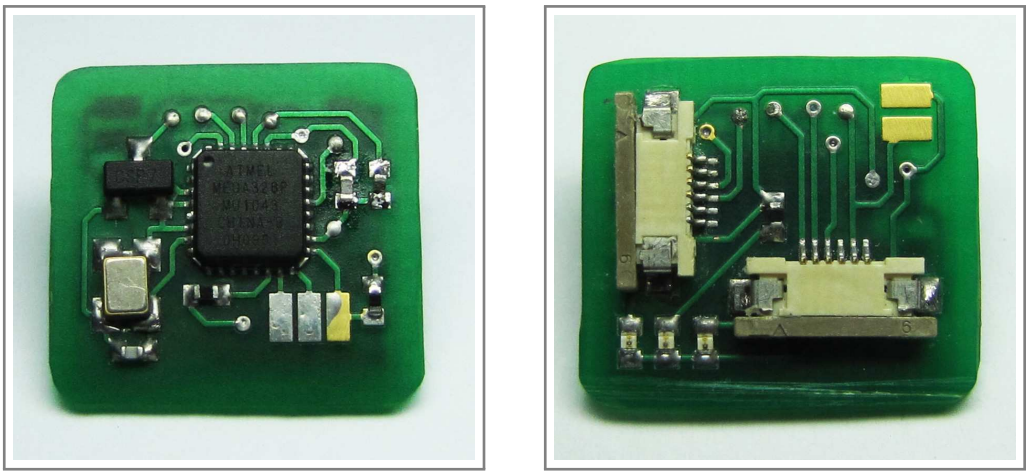

(a) Component side of CPU board (b) Interface side of CPU board

Figure 4.7: CPU board

The implementation of the Arduino software environment on an application specific circuit was a key component of the CPU board design. Substantial effort was thus put toward developing a system which allowed the same microprocessor as on the Arduino UNO to be used for the CPU board. A detailed description of this system and the necessary procedure for implementing the Arduino software on an application specific circuit can be found in Appendix E.

4.2.3 Sensor board

The sensor board represents the interface between the mechanical and electronic subsystems and thus makes up part of the appliance assembly. The circuit holds six ASIC chips, which are used for position sensing, force sensing

and controlling the Squiggle motors. Most importantly, all of the components housed on the sensor board use I2C communication and thus only four electronic connections are required for interfacing. Two are used for supplying power to the sensor board and the other two for the I2C communication.

The position sensors provide measurements of the mechanical effector positions relative to the sensor board. A multi-pole magnetic strip is mounted on the effector in such a way that it coincides with the interfacing plane and generates a changing magnetic field as it passes over the NSE-5310 position encoder (Austria Micro Systems, Unterpremstaetten, Austria). These small changes are detected using a linear hall array and are interpolated into fine steps which can then be read from the encoders. The NSE-5310 linear position encoder features a 12-bit resolution for measuring displacements over large distances and a high-speed I2C read-out frequency of 400 kHz.

Because no suitably small force sensor could be sourced, the previously described force transducer was built and a position encoder used to measure the stator displacement from which the force can be calculated. Similar to the previously described NSE-5310, the AS5510 encoder uses a hall sensor array to measure the magnetic field strength, but it is used in conjunction with a simple two-pole magnet instead of a multi-pole magnetic strip. The AS5000-MA4x2H-1 (Austria Micro Systems, Unterpremstaetten, Austria) two-pole magnet is mounted on the upper stator surface so that it coincides with the interface plane. The AS5510 position encoder can however only measure small displacements of up to ± 1 mm, depending on the desired resolution. The 1.46x1.10 mm AS5510 encoder is used to sense the required range and provides position measurements with 10-bit accuracy via an I2C interface in an extremely compact package. The final sensor board is 22x14x3 mm large and is shown in Figure 4.8.

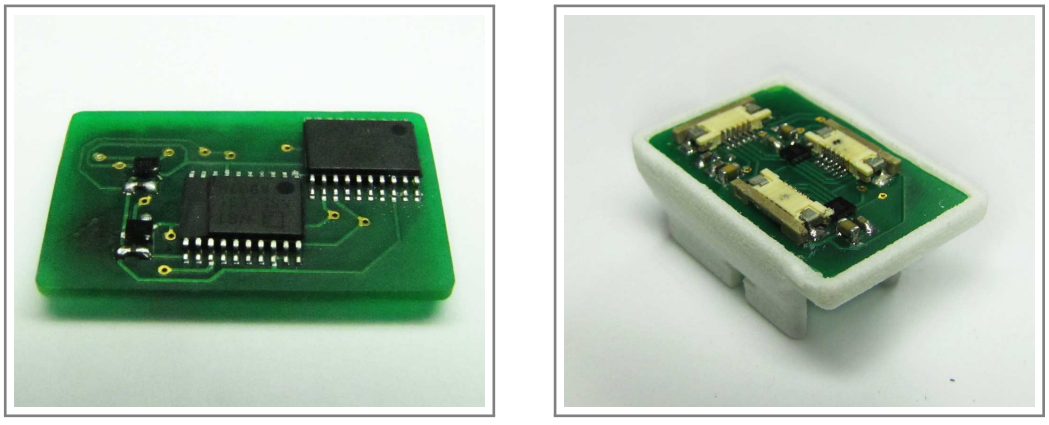

(a) Component side of sensor board

(b) Sensor board integrated into the appliance housing

Figure 4.8: Sensor board

4.2.4 Adaptor board

The adaptor board converts the serial communication protocol to USB or vice versa, which enables the orthodontic appliance to be connected and controlled directly from any computer with a USB port. A ATmega8U2 chip (Atmel, San Jose, California), programmed as a USB-to-serial converter, enables high-speed serial communication and data exchange via the USB port. The board is thus used to connect the CPU board to a computer and enables real-time viewing of position and force measurements on the GUI.

The adaptor board also acts as a battery charger for 3.7 V lithium-ion batteries. When connected to the USB port, three lithium-ion batteries can be charged simultaneously at 70 mA charge current. The time required for a complete charge cycle of the LPP 402025CE 150 mAh batteries (VARTA, Alpharetta, Georgia, USA) is thus just over two hours.

Lastly, the adaptor board incorporates a number of LEDs to provide feedback on the board status. A green light indicates that power is supplied to the adaptor board, while two orange LEDs indicate activity on the serial receive (Rx) and serial transmit (Tx) lines of the serial communication port as shown in Figure 4.9(a). The battery charger also includes a blue LED on each of the charger ports, which indicates when a battery is being charged. Figure 4.9(b) shows the charger state for a single battery being charged on port three.

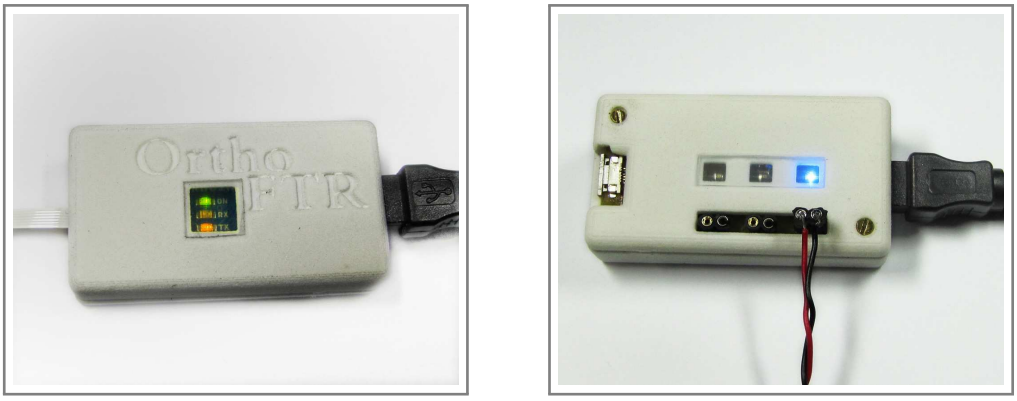

(a) Power is being supplied to board and serial communication is active

(b) Battery is currently being charged

Figure 4.9: Adaptor board

4.2.5 Power supply and management

Depending on the selected operating mode, the appliance is powered using either the USB connection or a rechargeable 150 mAh 3.7 V lithium-ion battery. It is important to note that the appliance can only be powered using either one of the two options and not both simultaneously. A switch is incorporated into the appliance allowing selection of the operating mode.

The method more commonly used is powering the appliance from the USB connection as this allows control via the GUI and viewing of the appliance measurements. The 5 V and GND connections on the USB cable are connected to the corresponding pins on the CPU board. Here a MCP1700 voltage regulator steps the 5 V down to 3.3 V, which is the operating voltage for all electronic components. The regulator includes a short circuit protection and is capable of supplying a maximum constant current of 250 mA.

The appliance operation can also be changed to battery mode by using the manual switch. The battery needs to be charged using the previously described charging circuit incorporated on the adaptor board. The 3.7 V battery supply voltage is stepped down to 3.3 V using the same MCP1700 regulator. This operation mode does not allow for data to be captured or displayed on the GUI, but can be used to apply a predetermined stimulus and is meant primarily for demonstration purposes.

Figure 4.10 shows the final appliance assembly being operated in battery mode. The flashing blue LED indicates that the software is being executed correctly.

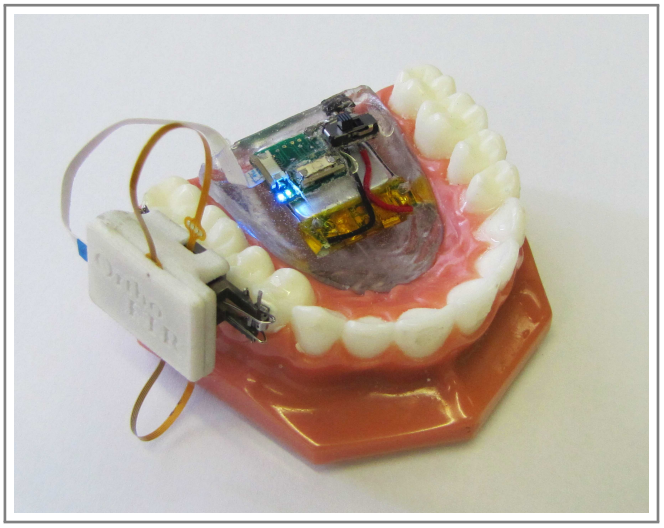

Figure 4.10: Final appliance assembly in battery operation mode

4.3 Software development

4.3.1 Overview

Two separate software programs constitute the development of the orthodontic appliance. The first is the GUI, which was designed and coded using the graphical user interface development environment (GUIDE) in Matlab. Its purpose is to provide the user with an easy-to-use interface which enables appliance connection, appliance control, as well as real-time viewing, recording

and reviewing of appliance data. The second piece of software was written for the CPU board to coordinate appliance functions. This appliance software was written using the Arduino IDE and is executed by the ATmega328P microprocessor on the CPU board. Its functions include communicating with the GUI, controlling the Squiggle motors and coordinating read/write operations to the sensors.

To achieve efficient communication between the appliance software and the GUI, programming of the two software elements was done in parallel. A simple communication protocol, described in more detail in Appendix D was devised to achieve efficient appliance interfacing. The primary focus during software development was fast and reliable data exchange between the CPU board and the GUI.

4.3.2 Graphical user interface

The GUI is specifically designed to provide an easy-to-use interface from which to control the orthodontic appliance. The layout makes use of the five different tabs seen in Figure 4.11, each of which feature certain high-level functions and commands that can be issued by the user. The functions associated with each of the five tabs are described below.

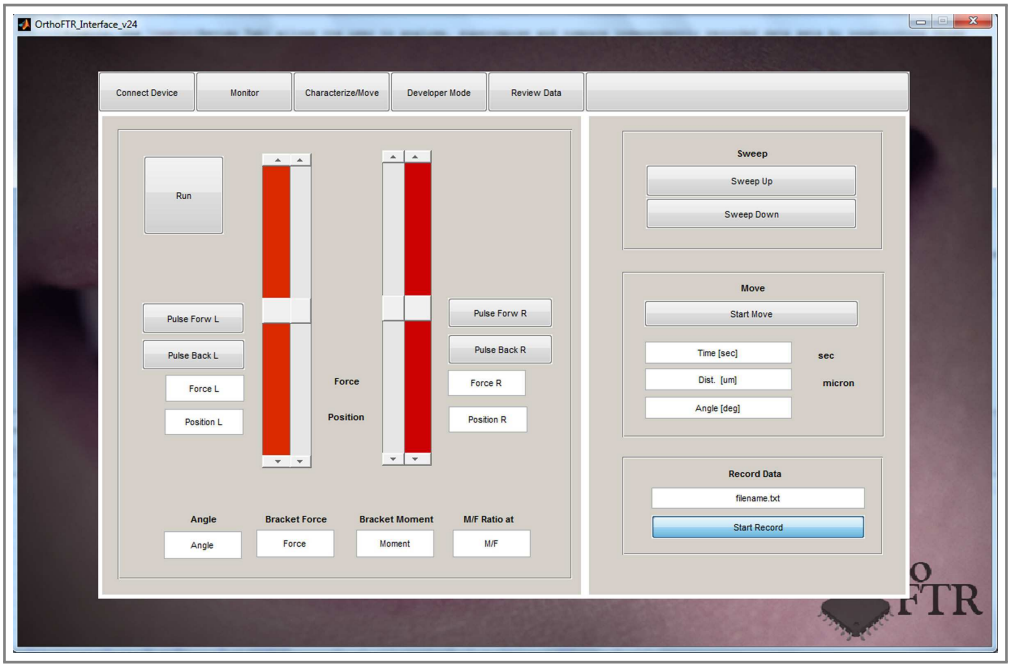

Figure 4.11: Screenshot of the GUI

When the GUI is first opened, the user will immediately be presented with the *Connect Tab*. This tab combines all the functions required for conveniently establishing and managing a serial connection to the appliance via the USB

port. Before connecting the appliance, the appropriate COM port has to be entered manually. The default serial communication speed is already set to correspond to that of the appliance at 115200 kbps. By pressing the *Connect* button, the serial connection is initialized and a confirmation sent by the appliance software is displayed on the GUI. Once a reliable connection has been established, commands can be sent and appliance data read from the CPU board using the functions on the other tabs.

The *Monitor Tab* allows the user to monitor the effector positions and forces in real-time as well as other important orthodontic parameters. A *Run* button is used to start the data acquisition and display the acquired information in real-time. Four sliders are used to provide a clear graphical representation of the two effector positions and the force applied to each of the effectors. Additionally, the numerical values of said parameters are displayed to provide more accurate readouts. The force and sensor information is used to calculate further parameters significant to orthodontic stimuli and movement. The bracket angle in degrees, moment magnitude in Nmm and the moment-force ratio MF can be read from the *Monitor Tab*. Two additional buttons allow open-loop stepwise position control of the effectors. Continuous controlled movements and case characterisation is achieved using the functions in the *Characterise/Move Tab*.

The *Characterise/Move Tab* comprises functions which are used to apply a stimulus to a tooth and record the resulting relative displacement, or to move a tooth by a prescribed distance and angle. The stimulus for the case characterisation is applied to a tooth by pressing either a *Sweep Up* or *Sweep Down* button. The sweep command directs the effectors to perform a continuous motion in the prescribed direction until the mechanical resistance causes the Squiggle motors to stall. This function is typically used in conjunction with the *Record* function in the *Characterise/Move Tab*, which measures both the effector positions and forces and saves these to an external file on the computer hard drive. Recording such data for repeated sweep motions allows the relationship discussed in Chapter 3 between the bracket force and the resulting tooth movement to be established.

Additionally, the *Characterise/Move Tab* features a *Move* function, which allows controlled, closed-loop movement of a tooth over a certain time. The *Move* option requires the user to enter the displacement and the angle by which a tooth is to be moved, as well as the time over which this movement should take place. Of importance is that the parameters entered by the user represent displacements relative to the starting position and do not allow for absolute position control. The starting position relative to which movement should occur is set using the *Developer Tab*.

The *Developer Tab* allows calibration of the effector positions and force. Because the appliance is designed to control relative displacements only, the effector positions need to be set to zero before each movement. The forces can also be zeroed using the *Developer Tab*.

Finally, the *Review Tab* allows the user to analyse, superimpose and compare independently recorded data sets by constructing three different types of graphs. The first type plots the individual as well as the average effector position vs. time. The latter is important as this is representative of the orthodontic bracket position. The second option constructs a force vs. time graph for the selected data set. Again, both individual effector forces and the combined force are plotted. The third option allows the force vs. displacement relationship to be plotted. As discussed in Chapter 3 this relationship is important as it could be used in determining case specific parameters. Acquired data will be discussed in more detail in Chapter 5.

4.3.3 Appliance software

The Arduino IDE was used for programming the appliance software. Using the Arduino environment allowed for software development and testing on a Arduino UNO board prior to adapting it to the application specific CPU board. Thus, a large part of the software could already be written before completion of the electronic design and manufacturing.

Because the appliance software uses the Arduino programming language, it requires specific firmware to be uploaded to the ATmega328P microprocessor. This firmware, also referred to as a 'bootloader', is programmed to the microprocessor using the procedure and hardware described in Appendix D. Once the bootloader has been written to the ATmega328P, the appliance software can be written to the microprocessor using the serial interface of the adaptor board. When executed by the ATmega328P the software follows the process flow diagram in Figure 4.12, which will be elaborated on in the following paragraphs.

The initialization process starts as soon as power is provided to the CPU board. Variables are declared and corresponding pins are set to output mode to drive the two status LEDs on the CPU board. Thereafter, parameters for the I2C communication protocol are set which enables control of the sensor board, and if available, the serial port to the computer is opened. Position and force variables are restored to pre-shutdown values by reading these from the internal EEPROM memory. Subsequently, the NSE-5310 and AS5510 encoders are initialized using the I2C lines and the NSD-2101 motor drivers are calibrated. After completion, a message is sent to the GUI to confirm successful initialization and the program enters the main function.

The main function is a recurring function from which other functions are called to perform specified tasks. During its routine the main function calls three other functions, namely the *Heartbeat* function, the *Serial* function and the *Mode* function.

Firstly, the *Heartbeat* function provides a means for providing reliable feedback to the user on the status of the CPU board. This function causes a blue LED to flash at one second intervals, which indicates that the software is run-

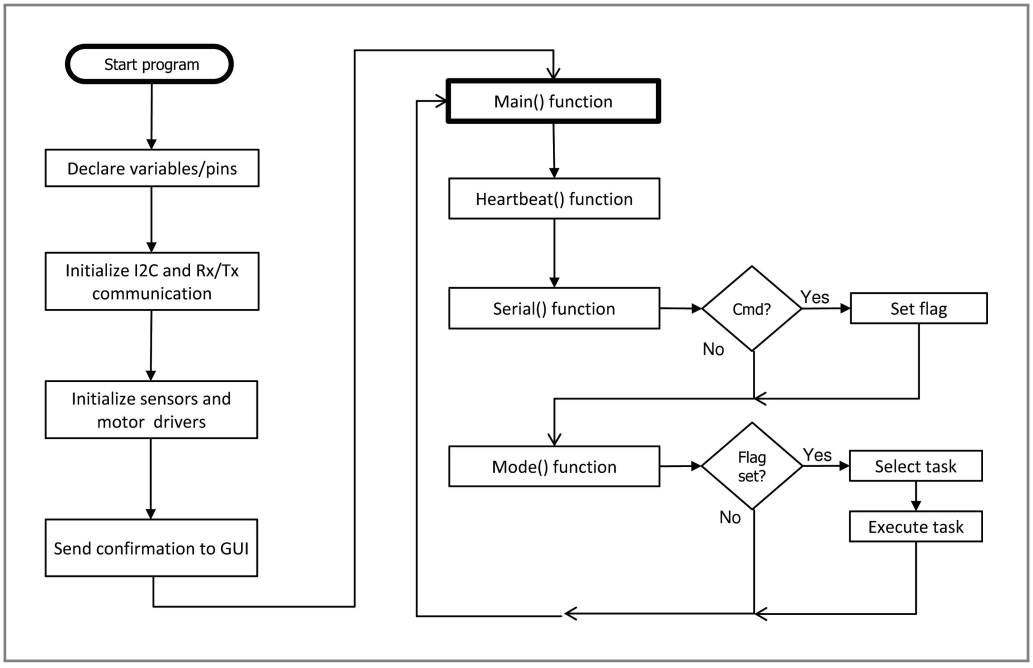

Figure 4.12: Functional flow diagram of appliance software

ning correctly and the main function is being executed repeatedly. In other words, if the green LED is illuminated indicating power is being supplied to the board, but the blue LED does not flash as described, this indicates an incomplete execution of the *Main* function or faulty software.

Secondly, the *Serial* function tests the availability of data on the serial port and reads such data. If the *Serial* function confirms that data is indeed available on the Rx line, the single first byte is read and treated as a *command* byte for further instructions. It specifies whether further bytes should be read from the serial port, how this data should be managed and what specific function should be performed. Depending on the *command* byte, the *mode* flag is also set for single-execution or repeated functions called by the *Mode* function.

Thirdly, the *Mode* function evaluates the *mode* flag and based on its value calls smaller functions to perform specific tasks. In comparison to the *Serial* function, this function has the advantage that it allows tasks to be performed repeatedly until the flag is reset, without the need for a command being sent from the GUI. The user can, for example, choose to view the appliance data in real-time from the GUI. To activate this feature, the user presses the *Run* button on the GUI, which sends a command to the CPU board via the serial port. The mode flag is set to *Run* causing the position and force sensors to be read every 20 ms. The acquired measurements are sent back to the serial port and are displayed on the GUI until the user presses the *Stop* button. After the *Main* function has been executed, the program returns to the beginning and the described process is repeated as illustrated in Figure 4.12.

Chapter 5

Testing and results

The following chapter provides information pertaining to the appliance evaluation and test procedures as per Objective 6. In the first section a brief overview of the experimental procedure is provided. Thereafter, the appliance functionality is evaluated and specific properties are investigated in more detail. Following the appliance evaluation, three experiments are described which were used to test the electromechanical orthodontic appliance with regard to the hypothesis put forth in Chapter 3.

5.1 Overview

Several tests were done to examine appliance functionality with regard to the design specifications set forth in Chapter 3. The measurement accuracy of the position sensors was evaluated using the supplier specifications for the individual components. Both types of FTS were tested using additional measurement instruments. The linearity of both systems was also evaluated and the hysteresis error of the force sensors further examined.

Following appliance testing, three independent experiments were conducted to further test the orthodontic appliance with regard to the hypothesis developed in Chapter 3. Firstly, the force vs. displacement curve was obtained for various dental models to test the case characterisation ability of the orthodontic appliance. Secondly, the ability to produce controlled movement of an orthodontic bracket was examined by specifying the displacement and tipping angle and tracking the effector positions throughout the movement. Lastly, the ability of applying advanced mechanical stimuli which include an oscillatory component was investigated. A sinusoidal position input was provided to the appliance and the output recorded to obtain the frequency response characteristics.

5.2 Appliance testing

5.2.1 Position sensor

The position sensor performance was evaluated according to the technical specifications provided by the supplier. Due to the high resolution offered by the NSE-5310 encoder, no external system with a higher resolution could be sourced to confirm the encoder reading. As such, the resulting accuracy is based on the technical specifications. The accuracy of the position sensor depends both on the NSE-5310 linear position encoder as well as the multi-pole magnetic strip, which is mounted on the effector. The technical specifications provided by the magnet and encoder supplier are summarised in Table 5.1 below.

Table 5.1: Position sensor specifications

Parameter	Min.	Typ.	Max.	Unit
Magnet specifications				
Pole length		1		mm
Pole length deviation		1	12	µm
Magnetic field amplitude at 0.8 mm	10			mT
Amplitude variation			0.2	mT
Encoder specifications				
Resolution		0.488		µm
INL_{opt}			±5.6	µm
INL_{worst}			±35.6	µm

The sensor accuracy is limited largely by imperfections of the magnetic strip while linearity errors of the encoder are small. The optimal non-linearity (INL) for an ideal magnet is only 5.6 µm while this value increases to 35.6 µm if the errors from the magnetic source are considered. The supplier specifications indicate that inaccuracies resulting from varying temperatures are practically negligible for the operating conditions of the orthodontic appliance. The inaccuracy over a 2 mm magnetic pole pair is thus less than 35.6 µm.

Inaccuracies of the mechanical system could potentially also affect the position sensor. Even though the NSE-5310 position encoder has several features such as an auto-gain function to correct for a varying magnetic field strength, the extent to which these are effective is not measurable. It is therefore possible that the movement of the effector relative to the position encoder over the entire operating range of 5 mm could affect the position measurement.

The effect of the mentioned inaccuracies is limited, however, by the fact that relative displacements are measured rather than the absolute position.

Before each experiment, the appliance sensors are calibrated so that only a relative displacement from the initial position is sensed. The high resolution of 0.488 µm thus allows for an accurate reading of small displacements, while the encoder non-linearity and magnetic errors only become apparent for larger displacements. All experiments conducted during this study involved relative movements below 1 mm. To summarise these results, the resolution of the position encoder is 0.488 µm and the inaccuracy within 1 mm of the initial position is less than one half of INL_{worst} or 17.8 µm.

5.2.2 Force transducer system

Both the NiTi and steel wire FTS were evaluated using a Precisa 40SM-200A balance (Dietikon, Switzerland). The Precisa balance has a range of 200 g and a sensitivity of 0.1 mg, which made it ideal for evaluating the two force transducers. During the tests, the appliance assembly was attached to a semi-rigid structure and positioned above the balance so that the effectors pressed down onto the balance when extended. Each effector was tested individually by gradually increasing the force applied to the balance. During this process, the encoder reading on the GUI and the force indicated on the balance in grams were recorded. The results were used to evaluate the effector force as a function of the encoder reading as described by Equation 4.7.

A limitation of this test procedure is that the force transducers were only tested for a compressive force being applied by the effector and not for the application of a tensile force. Also, measurements were only recorded during the force application and not its removal. The reasons therefore were primarily to eliminate the effects of hysteresis and friction, which were dealt with in a separate experiment.

Figure 5.1 presents the results for the NiTi and steel wire force transducer tests. Two straight lines were fitted to the raw data according to the linear relationship given by Equation 4.5. The gradient of the straight line was determined using a linear least-squares method with an equality constraint at the origin. The dotted line represents the design value for the FTS as specified by Equation 4.5 in Chapter 4. As mentioned, this value was used only during the design of the FTS, and the deviation of the design value from the experimental values does not affect the FTS accuracy.

The results for the NiTi FTS show that a linear relationship can be used to approximate the effector force for small forces, but that this relationship becomes increasingly non-linear for forces exceeding 40 cN. This non-linearity is likely accounted for by the uncertainties regarding material properties and exact wire geometries listed in Chapter 4. A further factor to potentially cause the observable non-linearity is varying amounts of friction. The wire deflection would result in a small moment applied to the stator, which could ultimately increase the normal forces on touching surfaces and thereby increase the measured friction force such as that seen in Figure 5.1.

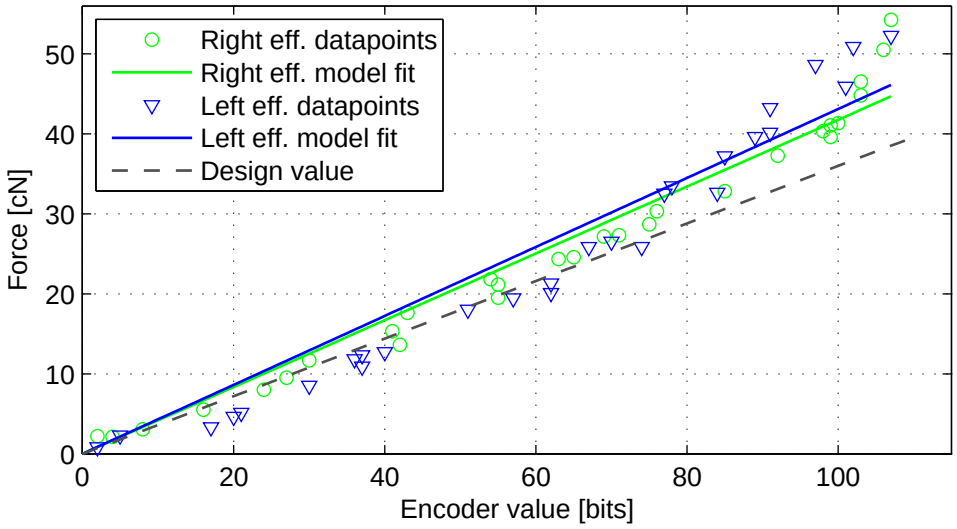

(a) NiTi wire force transducer

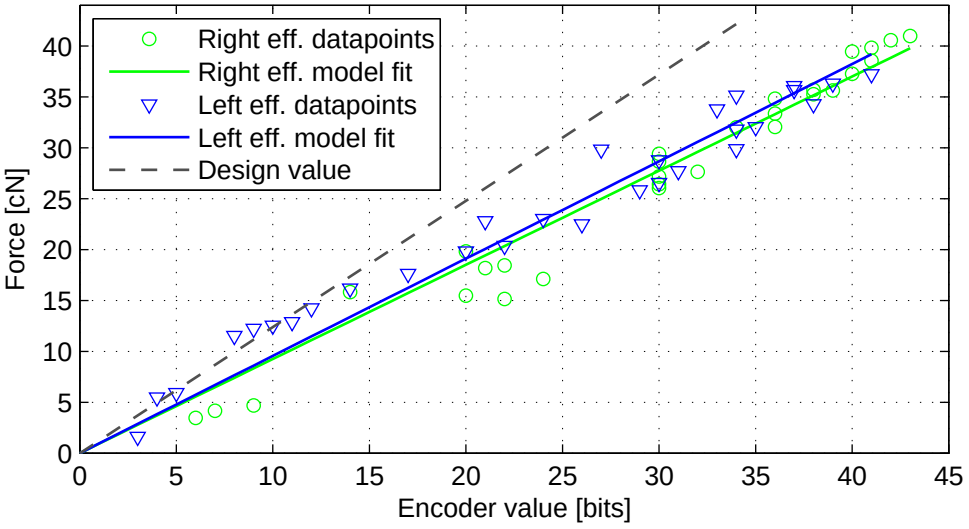

(b) Steel wire force transducer

Figure 5.1: Force transducer test results

In comparison, the results obtained for the steel wire FTS by the same procedure indicate a constant linear relationship throughout the positive force range. As expected, the gradient is increased due to a higher Young's Modulus than that of the NiTi, but the same force range can be measured using this FTS.

An average value of k was calculated from the measurements and used to calibrate the FTS. To restate, k combines the constant mechanical system parameters and is defined by

$$k = \frac{24EI}{\alpha_M S_F \mathrm{L}^3} \tag{5.1}$$

The variance of the design value and that calculated from the experimental results is likely to result from inaccuracies in the theoretical design variables and as such, the measured results were used to calibrate the transducers. The good correlation between the experimental results for the left and right effector allowed an average value of k to be calculated for each type of transducer.

To evaluate the variance of the data points from the fitted value, the standard deviation was calculated by

$$SD = \sqrt{\frac{1}{N}\sum (x_i - \mu)^2} \tag{5.2}$$

where N is the number of data points, x_i is the observed position and μ is the fitted average value. It should be noted that the calculated standard deviation is not representative of the overall accuracy of the FTS over the entire measurement range, but only for the measurements taken during the FTS evaluation.

Finally, for the NiTi FTS the calibration constant was found to be $k_{NiTi} = 0.424\,\mathrm{cN/bit}$ with a SD of 3.51 and thus the output of the NiTi FTS is

$$F(O_{NiTi}) = 0.424 O_{NiTi} \tag{5.3}$$

For the steel wire FTS the corresponding values are $k_{Steel} = 0.94\,\mathrm{cN/bit}$ with a SD of 2.00 and thus the force output is

$$F(O_{Steel}) = 0.94 O_{Steel} \tag{5.4}$$

The results indicate that the steel FTS is less susceptible to material uncertainties and linearity errors but that a better resolution is obtained with the NiTi FTS. Hence, both FTS will be used and their results compared.

5.2.3 Hysteresis analysis

Both types of FTS were found to exhibit some hysteresis, which was further analysed in the following experiment on the steel wire FTS. The steel wire FTS was mounted as in the previous test, so that the effector pressed down on the Precisa 40SM-200A. In this case the FTS output and the true force on the Precisa 40SM-200A were measured during repeated cycles of increasing and decreasing force strokes. The data was separated into forward stroke and reverse stroke and a straight line fitted to each of the resulting datasets as shown in Figure 5.2. The difference in the FTS force between the forward and

the backward stroke, indicated by H on the graph, represents the hysteresis. The hysteresis error for the right effector varies between 7 cN and 19 cN with an average of approximately 13 cN, whereas that of the left effector stays constant throughout the stroke at approximately 12 cN.

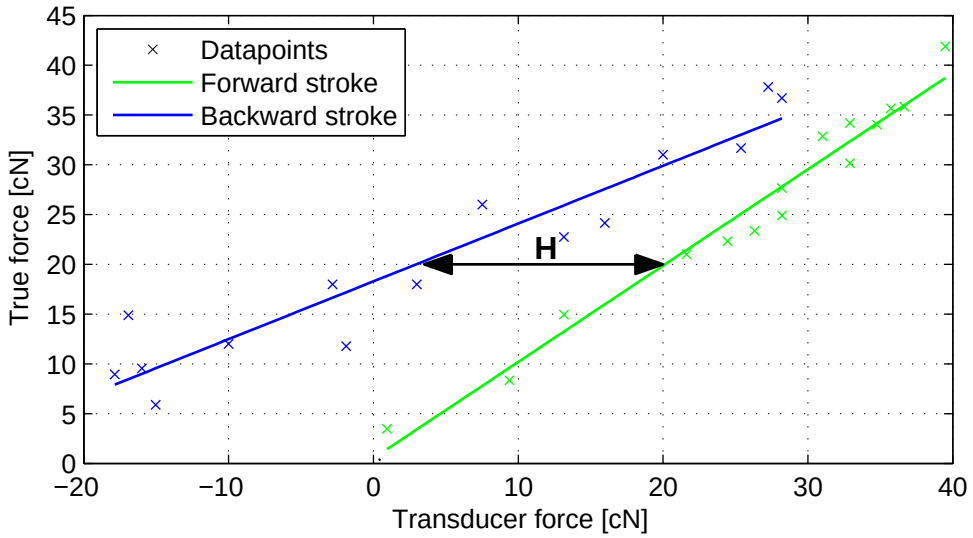

(a) Hysteresis measurement for right effector

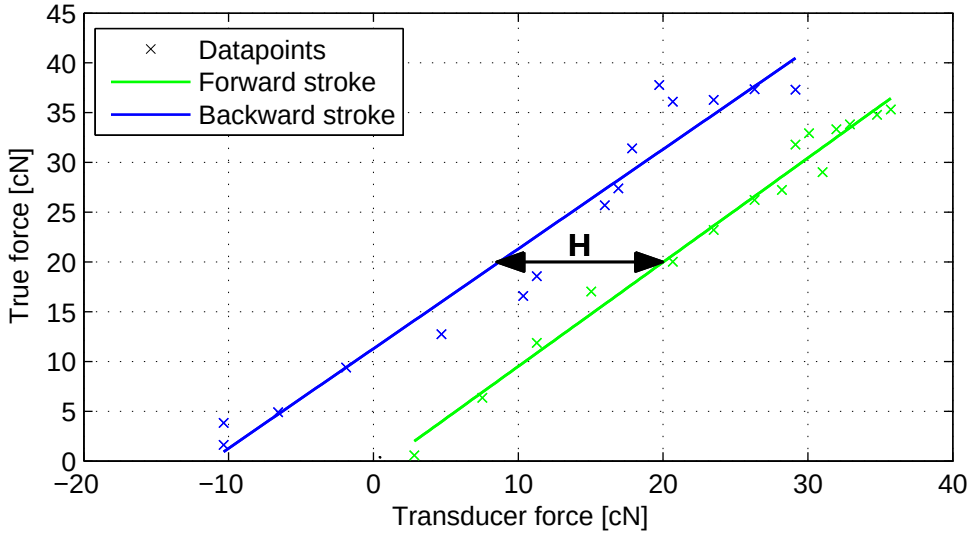

(b) Hysteresis measurement for left effector

Figure 5.2: Hysteresis analysis

The hysteresis error as measured by the described test was identified as one of the major shortcomings of the orthodontic appliance. Mechanical components were examined under a microscope to provide insight into the factors

potentially affecting their movement. A detailed examination which is documented in Appendix B, showed a rough surface finish on the effectors and a low tolerance on the manually machined dental interfacing features. In combination, these factors are believed to be responsible for backlash and the observable hysteresis. Because no improvement could be made to the mechanical system, it was decided that the hysteresis error should be compensated for during the data processing procedure.

5.3 Experiment 1: Case characterisation

5.3.1 Experimental objective

This experiment investigated the effectiveness of the electromechanical orthodontic appliance in determining case specific parameters. More specifically, an attempt was made to characterise orthodontic cases according to the relationship between the force magnitude and the immediate coronal tooth displacement, as described by the hypothesis developed in Chapter 3. This was done by applying a force to, and measuring the displacement of a tooth, which formed part of the dental models described in the following section. A direct comparison of the curves for each of the orthodontic cases was made.

5.3.2 Model manufacturing and verification

Case characterisation experiments were conducted on custom made dental models, as the appliance was not suitable for in-vivo testing. None of the commercially available models were found to include an accurate replica of the PDL, which was essential for the case characterization experiments. As such, custom made dental models were designed, manufactured and analysed. The models comprised a replica of the tooth, the alveolus and the PDL.

The dental models were manufactured using multiple moulds. First a rubber mould was made from an anatomically correct replica of a tooth. Using the mould, three identical models of the tooth were produced using acrylic (poly methyl methacrylate). The replica were then covered in a wax layer with approximately the same thickness as the desired PDL, which acted as a temporary space-holder. The alveolar replica was then built up around the wax layer using acrylic. Once the acrylic had cured, the tooth was extracted from the alveolar model and the was layer was removed. Upon re-insertion a space was left between the tooth and the alveolar wall, with a width equivalent to that of the wax layer and ultimately the PDL thickness.

To construct the PDL, the jig shown in Figure 5.3(a) was built to position the tooth relative to the alveolar model. The space between the alveolar wall and the root of the tooth was then filled with black Dragon Skin 10 silicon (Smooth-On, Easton, Pennsylvania, USA). Finally, the jig was discarded leav-

ing the final model shown in Figure 5.3(b). The final model comprises the acrylic tooth (pink), the alveolus (clear) and the soft silicon PDL (black).

Additionally, a frame was built on which the different dental models could repeatedly be mounted in the same configuration for the case characterisation experiments. Figure 5.4(a) shows the molar and premolar model mounted on the frame, without the appliance, while Figure 5.4(b) shows the appliance connected to the teeth. Further details regarding the experimental set-up are provided in Section 5.3.3.

(a) Moulding jig used for PDL construction

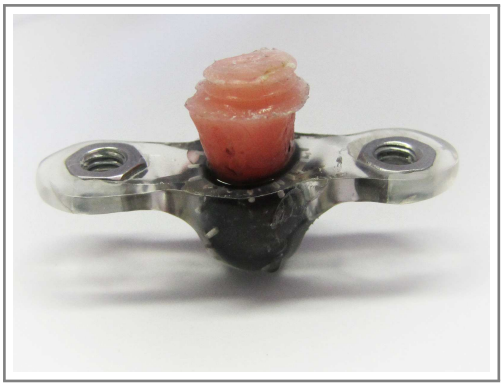

(b) Completed model comprising the tooth (pink), the alveolus (translucent) and the PDL (black)

Figure 5.3: Manufacturing of dental models

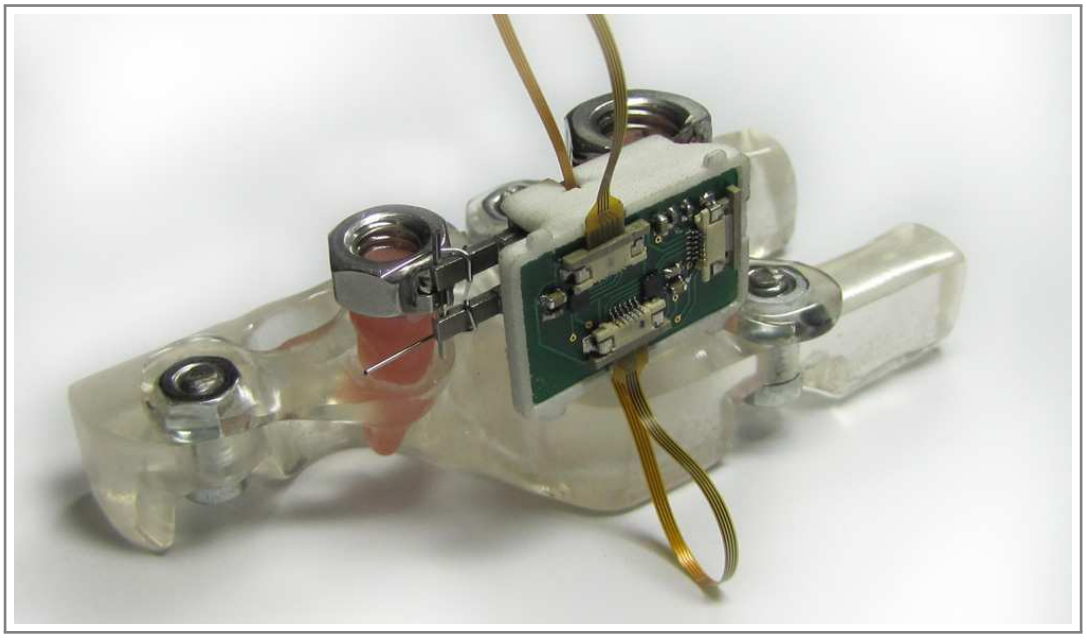

Figure 5.4: Appliance mounted to dental models

In order to verify model parameters, micro-focus X-ray Computed Tomography (CT) scans were done to analyse the dental models. The instrument used was a VTomeX L240 CT scanner (General Electric, Fairfield, Connecticut, USA) and scans were done at 60 kV, 240 µA, 500 ms exposure per image and 1500 images in a rotation, which resulted in a 14 µm resolution. Virtual 3-D CAD models, such as that in Figure 5.5, were constructed from the data offering an excellent means for analysing the dental models. VG Explorer Integration software (Volume Graphics GmbH, Heidelberg, Germany) was used to distinguish between materials of different densities and thus proved useful in analysing the silicon PDL between the two acrylic elements.

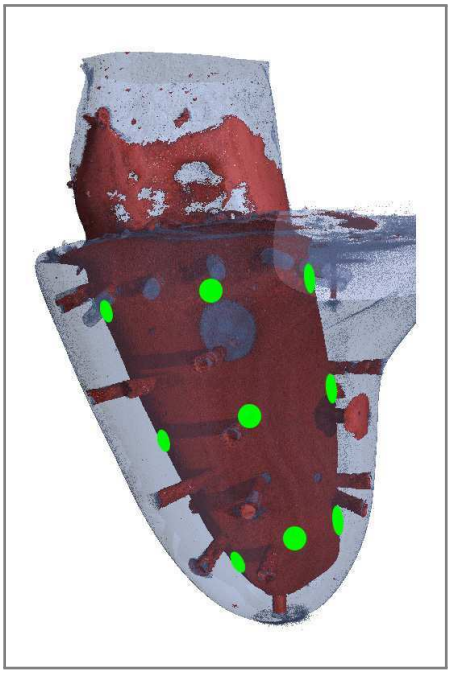

Figure 5.5: Virtual 3-D representation of premolar model

Scans were conducted for the one molar model and the two premolar models which include a PDL. Thereafter, virtual 3-D models were constructed to examine the PDL thickness and compare it with the desired values. A total of twelve individual measurements of the PDL thickness were taken at different locations on the root of the tooth, of which nine are illustrated in Figure 5.5. The measurement results provided in Table 5.2 show that the average thickness is close to the desired value, but that significant variations in localised PDL thickness are present.

This result is important because the tooth movement is governed by the minimal PDL thickness rather than the average value. The premolar model for example shows a decreased PDL thickness in the apical region with a minimum value of 0.091 mm. The thinned area is likely to limit the apical displacement

causing the centre of resistance $CRes$ to be shifted toward the apex. Further analyses were done to identify such possible changes in dynamic behaviour due to a non-uniform PDL thickness.

Table 5.2: Average PDL thickness of dental models

Model 1: Molar 0.2 mm PDL					
	PDL thickness [mm]				
Location	**Lingual**	**Mesial**	**Labial**	**Distal**	**Average**
Alveolar crest	0.283	0.438	0.164	0.392	0.319
Center	0.273	0.435	0.098	0.217	0.256
Apex	0.391	0.198	0.106	0.331	0.257
					0.277

Model 2: Premolar 0.2 mm PDL					
	PDL thickness [mm]				
Location	**Lingual**	**Mesial**	**Labial**	**Distal**	**Average**
Alveolar crest	0.215	0.131	0.226	0.304	0.219
Center	0.239	0.379	0.331	0.348	0.324
Apex	0.091	0.341	0.104	0.117	0.163
					0.236

Model 3: Premolar 0.5 mm PDL					
	PDL thickness [mm]				
Location	**Lingual**	**Mesial**	**Labial**	**Distal**	**Average**
Alveolar crest	0.340	0.789	0.587	0.809	0.631
Center	0.289	0.810	0.420	0.817	0.584
Apex	0.332	0.707	0.193	0.654	0.472
					0.562

To characterize the expected coronal tooth movement upon application of a mesio-distal force, the virtual 3-D models were used to identify areas of minimum PDL thickness. Figure 5.6 shows two views of the virtual premolar model in which the variations in PDL thickness can clearly be seen and localised areas of minimum thickness are indicated by circles. Further images as well as a more detailed discussion on the outcomes of the model analysis using CT scans is provided in Appendix F. Images of the other virtual models are presented and areas of localised PDL thinning are highlighted. Technical details on the CT scans are also provided in the appendix.

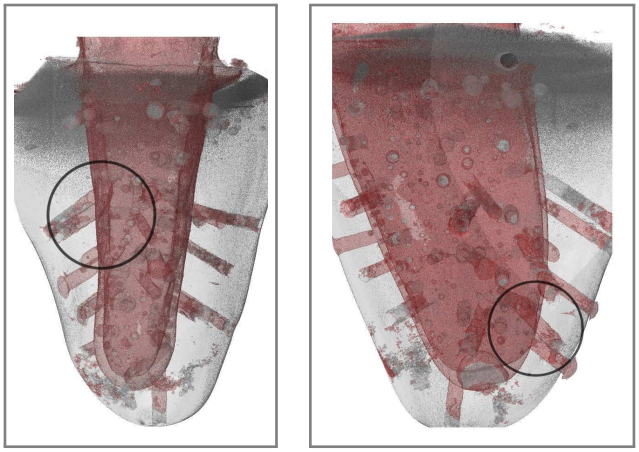

(a) Labial view (b) Mesial view

Figure 5.6: Localised thinning of the 0.2 mm PDL of the premolar model

In an attempt to formulate the expected movement constraints of the tooth, areas of PDL thickness below 0.05 mm were identified on each of the models. Observations and outcomes of this analysis are summarised by the following statements:

- **Molar with 0.2 mm PDL**
  The molar model features a thinning of the PDL along the linguo-distal surface of the root from the alveolar crest to the centre of the root. The labial surface of the mesial part of the root also shows a PDL thickness below 0.05 mm. The thinning of the PDL close to the alveolar crest could shift the CRes upward and restrict coronal movement. Because both these areas are fairly large and lie on opposite sides of the molar root, it is expected that the possible mesio-distal movement will be limited.

- **Premolar with 0.2 mm PDL**
  The premolar model shows a minimum PDL thickness on the lingual surface of the root apex. Because this point is toward the lingual side of the root, it is not expected to significantly affect the mesio-distal movement. A larger area featuring a PDL thickness below 0.05 mm is found along the distal surface in the middle portion of the root. It is considered large enough to potentially limit the mesio-distal displacement of the tooth.

- **Premolar with 0.5 mm PDL**
  The 0.5 mm PDL premolar model shows a relatively uniform PDL thickness with a single point of reduced thickness at the root apex. At this point the PDL thickness is below 0.05 mm toward the labial and mesial directions. Although the thinning of the PDL at this location might shift the CRes downward slightly, it is not expected to significantly affect the mesio-distal movement.

5.3.3 Experimental procedure

The appliance was mounted between two orthodontic brackets attached to the molar and premolar models as shown in Figure 5.4. The appliance base was fixed to the vertical slot bracket on the molar using elastic ligatures. Thereafter, the two effectors were connected to the premolar using the Speed bracket system. The sweep function was then used to repeatedly apply alternating force cycles ranging from −100 cN to +100 cN to the premolar, while recording the relative displacement between the molar and the premolar. A positive relative displacement thus represents a mesial movement of the premolar crown and a distal movement of the molar crown, while a negative value represents distal premolar and mesial molar movement.

A basic closed-loop proportional control function implemented on the CPU board was used to apply the same force magnitude with each of the effectors, thereby minimizing the moment-force ratio applied at the bracket. The purpose thereof was to apply a single force vector, without a rotational component, and measure the resulting coronal tooth displacement resulting from pure tipping. During this process, the record function was used to record the time, the effector forces and the effector positions.

Table 5.3: Case characterisation experiments

Experiment	Molar PDL thickness [mm]	Premolar PDL thickness [mm]	FTS type
RR_{NiTi}[a]	0	0	NiTi
RM_{NiTi}[b]	0	0.2	NiTi
RT_{NiTi}[c]	0	0.5	NiTi
MR_{NiTi}	0.2	0	NiTi
MM_{NiTi}	0.2	0.2	NiTi
MT_{NiTi}	0.2	0.5	NiTi
RR_{Steel}	0	0	Steel
RM_{Steel}	0	0.2	Steel
RT_{Steel}	0	0.5	Steel
MR_{Steel}	0.2	0	Steel
MM_{Steel}	0.2	0.2	Steel
MT_{Steel}	0.2	0.5	Steel

[a] R - rigid, no PDL
[b] M - medium, 0.2 mm PDL
[c] T - thick, 0.5 mm PDL

To evaluate appliance functionality twelve experiments listed in Table 5.3 were conducted. Two different molar models, each in combination with the

three different premolar models were characterised by both FTSs. The designation used for the experiments consists of one letter which refers to the thickness of the molar model, while a second letter indicates the premolar thickness. The three abbreviations used are R which indicates a PDL thickness of 0 mm or rather a rigid connection between the tooth and the alveolus, M which indicates a medium PDL thickness or 0.2 mm PDL, and T which indicates a thick PDL of 0.5 mm. An experiment which tests a molar with a medium PDL in conjunction with a premolar with a rigid connection will thus have designation $MR_{FTStype}$.

5.3.4 Data processing

Raw data measurements for the force vs. displacement relationship exhibited significant hysteresis and data processing in Matlab (Mathworks, Natick, Massachusetts, USA) was necessary. The processing was done primarily to enable a direct comparison between the measurements for various orthodontic cases. This is vital to evaluate the ability of the appliance to distinguish between these various cases.

Firstly, the acquired data shown as grey points in Figure 5.7, was split into two sets corresponding to the forward and backward sweep movement. A spline was then fitted to each of the data sets as shown by the red and blue dotted lines in Figure 5.7. The splines corresponding to the forward and backward sweep were then used to calculate the average force measured at each specific displacement. Further details on the data processing procedure are presented in Appendix G.

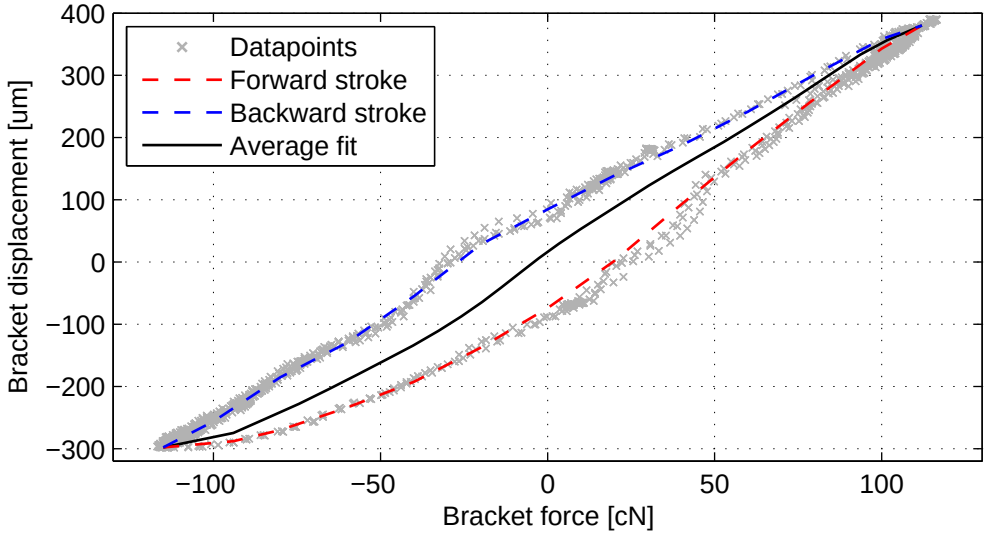

Figure 5.7: Data processing procedure

To allow a direct comparison of the different orthodontic cases by superimposing the fitted splines, calibration errors were corrected by centring the results about the origin.

The same data processing procedure was applied to all further case characterisation experiments. Using the same procedure allowed for a direct comparison of the curves for each orthodontic case. The following section presents the outcomes for all of the experiments listed in Table 5.3.

5.3.5 Results

As mentioned, six experiments were conducted with the NiTi FTS and the same six experiments were repeated with the steel wire FTS. All experiments were conducted on the same models. The results for the NiTi FTS and the steel wire FTS are provided in Figures 5.8 and 5.9 respectively. The results are further discussed with reference to the expected tooth movement as defined by the dental model analysis. Lastly, limitations of the presented results are mentioned.

The results obtained using the FTS clearly show that a distinction can be made between different orthodontic cases. Considering Figure 5.8(a), the relative displacement is shown to increase for a thicker PDL. The largest distalization of 350 µm was measured for the RT case, while a negative force of equal magnitude caused a relative displacement of approximately -300 µm.

The force vs. displacement curves for a molar model with a 0.2 mm PDL and varying premolar PDL are shown in Figure 5.8(b). A larger relative movement was observed for all three cases, when comparing these to the cases for which a rigid molar alveolus was used.

Comparable results, which are presented in Figure 5.9 were obtained using the steel wire FTS. Again, it can be seen that the appliance was able to characterise each of the cases according to the force vs. displacement curve. As expected, a larger bracket displacement was observed for the dental models featuring a thicker PDL. This observation also holds when comparing Figure 5.9(a) and Figure 5.9(b), which shows that the molar PDL also leads to an increase of the relative bracket displacement for the same forces.

In the previous section the dental models were analysed using CT scans and the expected movement constraints were formulated for each of the three dental models featuring a PDL. The 0.2 mm molar PDL as well as the 0.2 mm premolar PDL showed significant thinning of the PDL which was expected to limit the mesio-distal movement. In comparison, the thickness of the 0.5 mm premolar PDL was below 0.05 mm only at the root apex and the movement of the premolar housed within the thick PDL was thus expected to be greatest. As will be explained, the experimental results were able to confirm these predictions.

When considering Figures 5.8 and 5.9, the gradient of the RT and MT curves is significantly larger, while the RM and MM curves show only a

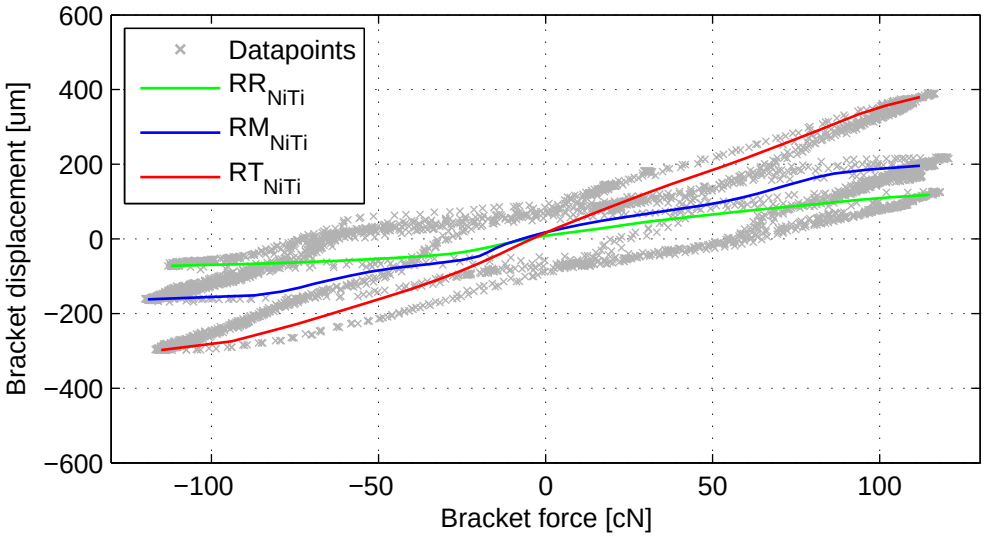

(a) Rigid molar alveolus with variable premolar PDL

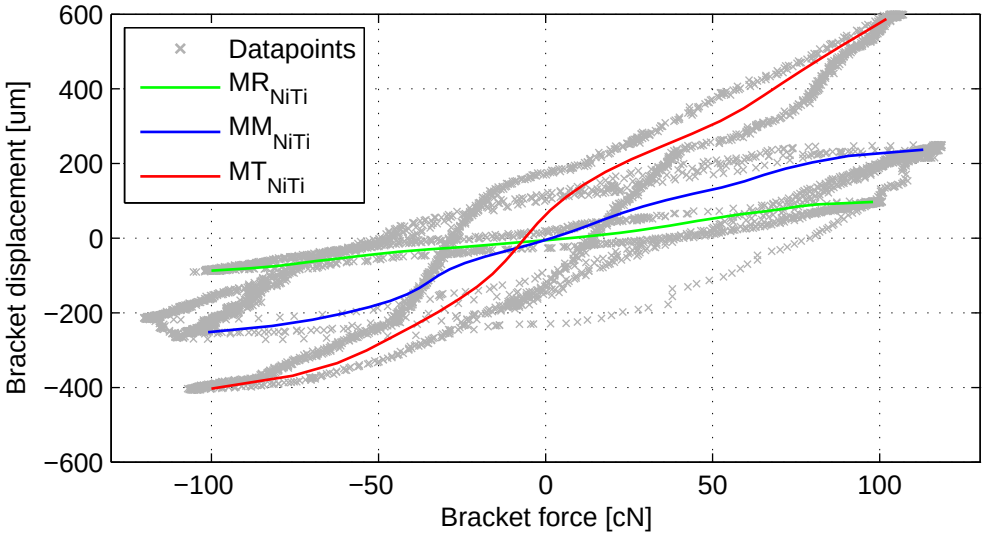

(b) Molar PDL of 0.2 mm with variable premolar PDL

Figure 5.8: Case characterisation using NiTi FTS

slight increase from the cases in which a force was applied to the rigid premolar. This indicates that the compression of the thick premolar PDL allowed a larger relative displacement of the tooth. The thinning of the 0.2 mm PDL in comparison limited the premolar displacement.

Similarly, when comparing Figure 5.8(a) to 5.8(b) and Figure 5.9(a) to 5.9(b), the effect of the molar PDL is observable. Even though the relative displacement did increase due to the molar PDL in each case, this increase was small in comparison to the movement facilitated by the thick premolar PDL.

To critically evaluate the presented results, certain limitations of the ac-

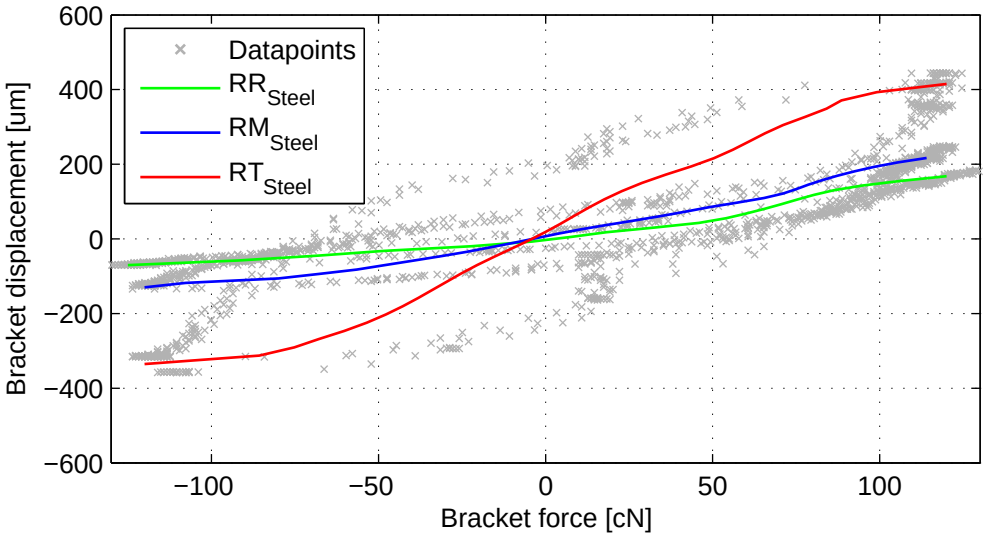

(a) Rigid molar alveolus with variable premolar PDL

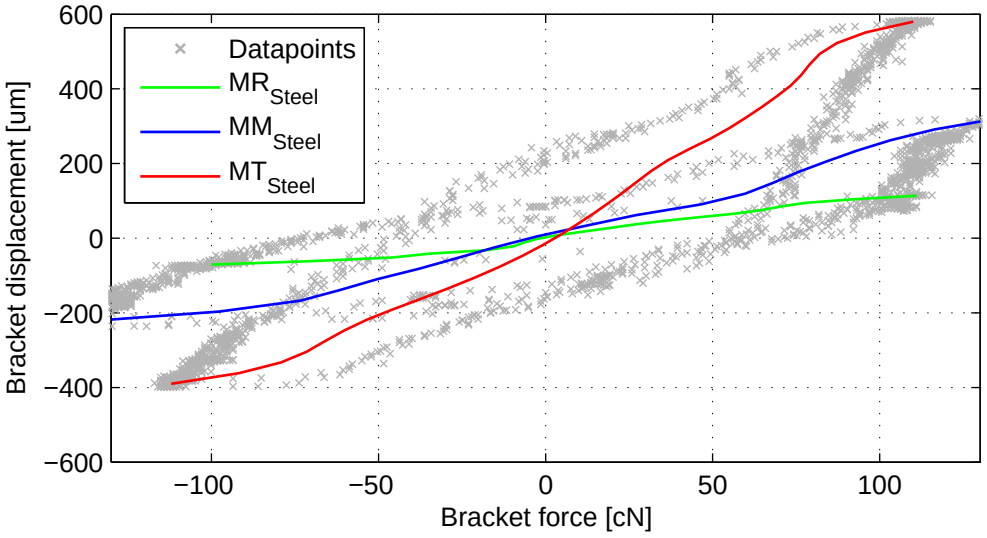

(b) Molar PDL of 0.2 mm with variable premolar PDL

Figure 5.9: Case characterisation using steel FTS

quired data need to be addressed. Firstly, it is evident that a relative displacement of approximately 100 µm was observable in the *RR* cases. Because, the acrylic teeth and alveolus are considered rigid, practically no displacement should be measurable when using an ideal system. The observed relative movement can thus not result from the compression of the PDL, but must be accounted for by other possible sources such as inaccuracies of the mechanical interfacing features. The wire inserted into the Speed bracket, for example, is not perfectly rigid and would thus likely contribute to the displacement such as that measured for the *RR* cases.

Some of the measured curves also show inconsistencies when compared to the remaining data sets. The MT_{NiTi} case, for example, reveals a displacement step at the origin, which is not present in any of the other results. Such relatively large movements due to a small change in the applied force could possibly be accounted for by the wire of the dental interface being able to move slightly within the slot of the Speed bracket.

Lastly, when considering the raw data, which is shown in grey in the Figures, some of the experiments are seen to exhibit considerably more hysteresis than others. As was previously mentioned, the hysteresis is thought to result from friction between the mechanical components. This effect is worsened if forces are exerted on the effectors, perpendicular to their line of action. Even though the experimental set-up was designed to minimize any such forces, it is likely that these do affect the hysteresis leading to the observable difference.

5.4 Experiment 2: Controlled tooth movement

5.4.1 Experimental objective

The controlled movement experiment aimed to evaluate the ability of the orthodontic appliance to move a tooth by a relative distance and angle over a certain period of time, under no load conditions. According to the system specifications both the tooth position and the tipping should be controllable. The following results present measurements for various types of specified movements including forward and reverse tipping.

5.4.2 Experimental procedure

The appliance was mounted between two orthodontic brackets, which were moved relative to one another. Unlike the previous experiment in which the brackets were fixed to dental models, the appliance was mounted on a flat surface. None the less, the same anatomical terms of reference which are indicated in Figure 5.10(a) are used for description purposes. The molar bracket was fixed to the surface, whereas the premolar bracket could be moved freely parallel to the surface as shown in Figure 5.10(b). The extension shown in red was attached to the premolar bracket for measurement purposes.

The desired relative movement was specified in the GUI as well as the time over which said movement was to be induced. Before the experiment, the position sensors were calibrated and the initial position was set as the reference position. Thereafter, the desired bracket translation in microns was specified as well as the desired tipping angle in degrees. Both values can be positive or negative. A positive value indicates a mesial translation or mesial tipping, while a negative value indicates a distal translation or tipping. The time over which the movement should be achieved was specified in seconds and

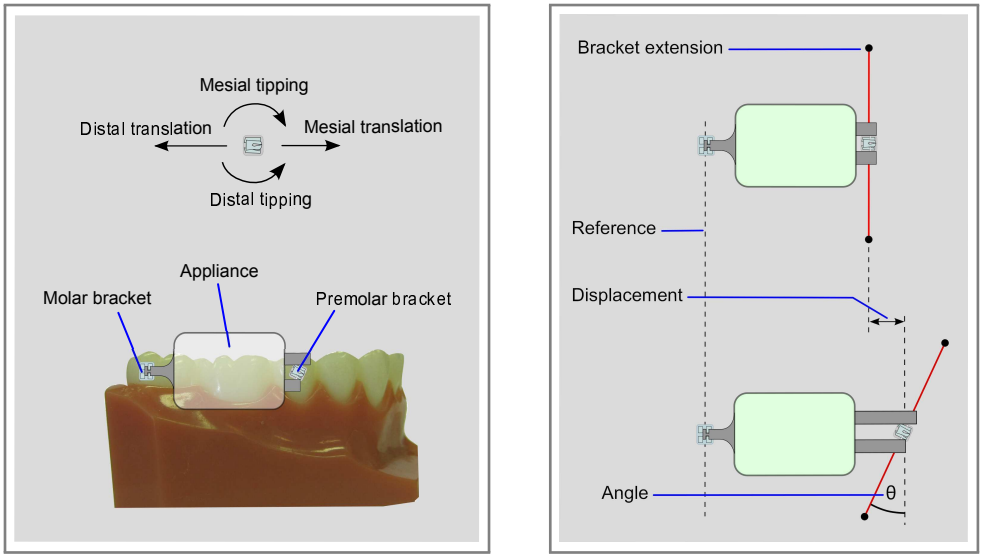

(a) Experiment reference (b) Measurement method

Figure 5.10: Controlled movement experimental set-up

only short times of less than three minutes were tested. The effector position was recorded over the duration of movement and plotted as a function of time. Results are presented in Figure 5.11 for which the graphs were plotted using Matlab.

Due to the extremely small bracket displacement, the appliance position sensor was used to measure the effector position and no secondary measurements of the bracket position were obtained. Even though measuring the bracket translation was problematic, it was possible to measure the relative bracket angle by attaching extensions to the orthodontic bracket to exaggerate the movement, as shown in Figure 5.10(b). Using vernier callipers, the displacement of the extension endpoints was measured and used to calculate the bracket angle. The extension length of 120 mm allowed a half a degree angle, for example, to be measured as a 1.05 mm translation. The results for this method are tabulated in Table 5.4.

Certain limitations of the current experimental set-up need mentioning. Firstly, the measurements obtained during this experiment represent the effector position and the actual bracket position could deviate slightly due to inaccuracies pertaining to the mechanical dental interface. As mentioned, this was manufactured by hand and it is thus likely that relative movement could occur between the bracket and the effectors. Secondly, the current experiments were conducted with no force being applied to the effectors. Applying a force to the premolar bracket would likely alter the response, increasing the time needed for a tooth to reach the desired position. However, given enough time, this would not affect the tracking ability of the appliance, which is to be examined. No data processing was required during this experiment.

5.4.3 Results

The results shown in Figure 5.11 correspond to the right and left effector positions over the duration of movement. Excellent correlation can be observed for the average effector position and the reference signal. The bracket angle is defined by the difference between the two effector positions.

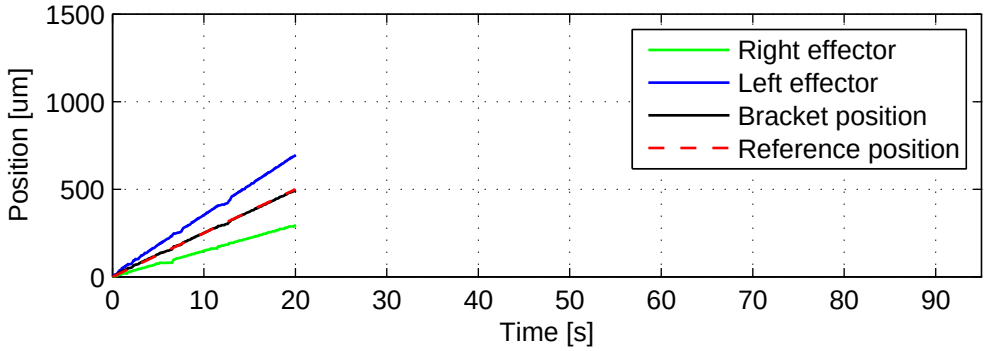

(a) Desired tooth movement: 500 µm mesially with 5° mesial tipping over 20 s

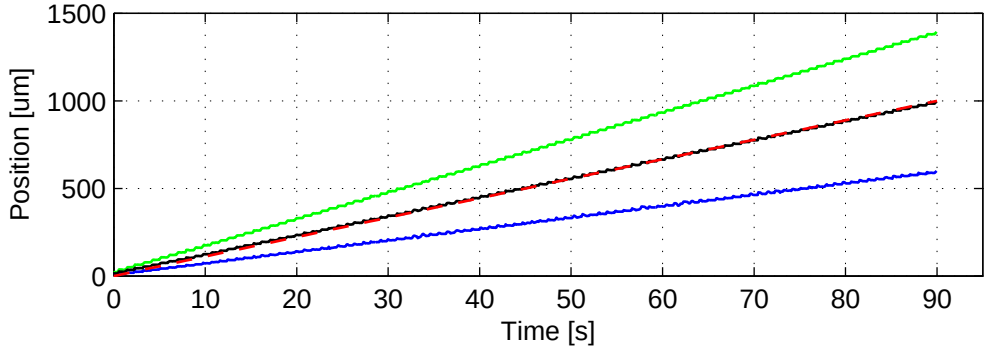

(b) Desired tooth movement: 1000 µm mesially with 10° distal tipping over 90 s

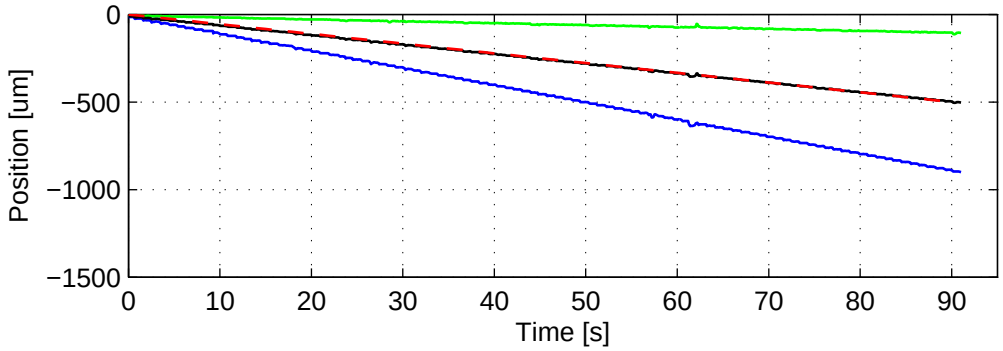

(c) Desired tooth movement: 500 µm distally with 10° distal tipping over 90 s

Figure 5.11: Controlled tooth movement results

The first graph provides the reference signal and effector positions for a 500 µm mesial translation and 5 ° mesial tipping over 20 s.

Figure 5.11(b) presents the results obtained for a 100 µm mesial translation combined with 10 ° distal tipping. Distal tipping was achieved by a larger movement of the right effector. The duration of movement was 90 s.

Lastly, Figure 5.11(c) presents the data recorded for a 500 µm distal premolar movement. The desired distal tipping was achieved by a larger retraction of the left effector and the duration of movement was once again 90 s.

To further examine the effect of the mechanical interfacing inaccuracies, various movements were specified and the final angular displacement of the bracket extension recorded. Table 5.4 lists the values for the reference angle θ_{ref}, the angle as calculated by the appliance sensors θ_{app} and the angle as measured from the bracket extension θ_{ext}. The error between the reference angle and the observed value was calculated in order to evaluate the movement accuracy.

The results in Table 5.4 show that the appliance is able to control the angle well for angles smaller than 10 °, but that deviations exist between the angles measured by the appliance and those measured using the bracket extensions. The variance between θ_{app} and θ_{ext} is thought to result from the connection between the effectors and the orthodontic bracket, which allows a slight relative movement. It can further be seen, that for a large reference angle of 15 °, the appliance is not able to track the reference angle accurately. The V-shaped slots, which were machined into the effectors allow for small angular displacements but limit the effector movement for larger angles causing a deviation from the reference value.

Table 5.4: Controlled tooth tipping

Experiment	Angle [°]				
	θ_{ref}	θ_{app}	Abs. Error	θ_{ext}	Abs. Error
Movement 1	10	9.71	0.29	10.22	0.22
Movement 2	15	12.83	2.17	10.79	4.21
Movement 3	−10	−9.79	0.21	−10.94	0.94
Movement 4	−3	−2.44	0.56	−3.48	0.48
Movement 5	5	4.96	0.14	4.46	0.54
Movement 6	7	6.35	0.65	6.59	0.41
Movement 7	2	2.28	0.28	2.54	0.54
Movement 8	−5	−4.96	0.04	−3.71	1.29
Movement 9	−10	−9.81	0.19	−8.75	1.25
Movement 10	5	4.86	0.14	4.83	0.17

5.5 Experiment 3: Frequency response

5.5.1 Experimental objective

The third and final experiment was conducted to evaluate the ability of the orthodontic appliance to apply time-varying mechanical stimuli to a tooth. According to the requirements, both a static as well as a stimulus with temporal characteristics should be possible. A sinusoidal position input was provided to the appliance with no load applied to the effectors and the resulting effector position was recorded. By doing so, the ability of the appliance to generate a vibratory signal such as that generated by the AcceleDent appliance, could be determined. The objective was thus to measure the movement response to a sinusoidal signal over a frequency range from 1 Hz to 45 Hz.

5.5.2 Experimental procedure

A sinusoidal signal with a constant amplitude of 100 µm and increasing frequency was provided as a reference position and the resulting effector position was recorded. Even though the relatively large amplitude of 100 µm did not allow accurate tracking by the effectors at increased frequencies, it did allow the physical limitations of the Squiggle motors to be determined. The initial frequency of 1 Hz was gradually increased by 0.2 Hz every 2 s until a maximum frequency of 45 Hz was reached.

Due to high oscillatory frequencies of up to 45 Hz data was acquired using a different serial communication platform than the GUI. Because the GUI receives and displays data in real-time, its acquisition speed is limited to 20 Hz, which was not sufficient for sampling the 45 Hz signal. Instead, a low-level interface, which allowed a sampling frequency of 255 Hz was used which is significantly higher than the minimum Nyquist rate of 90 Hz for this problem. The recorded data was imported into Matlab for processing.

5.5.3 Data processing

The root mean square (RMS) value of the oscillatory signal was calculated in Matlab. For the finite number of data points the RMS value was calculated by

$$x_{RMS} = \sqrt{\frac{1}{N}\sum_{i=1}^{N}|x_i|^2} \tag{5.5}$$

Here x_{RMS} is the RMS amplitude of the effector position at the given frequency, N is the number of data points recorded during each of the frequency intervals and x_i is effector position of each data point. Additionally, the time

delay between the input signal and the effector movement was measured and used to calculate the phase shift in degrees at each of the frequency intervals.

The resulting frequency response characteristics were visualised by plotting the normalised magnitude, that is the ratio between the output signal and the input signal, and the phase shift. The frequency is plotted on the horizontal axis using a logarithmic scale, whereas the normalised oscillatory magnitude and the phase shift are plotted on linear vertical axes.

5.5.4 Results

The frequency response characteristics of the orthodontic appliance are presented in Figure 5.12. Figure 5.12(a) shows the magnitude of the effector movement while Figure 5.12(b) shows the phase shift as a function of the frequency.

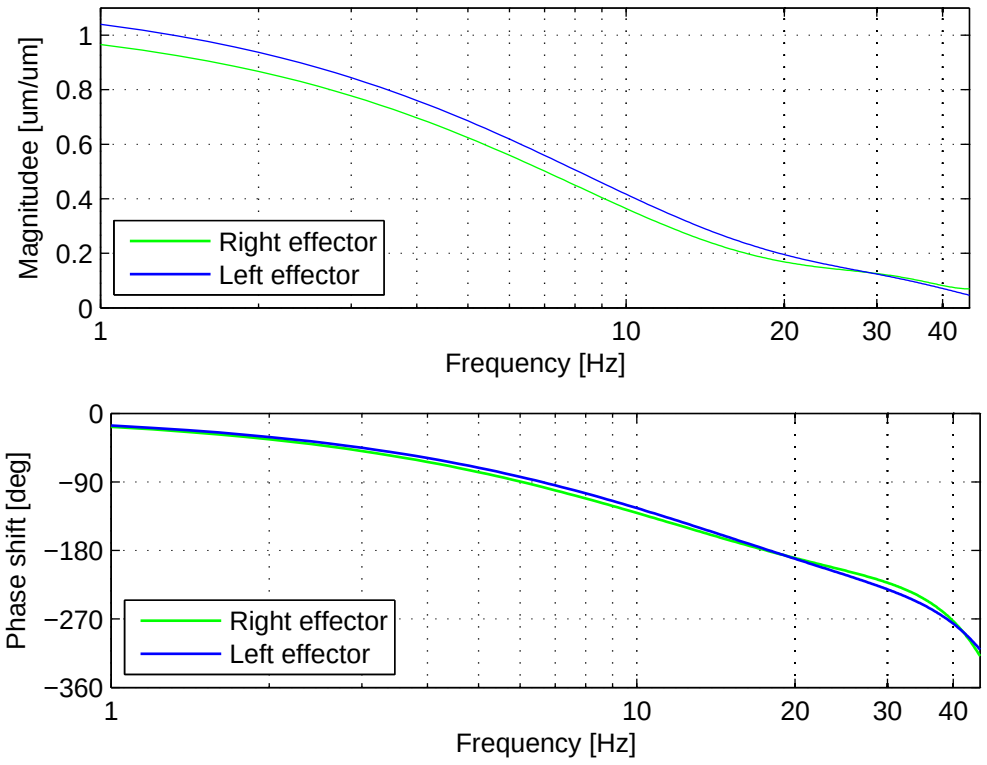

Figure 5.12: Frequency response results

The magnitude plot shows the RMS value of the oscillating effector position relative to the RMS value of the input signal. For low frequencies of 1 Hz this value for both effectors is close to 1 , which indicates that the input signal can be tracked accurately. As the frequency increases to 10 Hz the magnitude decreases to 0.38 When doubling the frequency to 20 Hz the amplitude is halved

to 0.19 , indicating that the achieved amplitude is inversely proportional to the input frequency. At a frequency of 40 Hz the RMS magnitude is decreased to approximately 0.08 Even though larger amplitudes might be desirable the achieved amplitude is likely enough to affect the underlying effects of tooth movement.

The phase plot confirms a close correlation between the input and output signals at low frequencies with an increasing phase shift at higher frequencies. At 1 Hz a small delay of approximately 15 ° is measured. This gradually increases for higher input frequencies, with a phase shift of −180 ° being reached at 18 Hz and a −270 ° delay at 40 Hz. These results highlight the physical system limitations as well as the tracking limitations of the basic proportional control, which is used to control the Squiggle motors.

Nevertheless, the actual mechanical stimulus which can be transferred to a tooth is considered more important than the tracking ability of high frequency signals. Extracts from the recorded data demonstrate the ability of the appliance to produce sinusoidal vibrations even at high frequencies. Figure 5.13(a) shows a maximum oscillatory amplitude of approximately 40 µm at 10 Hz, which decreases to 20 µm at 20 Hz. Even though the amplitude diminishes further for high frequencies, both effectors are able to produce a 10 µm sinusoidal vibration at frequencies of up to 40 Hz as shown by the results in Figure 5.13(d).

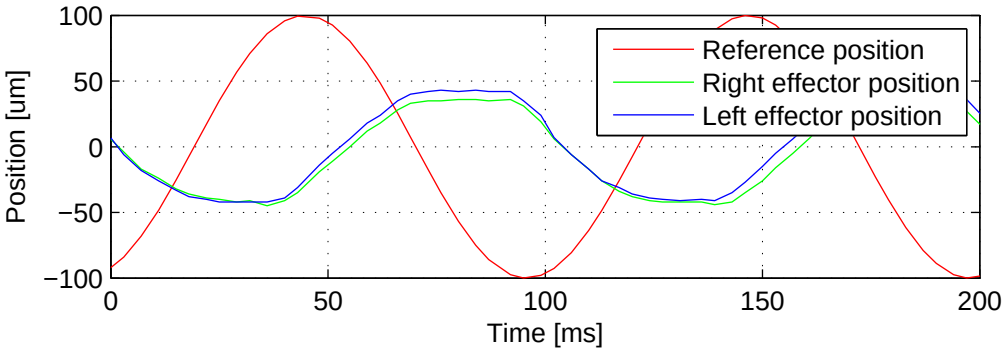

(a) Response to 10 Hz sinusoidal input

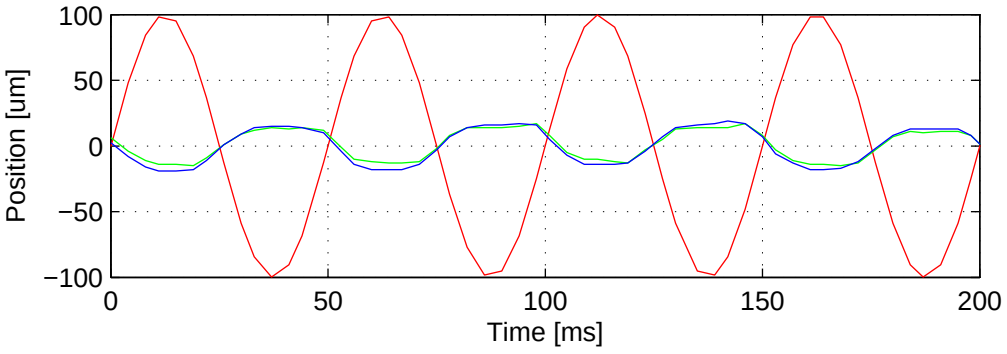

(b) Response to 20 Hz sinusoidal input

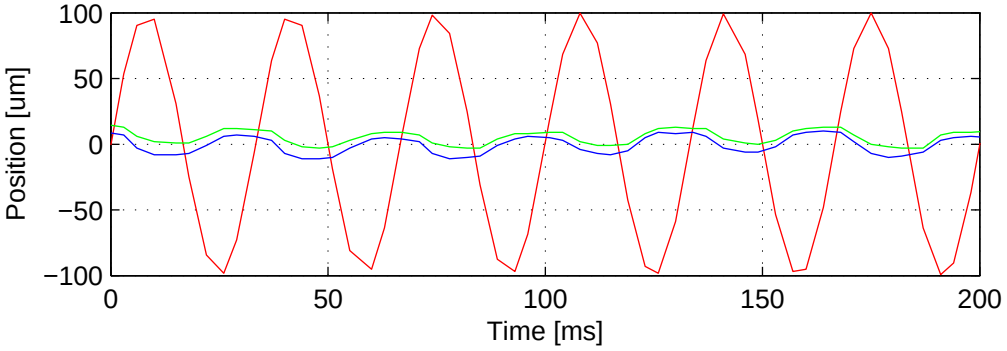

(c) Response to 30 Hz sinusoidal input

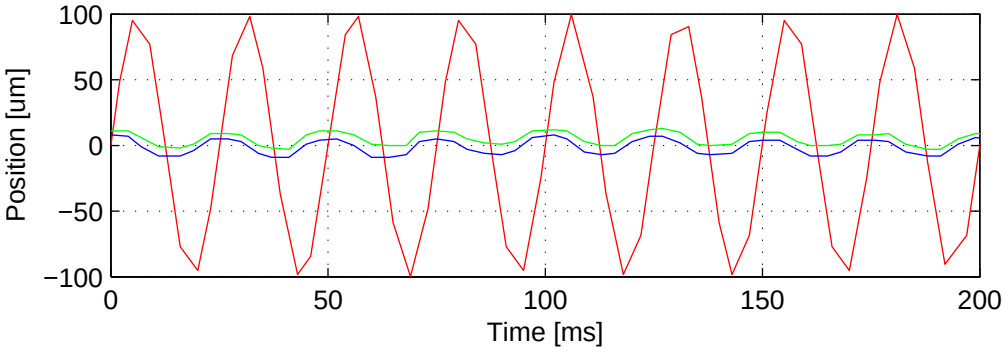

(d) Response to 40 Hz sinusoidal input

Figure 5.13: Response extracts for various frequencies

Chapter 6

Discussion of results

The following chapter presents a discussion of the electromechanical orthodontic appliance based on the outcomes of the experimental results presented in Chapter 5. Previously identified system limitations are discussed and likely causes thereof described. The achieved functionality is also highlighted and a comparison to existing systems is drawn. Lastly, the relevance of the experimental data to the orthodontic field is emphasized, thereby addressing Objective 7.

6.1 Orthodontic appliance evaluation

The appliance development could be completed to satisfy the system requirements as well as the engineering specifications set forth in Chapter 3, but limitations due to the mechanical system were identified. It was found that even though the desired functionality was achieved, the reliability and accuracy of feedback systems were negatively affected by properties of the mechanical system.

Appliance testing revealed that both FTS experienced a significant degree of hysteresis, which influenced the measurement results. The design of the custom FTS uses a force-displacement transducer which relies on small relative movements of the mechanical components to measure orthodontic forces. The manufacturing of the effectors by WEDM resulted in a relatively rough surface finish, creating friction between the effectors and the base, and ultimately causing the hysteresis exhibited by the FTS. Limited micro-manufacturing capabilities and budget constraints did not allow for improved manufacturing of the mechanical system.

As with the FTS construction, the inaccuracies pertaining to the dental interface features can be contributed to the mechanical manufacturing limitations. These features were omitted from the initial design to reduce manufacturing costs, and were manually cut into the components resulting in a low tolerance and relative movement between the effectors and the bracket.

Despite the deficiencies regarding the mechanical system, the desired static and dynamic mechanical stimuli could be applied to a tooth. The appliance allowed the mechanical stimuli to be varied in a controlled manner without making any physical system changes. Primary factors affecting tooth movement which can be controlled using the developed appliance include the force magnitude, the direction and frequency of application, the duration of application, the oscillatory frequency and the oscillatory amplitude.

The electromechanical appliance was further able to measure the applied force as well as the resulting tooth displacement, both of which could be displayed in real-time and recorded. Apart from the hysteresis error on the FTS, the sensors were able to satisfy the feedback requirements and sufficiently high data acquisition speeds could be achieved.

Based on the described functionality, the appliance was capable of characterising different orthodontic cases. The applied force which represented the controllable primary factors, as well as the resulting coronal tooth movement which represented the secondary factors, could be measured and their relationship could be described. This relationship between the primary and secondary factors enabled the appliance to clearly distinguish between various orthodontic cases and successfully characterise different PDL thicknesses.

Controlled movements of the orthodontic bracket could also be achieved. By specifying relative displacement parameters in the GUI the desired translation and tipping could be induced and reference signals could be accurately tracked by the appliance. The controlled movement experiment also highlighted the deviation of the true bracket position from that sensed by the appliance, due to relative movements resulting from the dental interface.

The electronically controllable actuators further proved to be suitable for generating time-varying orthodontic forces. The ability to apply a vibratory stimulus was evaluated by measuring the frequency response characteristics of the appliance. Even though the physical limitations of the Squiggle actuators limited the amplitude of the oscillatory stimulus, vibrations of significant magnitude could be generated at frequencies of up to 40 Hz.

To summarise the appliance evaluation, even though mechanical system limitations were found to affect appliance feedback, advanced mechanical stimuli can be generated and different orthodontic cases characterised by the orthodontic appliance. Controlled movement can also be induced using closed-loop feedback, and oscillatory stimuli of significant amplitude and frequency can be generated. The appliance is capable of providing feedback and thereby gives important insights into orthodontic tooth movement, which are not observable using existing orthodontic systems. No other orthodontic systems featuring a comparable functionality could be found during the literature review.

6.2 Significance of results

The case characterisation experiments indicate that it is possible to determine the relationship between primary and secondary factors affecting tooth movement using an electromechanical orthodontic appliance, and to use these to distinguish between specific cases. The developed appliance is capable of producing force vs. displacement curves similar to those obtained by Melsen *et al.* (2007), who made use of FEA methods. In comparison, the experimental procedure does not require CT scans of the root morphology or the development of virtual models. It is also independent of other model parameters such as the properties of the PDL, which need to be specified during FEA simulations.

The electromechanical appliance could further aid in addressing some of several problems regarding the study of orthodontic tooth movement listed in the literature review. Because the current appliance integrates both stimulatory and measurement systems into one compact system, greater repeatability can be achieved and the error arising due to different experimental set-ups is reduced. Generating comparable data previously required complex experimental set-ups and extra-oral measurement instrumentation (Yoshida *et al.*, 2000; Sia *et al.*, 2009).

Most significant is perhaps the fact that the force vs. displacement curve of an actual tooth could be determined within seconds. The time to generate a single force vs. displacement curve, such as those measured during the case characterisation, is typically less than one minute. By implementing the data processing procedure directly on the microprocessor within the appliance, this time could be reduced to seconds. This further allows such a relationship to be determined repeatedly over extended periods of time, thereby generating the data necessary to characterise the three-dimensional relationship between force, displacement and time. According to the author's knowledge, no such model has previously been achieved.

Results of the controlled movement experiments show that by using electromechanical components, the accurate movement of teeth could be achieved without the need for physical changes to the orthodontic appliance. Translation as well as tipping in the mesio-distal plane could be controlled accurately, while in contrast to conventional systems, the desired mechanical stimulus could be applied continuously throughout the entire movement. The introduction of electromechanical systems, such as the one developed during this study, would enable the practitioner to control the desired movement trajectory, make changes thereto or even reverse the tooth movement without touching the orthodontic appliance.

Lastly, the frequency response characteristics ascertain that advanced time-varying stimuli and vibrations can also be transmitted to a tooth using the electromechanical orthodontic appliance. The current appliance could thus aid in studying the short and long term effects of increased mechanical stimulation to a tooth. In contrast to appliances such as AcceleDent, this approach allows

the application of various different vibrations while measuring the immediate effects thereof. The electromechanical appliance could thus greatly benefit researchers in the orthodontic field by enabling the application of advanced mechanical stimuli and measuring their effect on tooth movement without inconveniencing the patient.

Chapter 7

Conclusion

The objectives for developing an electromechanical orthodontic appliance using non-conventional methods were put forth in Chapter 1. The following section reviews the project outcomes and states to what extent these contribute to the attainment of the initial objectives. Recommendations for further development of the appliance are made and a final conclusion to the presented thesis is drawn.

7.1 Attainment of objectives

7.1.1 Objective 1

Objective 1 dealt with developing a fundamental understanding of the background of orthodontics, the current orthodontic treatment approach and existing orthodontic systems. The history of the orthodontic profession was briefly reviewed and its advancement to the current state of the art discussed in Chapter 2. An understanding of the current treatment approach and methods could be developed, thereby achieving Objective 1.

7.1.2 Objective 2

One of the major components of the current project was concerned with the study of the underlying biomechanical and physiological principles governing orthodontic tooth movement as specified by Objective 2. This objective was addressed during Chapter 2 in which a thorough review of the factors affecting tooth movement was provided.

Numerous academic studies from various fields including dentistry, orthodontics, orthopaedics, biomechanics and bone and mineral research were revised to construct a knowledge database of factors potentially affecting orthodontic tooth movement. The discussion in Chapter 2 presents the relevant outcomes and shows that an understanding beyond the basic orthodontic principles could be developed by the author.

7.1.3 Objective 3

The concluding section of Chapter 2 contributed to the completion of the third objective by critically evaluating the current state of the art in orthodontics with regard to the outcomes of Objective 2. It was suggested that the failure to ascertain several hypotheses presented by researchers can be accredited to the limitations of the methods and technologies currently employed in the orthodontic field rather than the inappropriateness of the hypotheses themselves.

7.1.4 Objective 4

Objective 4 was attained by the content presented in Chapter 3. A hypothesis for an improved treatment approach employing an electromechanical orthodontic appliance was formulated. The novel treatment approach proposed replacing purely mechanical components with electromechanical systems to address the complex nature of the underlying effects of orthodontic treatment. Importantly, a bottom-up approach was used, which takes into account said complexity instead of simplifying the problem statement.

A electromechanical system to facilitate the proposed treatment method was characterised based on the relationship between the primary and secondary factors affecting tooth movement. System requirements were laid out and relevant engineering specifications were listed in Chapter 3.

7.1.5 Objective 5

Objective 5 requires a functional physical prototype to be built. The development process as well as the resulting physical system is described in detail in Chapter 4. First the mechanical subsystem development is described followed by the development of the electronic subsystem and the software development. The content presented in Chapter 4 confirms the possibility of developing an electromechanical orthodontic appliance and therewith completes Objective 5.

7.1.6 Objective 6

The completion of Objective 6 is presented in Chapter 5. The appliance functionality was evaluated by testing the actuating and the FTS sensors. Results confirmed the desired system functionality, but also provided insight into the physical system limitations.

Three experiments were conducted to evaluate the orthodontic appliance functionality with regard to the hypothesis put forth in Chapter 3. For the first experiment, dental models featuring various PDL thicknesses were constructed. The electromechanical orthodontic appliance was then used to characterise different combinations of the molar and premolar models for which the force vs. displacement curves are illustrated in Figures 5.8 and 5.9. The case

characterisation experiments provided a clear indication that the appliance can reliably differentiate between orthodontic cases based on the relationship between the primary and secondary factors.

The ability of the electromechanical orthodontic appliance to initiate controlled movement was confirmed by the second experiment described in Section 5.4. The translation and tipping defined in the GUI could be tracked by the effectors over the prescribed duration of movement. Secondary measurements, however, indicated a divergence of the actual bracket position from that sensed by the appliance, thereby highlighting further system limitations resulting from inaccuracies of the mechanical interface to the teeth.

Objective 5 was completed by measuring the frequency response characteristics in order to investigate the ability of the orthodontic appliance to apply a time-varying mechanical stimulus to a tooth. Even though the physical system limitations result in a decreased tracking ability at high frequencies, an oscillatory stimulus could be generated at frequencies up to 40 Hz. The achieved amplitude is likely sufficient to affect the underlying principles of tooth movement.

7.1.7 Objective 7

As per Objective 7 experimental results were reviewed and their relevance to the field of orthodontics was discussed in Chapter 6. The appliance evaluation and limitations of the current project were summarised. Subsequently, the experimental outcomes were mentioned and their relevance with regard to current research in the orthodontic field illustrated. A comparison to the outcomes of other similar studies was drawn, illustrating the potential of using electromechanical orthodontic appliances such as that developed during this study.

7.2 Recommendations for future work

The current project signifies the first of many steps toward the introduction of electromechanical appliances to the field of orthodontics and thus leaves ample room for improvement. A hypothesis was developed, proposing a new orthodontic treatment approach. The following recommendations will focus on the improvement of the physical appliance design to better facilitate this novel approach.

One of the most apparent areas of improvement is the system miniaturisation. Even though this was one of the key factors during the design phase, limited resources and manufacturing capabilities did pose constraints to the system miniaturisation. In order to make the electromechanical orthodontic appliance suitable for in-vivo operation, both the mechanical and the electronic component manufacturing need to be improved.

To further improve the mechanical system, it is recommended that future appliances should be designed and manufactured by entities who specialise in micro-manufacturing. The appliance must not only be small but must also be able to accurately measure the applied forces and the resulting secondary factors. This requires a flawless system. The interface between the appliance and the tooth has been identified as a further limitation and more emphasis should be put on the reliability of the dental interface during future endeavours.

Recommendations for improving the electronic system include sourcing application specific electronic components and the use of low-level programming languages. The current design makes use of electronic components such as the NSE-5310 or the ATmega328P, which include unused features. The size of the electronic subsystem could be reduced by identifying and sourcing integrated circuits (IC) with only essential functionality. Also, instead of using the Arduino environment, the use of a low-level programming language to program the microprocessor would be advisable. This would enable a more efficient use of the microprocessor allowing for faster communication and the optimisation of power consumption.

An optimized power consumption will in turn benefit the battery operation mode of the orthodontic appliance, crucial to the intra-oral functioning of the appliance. In Chapter 3 is was stated that the use of medical grade implantable lithium-ion batteries was not viable for the prototype development. Medical grade batteries will however need to be sourced for future designs to ensure safety of the appliance.

Ultimately, the opportunities for improving the software algorithms implemented on the microprocessor are near to unlimited. Once a physical system which is sufficiently small, reliable and safe for extended periods of intra-oral use has been developed, its software can continuously be improved. Using the data from the feedback system, advanced algorithms for data analysis, optimal force characterisation and the improved application of an optimal orthodontic force can be implemented.

7.3 Conclusion

Based on a detailed study regarding the underlying principle of change to the dento-facial structures, this thesis presents a novel approach to orthodontic treatment. It is the view of the author that by further development, the proposed technology could revolutionise the orthodontic field and bring about the necessary paradigm shift. This would allow the transformation of the previously conservative approach used in orthodontics to one which is capable of harnessing the full potential of new technological developments. The prototype developed during the scope of this study successfully proves the concept of an electromechanical orthodontic appliance and its relevance to the orthodontic field.

List of references

AcceleDent (2012). *Accelerated tooth movement.* [Accessed: 2012, October 7]. Available at: `http://acceledent.com/orthodontists`

Alford, T.J., Roberts, W.E., Hartsfield, J.K., Eckert, G.J. and Snyder, R.J. (2011). Clinical outcomes for patients finished with the SureSmile method compared with conventional fixed orthodontic therapy. *The Angle Orthodontist*, vol. 81, no. 3, pp. 383–388.

Asbell, M.B. (1990). A brief history of orthodontics. *American Journal of Orthodontics and Dentofacial Orthopedics*, vol. 98, no. 3, pp. 206–213.

Baccetti, T., Franchi, L., Camporesi, M., Defraia, E. and Barbato, E. (2009). Forces produced by different nonconventional bracket or ligature systems during alignment of apically displaced teeth. *The Angle Orthodontist*, vol. 79, no. 3, pp. 533–539.

Bassett, C.A.L. (1968). Biologic Significance of Piezoelectricity. *Review Literature And Arts Of The Americas*, vol. 272, pp. 252–272.

Brown, T.D., Pedersen, D.R., Gray, M.L., Brand, R.a. and Rubin, C.T. (1990). Toward an identification of mechanical parameters initiating periosteal remodeling: a combined experimental and analytic approach. *Journal of Biomechanics*, vol. 23, no. 9, pp. 893–905.

Burstone, C.J. and Pryputniewicz, R.J. (1980). Holographic determination of centers of rotation produced by orthodontic forces. *American Journal of Orthodontics*, vol. 77, no. 4, pp. 396–409.

Cattaneo, P.M., Dalstra, M. and Melsen, B. (2005). The finite element method: a tool to study orthodontic tooth movement. *Journal of Dental Research*, vol. 84, no. 5, pp. 428–433.

Cattaneo, P.M., Dalstra, M. and Melsen, B. (2009). Strains in periodontal ligament and alveolar bone associated with orthodontic tooth movement analyzed by finite element. *Orthodontics & craniofacial research*, vol. 12, no. 2, pp. 120–128.

Cochran, G. (1972). Experimental methods for stimulation of bone healing by means of electrical energy. *Bulletin of the New York Academy of Medicine*, vol. 48, no. 7, pp. 899–911.

Darendeliler, M.A., Zea, A., Shen, G. and Zoellner, H. (2007). Effects of pulsed electromagnetic field vibration on tooth movement induced by magnetic and mechanical forces: a preliminary study. *Australian Dental Journal*, vol. 52, no. 4, pp. 282–287.

Daskalogiannakis, J. (2000). *Glossary of Orthodontic Terms*. Quintessence Books.

Dynaflex (2012). *Orthodontic appliances*. [Accessed: 2011, March 15]. Available at: `http://dynaflex.com/`

Graber, T.M. (1954). Extraoral force - Facts and fallacies. *American Journal of Orthodontics*, vol. 41, no. 7, pp. 490–505.

Halazonetis, D.J. (1996). Computer experiments using a two-dimensional model of tooth support. *American Journal of Orthodontics and Dentofacial Orthopedics*, vol. 109, no. 6, pp. 598–606.

Halazonetis, D.J. (1998). Ideal arch force systems: a center-of-resistance perspective. *American Journal of Orthodontics and Dentofacial Orthopedics*, vol. 114, no. 3, pp. 256–264.

Harmony (2012). *Harmony lingual braces*. [Accessed: 2011, October 23]. Available at: `https://www.myharmonysmile.com/`

Huang, X. and Liu, Y. (2001). Effect of annealing on the transformation behavior and superelasticity of NiTi shape memory alloy. *Scripta Materialia*, vol. 45, pp. 153–160.

IFDEA (2012). *International Federation of Dental Educators and Associations*. [Accessed: 2012, October 7]. Available at: `http://www.ifdea.org/Pages/Default.aspx`

Jónsdóttir, S.H., Giesen, E.B.W. and Maltha, J.C. (2006). Biomechanical behaviour of the periodontal ligament of the beagle dog during the first 5 hours of orthodontic force application. *European Journal of Orthodontics*, vol. 28, no. 6, pp. 547–552.

Kau, C.H., Nguyen, J.T. and English, J.D. (2011). The clinical evaluation of a novel cyclical force generating device in orthodontics. *Orhtodontic Practice US*, vol. 1, no. 1, pp. 10–15.

Kopher, R.a. and Mao, J.J. (2003). Suture growth modulated by the oscillatory component of micromechanical strain. *Journal of bone and mineral research : the official journal of the American Society for Bone and Mineral Research*, vol. 18, no. 3, pp. 521–8.

Kusy, R.P. and Tulloch, C. (1986). Analysis of moment/force ratios in the mechanics of tooth movement. *American Journal of Orthodontics and Dentofacial Orthopedics*, pp. 127–131.

Lanyon, L.E., Goodship, a.E., Pye, C.J. and MacFie, J.H. (1982). Mechanically adaptive bone remodelling. *Journal of Biomechanics*, vol. 15, no. 3, pp. 141–154.

Liu, Y., Xie, Z., Van Humbeeck, J. and Delaey, L. (1998). Asymmetry of stress-strain curves under tension and compression for NiTi shape memory alloys. *Acta Materialia*, vol. 46, no. 12, pp. 4325–4338.

Melsen, B., Cattaneo, P.M., Dalstra, M. and Kraft, D.C. (2007). The Importance of Force Levels in Relation to Tooth Movement. *Seminars in Orthodontics*, vol. 13, no. 4, pp. 220–233.

Mueller, H.-P. (2005). *Periodontology: The Essentials*. Georg Thieme Verlag, Stuttgart.

NewScaleTechnologies (2012). *Squiggle piezo motor - Linear micro actuators*. [Accessed: 2011, November 3].
Available at: `http://www.newscaletech.com/`

Nishimura, M., Chiba, M., Ohashi, T., Sato, M., Shimizu, Y., Igarashi, K. and Mitani, H. (2008). Periodontal tissue activation by vibration: intermittent stimulation by resonance vibration accelerates experimental tooth movement in rats. *American Journal of Orthodontics and Dentofacial Orthopedics*, vol. 133, no. 4, pp. 572–583.

Obaidi, H.A. (2009). The Influence of Different Ligature Ma- terials on Frictional Coefficient of Slided Bracket on Arch Wire. *Rafidain dental journal*, vol. 9, no. 2, pp. 199–202.

Oppenheim, A. (1942). Human tissue response to orthodontic intervention of short and long duration. *American Journal of Orthodontics and Oral Surgery*, vol. 28, no. 5, pp. 263–301.

Ormco (2011). *Damon clear braces*. [Accessed: 2011, October 23].
Available at: `http://www.ormco.com/`

Peptan, A.I., Lopez, A., Kopher, R.a. and Mao, J.J. (2008). Responses of intramembranous bone and sutures upon in vivo cyclic tensile and compressive loading. *Bone*, vol. 42, no. 2, pp. 432–438.

Pilon, J.J., Kuijpers-Jagtman, A. and Maltha, J.C. (1996). Magnitude of orthodontic forces and rate of bodily tooth movement. An experimental study. *American Journal of Orthodontics and Dentofacial Orthopedics*, vol. 110, no. 1, pp. 16–23.

Proffit, W., Fields, H. and Sarver, D. (2007). *Contemporary Orthodontics*. 4th edn. Mosby Elsevier.

Proffit, W.R. (1978). Equilibrium theory revisited: factors influencing position of the teeth. *The Angle orthodontist*, vol. 48, no. 3, pp. 175–86.

Qian, L., Todo, M. and Morita, Y. (2009). Deformation analysis of the periodontium considering the viscoelasticity of the periodontal ligament. *Dental materials : official publication of the Academy of Dental Materials*, vol. 5, pp. 1285–1292.

Quinn, R.S. and Yoshikawa, D.K. (1985). A reassessment of force magnitude in orthodontics. *American Journal of Orthodontics*, vol. 88, no. 3, pp. 252–260.

Reitan, K. (1957). Some factors determining the evaluation of forces in orthodontics. *American Journal of Orthodontics*, vol. 43, no. 1, pp. 32–45.

Reitan, K. (1967). Clinical and histologic observations on tooth movement during and after orthodontic treatment. *American Journal of Orthodontics*, vol. 53, no. 10, pp. 721–745.

Reitan, K. (1974 January). Initial tissue behavior during apical root resorption. *The Angle Orthodontist*, vol. 44, no. 1, pp. 68–82.

Ren, Y. (2004). Optimum force magnitude for orthodontic tooth movement: a mathematic model. *American Journal of Orthodontics and Dentofacial Orthopedics*, vol. 125, no. 1, pp. 71–77.

Ren, Y., Maltha, J.C. and Kuijpers-Jagtman, A.M. (2003). Optimum force magnitude for orthodontic tooth movement: a systematic literature review. *The Angle Orthodontist*, vol. 73, no. 1, pp. 86–92.

Ruan, W.-h., Chen, M.-d., Gu, Z.-y., Lu, Y., Su, J.-m. and Guo, Q. (2005). Muscular forces exerted on the normal deciduous dentition. *The Angle orthodontist*, vol. 75, no. 5, pp. 785–90.

Rubin, C.T. and Lanyon, L.E. (1984 March). Regulation of bone formation by applied dynamic loads. *The Journal of bone and joint surgery. American volume*, vol. 66, no. 3, pp. 397–402.

Rubin, C.T. and Lanyon, L.E. (1985). Regulation of bone mass by mechanical strain magnitude. *Calcified tissue international*, vol. 37, no. 4, pp. 411–417.

Rubin, J., Rubin, C. and Jacobs, C.R. (2006 February). Molecular pathways mediating mechanical signaling in bone. *Gene*, vol. 367, pp. 1–16.

Salzmann, J. (1950). *Principles of orthodontics*. Lippincott.

Saxe, A.K., Louie, L.J. and Mah, J. (2010). Efficinecy and Effectiveness of SureSmile. *World Journal of Orthodontics*, vol. 11, no. 1, pp. 16–22.

Schwarz, A. (1932). Tissue changes incident to orthodontic tooth movement. *American journal of orthodontics*, vol. 18, pp. 331–352.

Shapiro, E., Roeber, F.W. and Klempner, L.S. (1979). Orthodontic movement using pulsating force-induced piezoelectricity. *American Journal of Orthodontics*, vol. 76, no. 1, pp. 59–66.

Shivapuja, P.K. and Berger, J. (1994). A comparative study of conventional ligation and self-ligation bracket systems. *American journal of orthodontics and dentofacial orthopedics*, vol. 106, no. 5, pp. 472–480.

Sia, S., Shibazaki, T., Koga, Y. and Yoshida, N. (2009). Experimental determination of optimal force system required for control of anterior tooth movement in sliding mechanics. *American Journal of Orthodontics and Dentofacial Orthopedics*, vol. 135, no. 1, pp. 36–41.

Storey, E. and Smith, R. (1952). Force in Orthodontics and its Relation to Tooth Movement. *Australian Journal of Dentistry*, vol. 56, pp. 11–18.

SureSmile (2012). *Robotically bent archwires*. [Accessed: 2012, October 08]. Available at: `http://www.suresmile.com`

Turner, C.H. and Pavalko, F.M. (1998). Mechanotransduction and functional response of the skeleton to physical stress: the mechanisms and mechanics of bone adaptation. *Journal of orthopaedic science : official journal of the Japanese Orthopaedic Association*, vol. 3, no. 6, pp. 346–55.

von Boehl, M. and Kuijpers-Jagtman, A.M. (2009). Hyalinization during orthodontic tooth movement: a systematic review on tissue reactions. *European Journal of Orthodontics*, vol. 31, no. 1, pp. 30–36.

Wang, X. and Mao, J.J. (2002). Accelerated chondrogenesis of the rabbit cranial base growth plate by oscillatory mechanical stimuli. *Journal of bone and mineral research : the official journal of the American Society for Bone and Mineral Research*, vol. 17, no. 10, pp. 1843–1850.

Weinstein, S., Haack, D.C., Morris, L.Y., Snyder, B.B. and Attaway, H.E. (1963). On equilibrium theory of tooth position. *Angle Orthodontics*, vol. 33, no. 1, pp. 1–26.

Williams, W.S. and Breger, L. (1975). Piezoelectricity in tendon and bone. *Journal of Biomechanics*, vol. 8, no. 6, pp. 407–413.

Wolf, H.F., Rateitschak, K.H. and Hassell, T.M. (2005). *Color Atlas of Dental Medicine*. 3rd edn. Thieme.

Yoshida, N., Koga, Y., Kobayashi, K., Yamada, Y. and Yoneda, T. (2000). A new method for qualitative and quantitative evaluation of tooth displacement under the application of orthodontic forces using magnetic sensors. *Medical engineering & physics*, vol. 22, no. 4, pp. 293–300.

Zadno, D. (1989). Linear and Non-Linear Superelasticity in NiTi. In: *MRS International Meeting on Advanced Materials*, vol. 9, pp. 201–209.

2

Appendices

Appendix A

Anatomical terms of reference

Even though the anatomical terms of reference used in dentistry and orthodontics largely correspond to those used in other medical fields, a number of terms are specific to the oro-facial complex.

Figure A.1 illustrates three planes of reference which are used to describe anatomical positions within the dento-facial complex. Firstly, the frontal or coronal plane lies vertically, dividing the body in anterior and posterior sections. Secondly, the sagittal plane, also known as the median plane, lies vertically and divides the body in left and right halves. Finally, the occlusal plane is a surface passing through the points of occlusion of the teeth. Technically this is not a plane but is referred to as such. The occlusal plane is similar to the more generally used transverse plane dividing the body into upper and lower portions, but can also be curved and does not necessarily lie horizontally. It is defined by the points at which the teeth from the upper and lower jaw touch or rather the points of occlusion.

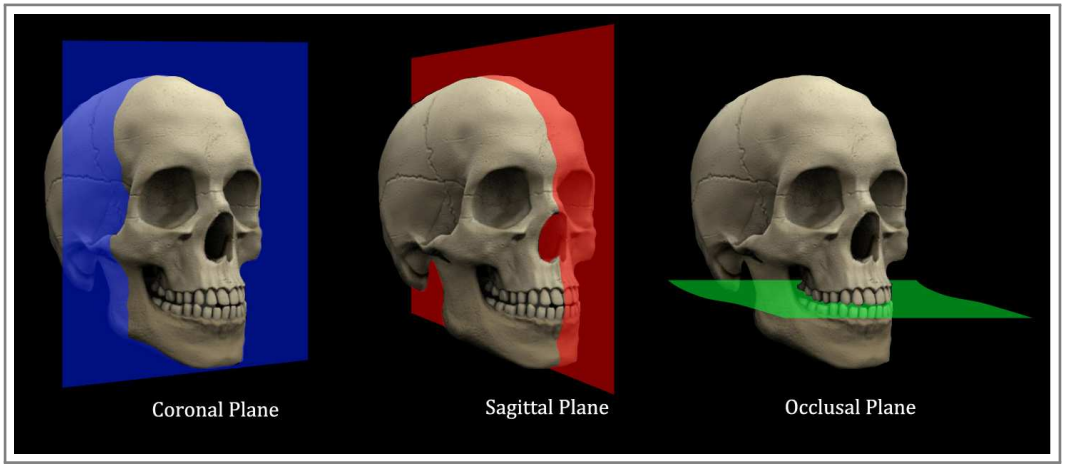

Figure A.1: Anatomical reference planes

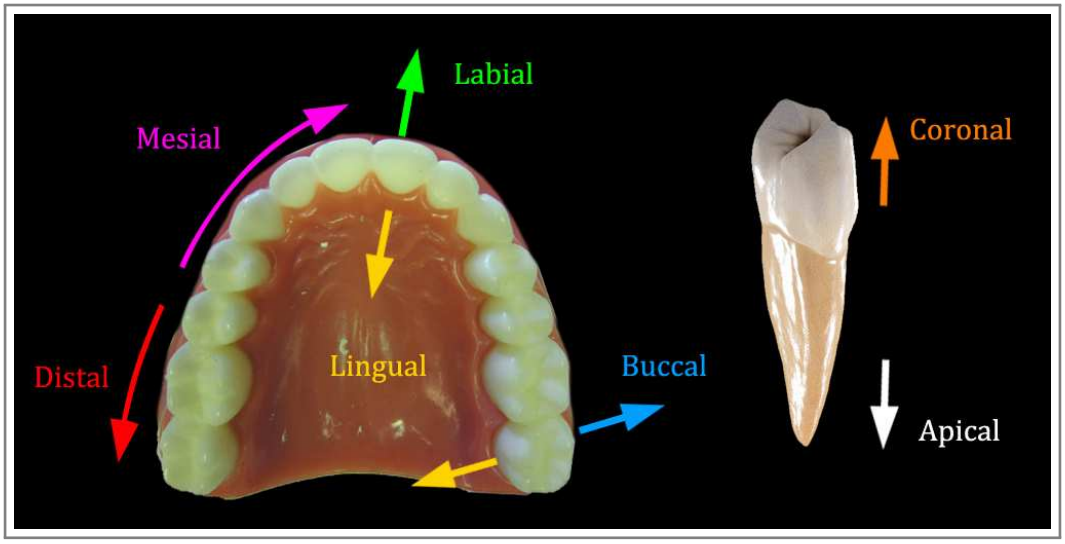

Figure A.2: Anatomical terms of reference

Figure A.2 illustrates additional important anatomical terms to describe the movement of teeth. The terms indicated in the figure are defined by the following statements:

- **Labial** means in the direction of or facing the lips. The labial surface of a tooth is thus the surface facing outward from the dental arch.
- **Lingual** means in the direction of or facing the tongue. The lingual surface is thus the inner surface of a tooth.
- **Buccal** means in the direction of the cheeks.
- **Mesial** means toward the mandibular symphysis, which is a small ridge at where the left and right portions of the mandible are joined.
- **Distal** means away from the mandibular symphysis.
- **Mesiodistal** means along the dental arch.
- **Labiolingual** means in a direction perpendicular to the dental arch. For anterior teeth this corresponds to a direction parallel to the sagittal plane. For posterior teeth this axis typically lies perpendicular to the sagittal plane and the term used is buccolingual.

Appendix B

Mechanical system considerations

The following section illustrate properties of the mechanical components. The surfaces resulting from the manufacturing processes are discussed and thereafter the dental interfacing features described. The surface finish is believed to cause significant friction on the effectors which represents one of the major system limitations and significantly affects appliance measurements. Figures B.1 and B.2 show images of the effector and stator components respectively.

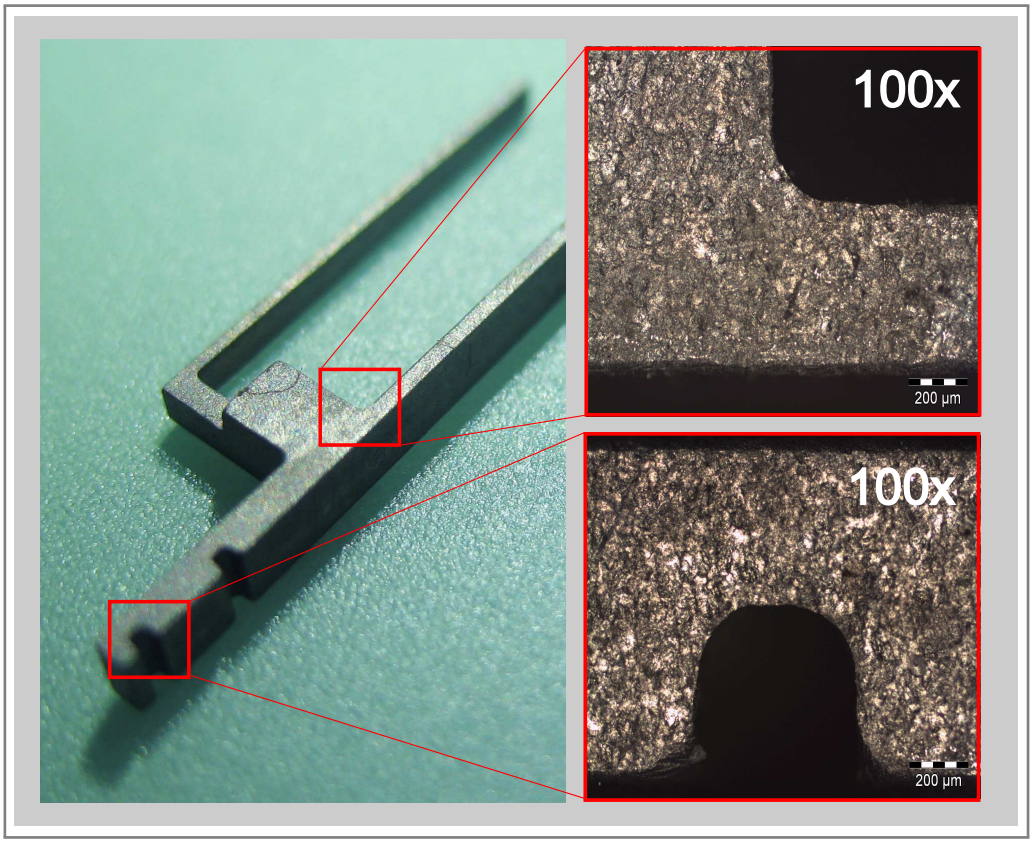

Figure B.1: Effector features viewed at 100x magnification

The effectors were manufactured using Wire Electrical Discharge Machining (WEDM). The WEDM process enabled the fragile features of the effector to be machined, but resulted in a relatively rough surface finish. The two insets in figure B.1 show images of the effector surface viewed at 100x magnification. The rough finish is thought to be responsible for the hysteresis error experienced by the FTS.

Figure B.2 shows the stator component which was machined using conventional milling. The insets show features of the stator viewed at a 100x magnification. It can clearly be seen that the surface finish is superior to that resulting from the WEDM.

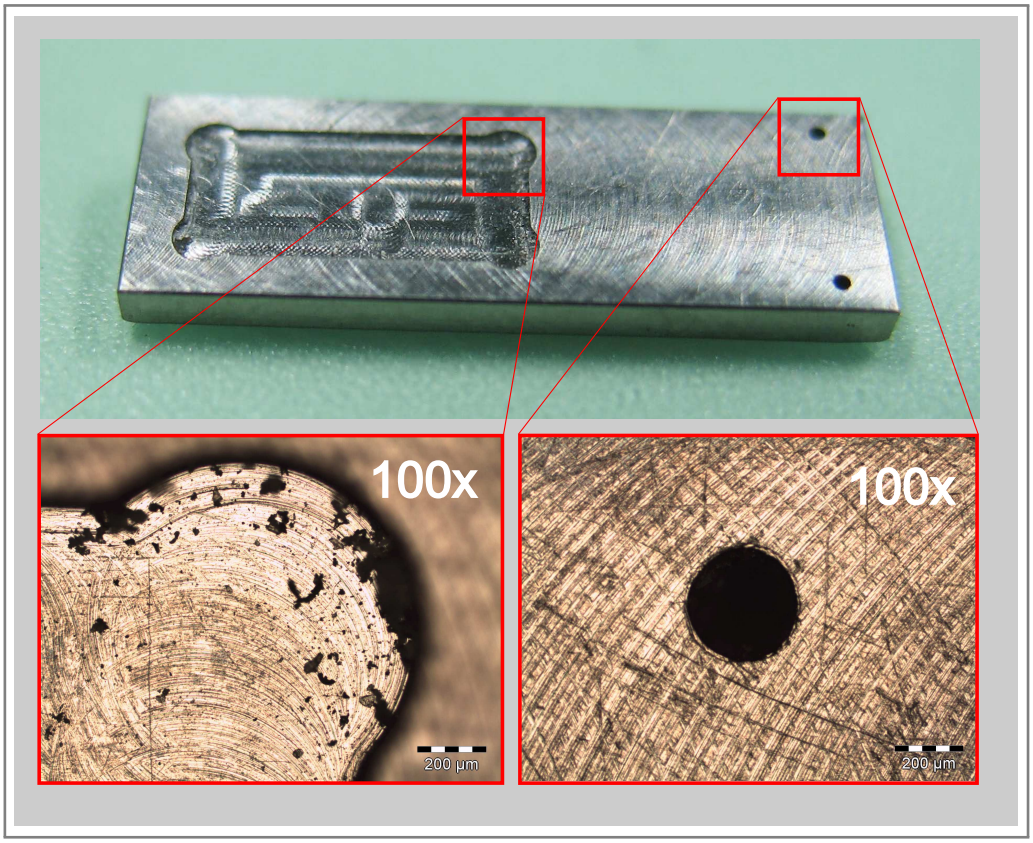

Figure B.2: Stator features viewed at 100x magnification

In an attempt to improve the surface finish of the effector components, two different methods for polishing the exposed surfaces were tested. The first method made use of a diamond impregnated silicon polishing disc, driven by the Dentalfarm micro motor, to polish the titanium surface. The resulting surface is shown in figure B.3. The silicon disc was found not to be suitable for polishing the titanium components due to their relatively soft material properties. Even though the surface finish did improve slightly, the silicon disc seems to smear the titanium particles rather than remove these. Because the

micro motor is hand held, and the disc does not have a flat surface with which to polish the effector surfaces, this method also created an uneven finish.

(a) Effector surface after WEDM

(b) Effector surface after polishing

Figure B.3: Polishing using diamond impregnated silicon disc

The second polishing method made use of a MD-Nap polishing cloth (Struers, Boksburg, South Africa). The polishing liquid used consisted of nine parts silica suspension and one part hydrogen peroxide (H_2O_2). Figure B.4 shows the improved surface finish achieved by the MD-Nap polishing cloth which did not create a 'smearing' effect, as experienced with the silicon polishing disc. Limitations of this method were however experienced, in that only flat outer surfaces could be polished and as such, not all surfaces affected by friction between the mechanical components could be accessed.

(a) Effector surface after WEDM

(b) Effector surface after polishing

Figure B.4: Polishing using Struers MD-Nap polishing cloth

The mechanical dental interfacing features also play an important role as they affect the relative movement experienced between the appliance and the teeth and thus have a direct effect on the measured results. Initial designs of the mechanical system included interfacing features which would allow the effectors to be connected to a tooth. The manufacturing thereof however required additional machining and increased manufacturing costs. They were thus omitted from the mechanical design and manually machined into the effector and the base component.

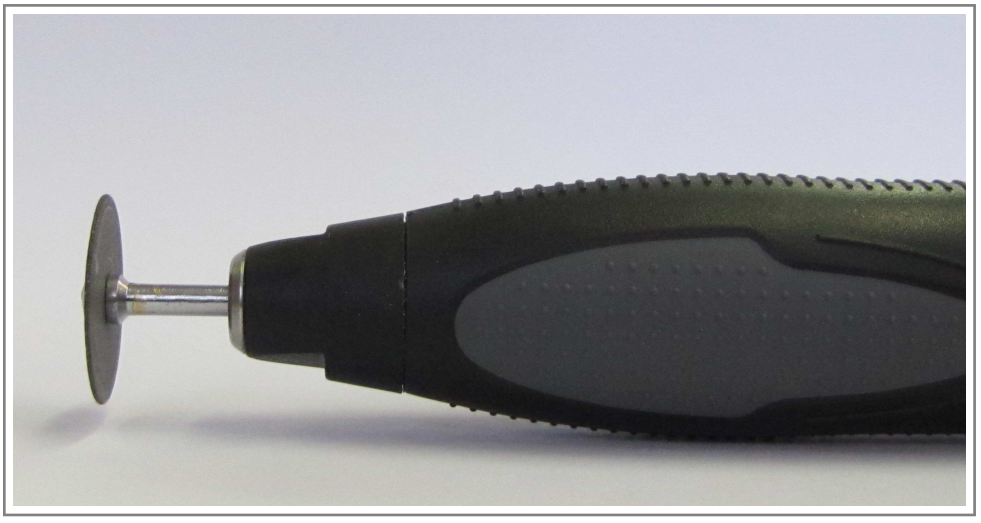

Figure B.5: Aluminium oxide cutting disc and Dentalfarm micro motor

The 0.5 mm aluminium oxide cutting disc and Dentalfarm micro motor shown in Figure B.5 were used to cut interfacing features into the base and the effector components. The T-shaped extension shown in Figure B.6(a) is inserted into the slot of a vertical slot orthodontic bracket and is held in place using elastic ligatures to provide a rigid connection in the working plane.

A method for connecting the effectors to a tooth which allowed for the desired tipping and translation to be controlled was also required. A V-shaped slot was cut into each of the effectors as shown in Figure B.6(b). The V-shaped slots accommodate a square wire which is free to rotate relative to the effectors but limits the translation.

During the testing phase, this interfacing method was however identified as one of the major shortcomings of the system. The low tolerance resulting from the manual manufacturing by means of the micro motor allowed for relative movement between the effectors and the tooth to occur. This movement was sensed by the appliance and affected the force vs. displacement curves according to which the various orthodontic cases were defined as could be seen in figures 5.8 and 5.9.

The photographs in Figure B.6 show the interfacing features when viewed at a 20x magnification. The images clearly show the inaccuracies pertaining to the mechanical features. Due to their small nature the small features required for interfacing the orthodontic appliance with the teeth should in future be manufactured using more accurate methods.

(a) T-feature machined into base component for engagement with a vertical slot bracket

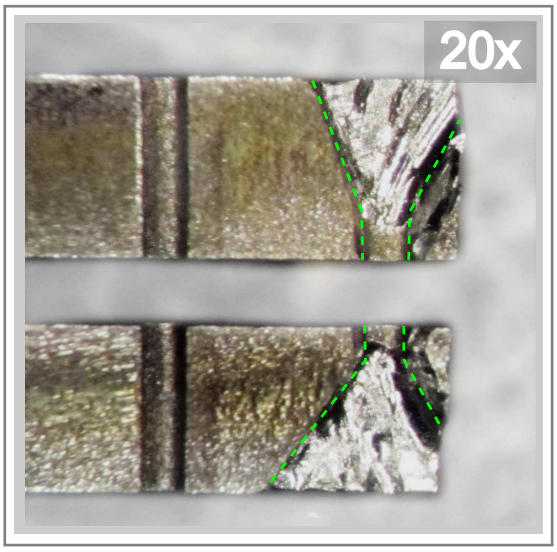

(b) V-shaped slots machined into effectors to accommodate a square wire

Figure B.6: Dental interface features viewed at 20x magnification

Appendix C

Electronic circuit specifications

The following sections provide details pertaining to the electronic circuit boards developed for the electromechanical orthodontic appliance. These are the CPU board, the sensor board, and the adaptor board. For each of the circuits, two tables provide information on the physical properties and list relevant specifications for the electronic interfacing connections, respectively. Only the key electronic components are listed and resistors, capacitors or other minor components are not tabulated.

C.1 CPU board

Even though the CPU board contains the microprocessor and is thus the most important of the electronic subsystems, it's dimensions are only 18x15 mm. Table C.1 lists all of the electronic components included on the physical circuit board along with their dimensions.

Table C.1: CPU board physical specifications

Description	Part No.	Qty	Dimensions [mm]
Outer dimensions			15 x 18 x 2
Microprocessor	ATmega328P-MU	1	9 x 9
Voltage regulator	MCP1700T-3302E	1	2.9 x 2.5
Clock	XO22050UITA-16.000	1	2 x 2.5
FPC connector	XF2L-0635-1A	2	6.9 x 3.5

The CPU board is required to connect to both the sensor board and the adaptor board. The smallest practical connection was achieved by means of 6-pin flexible printed circuits (FPC) featuring. Details required for interfacing with the CPU board are provided in Table C.2.

Table C.2: CPU board electronic specifications

Pin No.	Description	Symbol	Value	Unit
Adaptor/CPU port				
1	Reset	RST	$3.3 - 5$	V
2	Serial receive	RX	$3.3 - 5$	V
3	Serial transmit	TXD	$3.3 - 5$	V
4	Ground	GND	0	V
5	Power supply	V_{IN}	$3.5 - 6.5$	V
6	NC	-	-	-
Appliance/CPU port				
1	Power supply	VCC	3.3	V
2	Ground	GND	0	V
3	I2C data	SDA	400	kHz
4	I2C clock	SCL	400	kHz
5	NC	-	-	-
6	NC	-	-	-

The circuit layout used for manufacturing the CPU board is provided in Figure C.1. A detailed schematic illustrating the electronic interfacing of the components of the CPU board is provided in Figure C.2.

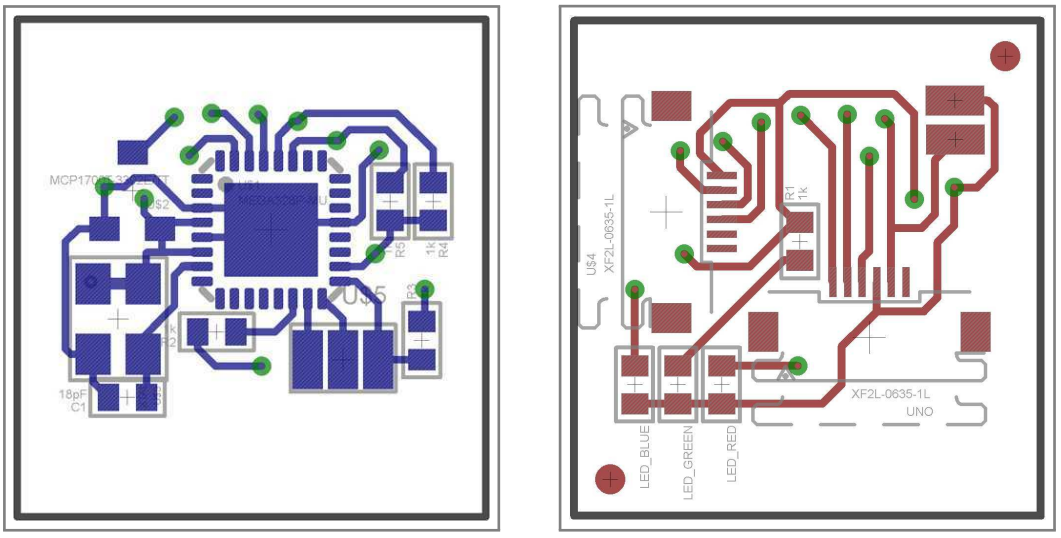

(a) Component side (b) Interface side

Figure C.1: CPU board circuit layout

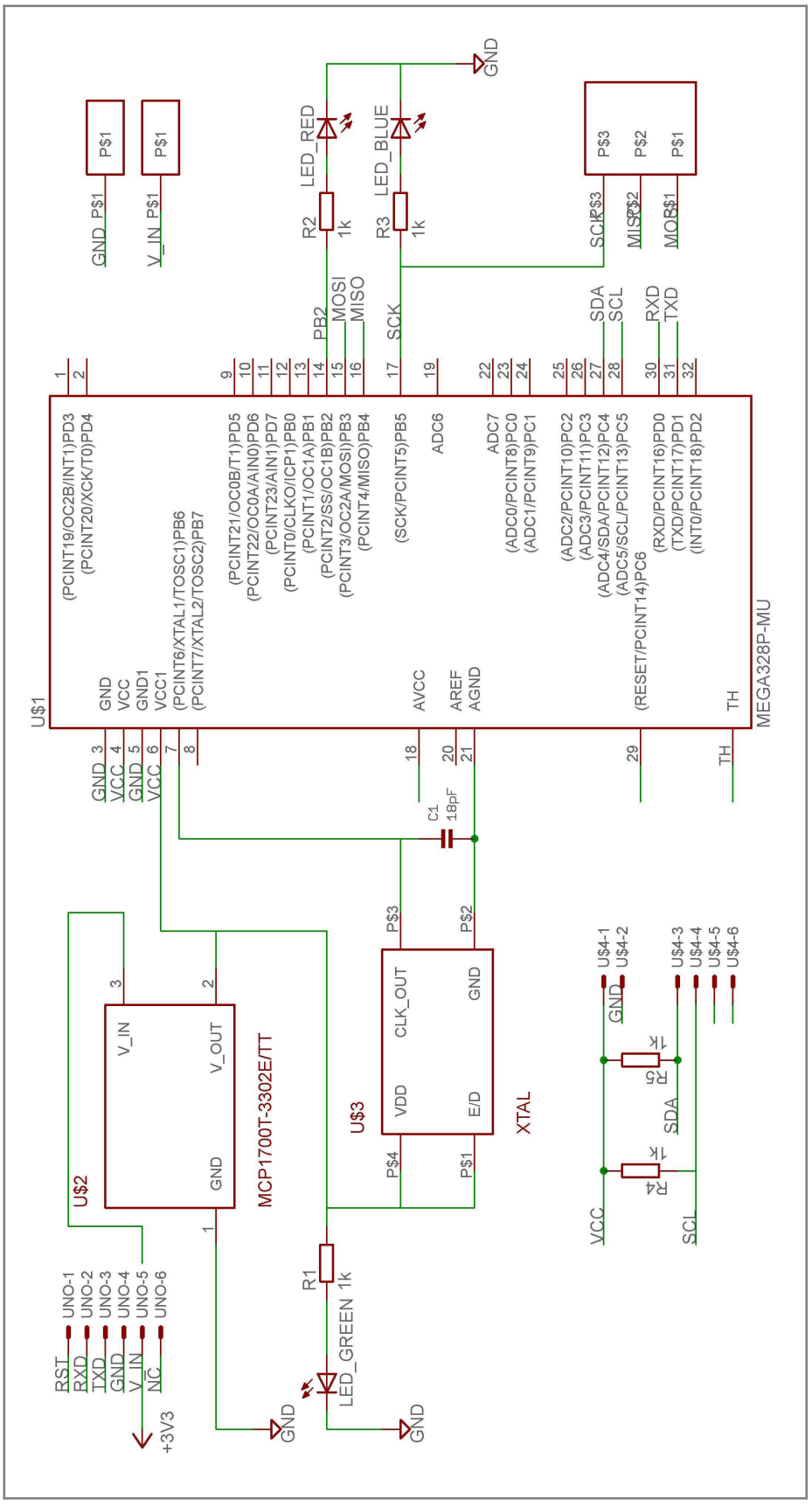

Figure C.2: CPU board schematic

C.2 Sensor board

Details for the sensor board design are provided in this section. The components comprised on the sensor board are tabulated in Table C.3. Table C.4 provides further details of the FPC connections used to interface the sensor board to the CPU board and to connect the Squiggle motors to the sensor board.

Table C.3: Sensor board physical specifications

Description	Part No.	Qty	Dimensions [mm]
Outer dimensions			22 x 14 x 3
Position encoder	NSE-5310	2	6.4 x 6.1
Position encoder (FTS)	AS5510	2	1.7 x 1.7
Motor driver ASICs	NSD-2101	2	1.64 x 1.1
FPC connector	XF2L-0635-1A	3	6.9 x 3.5

Table C.4: Sensor board electronic specifications

Pin No.	Description	Symbol	Value	Unit
Appliance/CPU port				
1	NC	-	-	-
2	NC	-	-	-
3	I2C clock	SCL	400	kHz
4	I2C data	SDA	400	kHz
5	Ground	GND	0	V
6	Power supply	VCC	3.3	V
Motor driver ports				
1	Phase 1	-	3.3	V
2	Phase 2	-	3.3	V
3	Phase 3	-	3.3	V
4	Phase 4	-	3.3	V
5	NC	-	-	-
6	NC	-	-	-

The circuit board layout of the sensor board played an important role as it integrated with the mechanical system of the orthodontic appliance and thus directly affected it's size. Significant effort was put toward designing the circuit layout presented in Figure C.3 to minimise the sensor board dimensions.

A specific layout of the magnetic encoders was also necessary to satisfy the requirements for interfacing of the magnets and the encoders. The component side of the sensor board is shown in Figure C.3(a) and includes the magnetic encoders, while the layout for the interfacing side is is shown in Figure C.3(b).

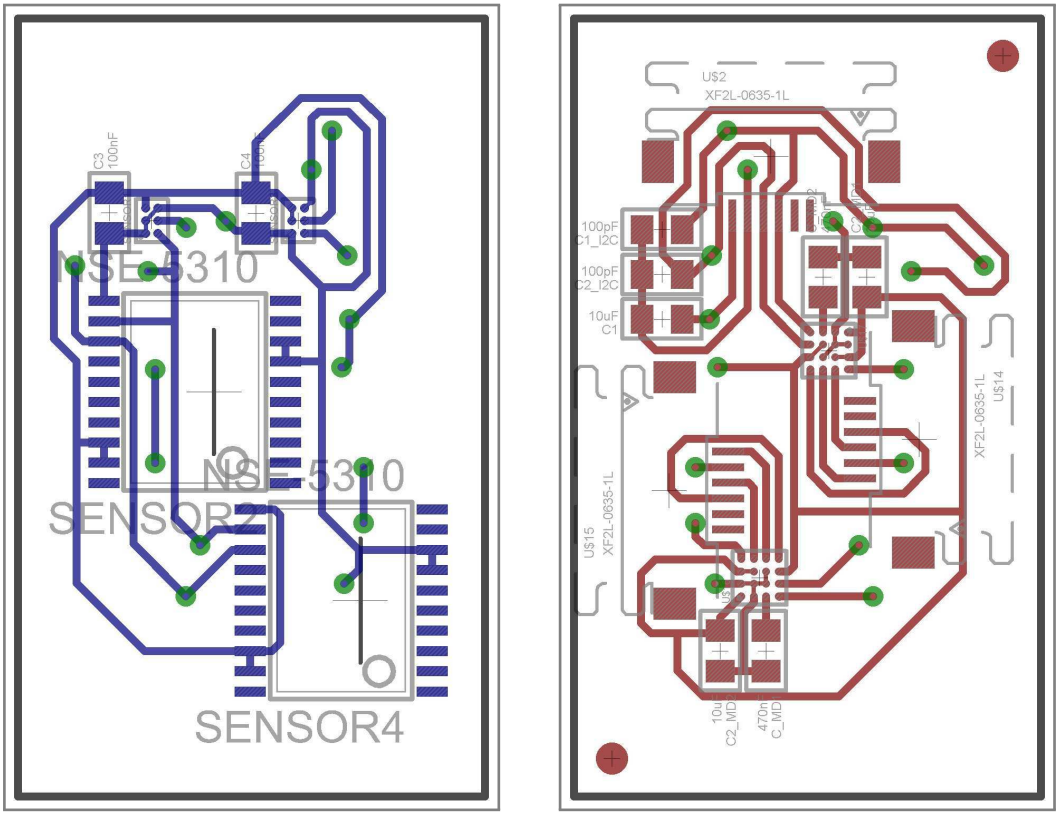

(a) Component side (b) Interface side

Figure C.3: Sensor board circuit layout

The schematic for the electronic design of the sensor board is shown in figures C.4 and C.5.

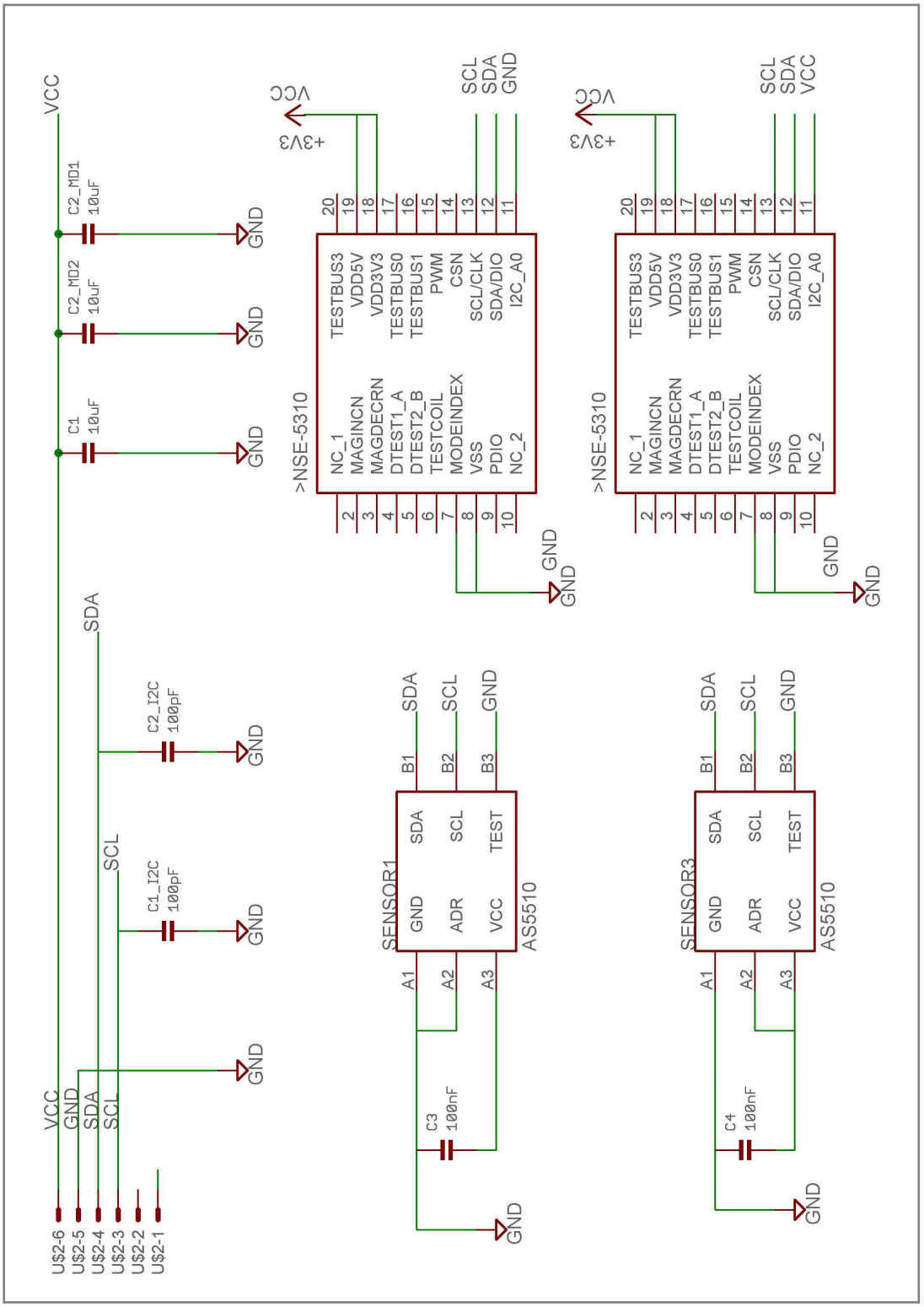

Figure C.4: Sensor board schematic (1 of 2)

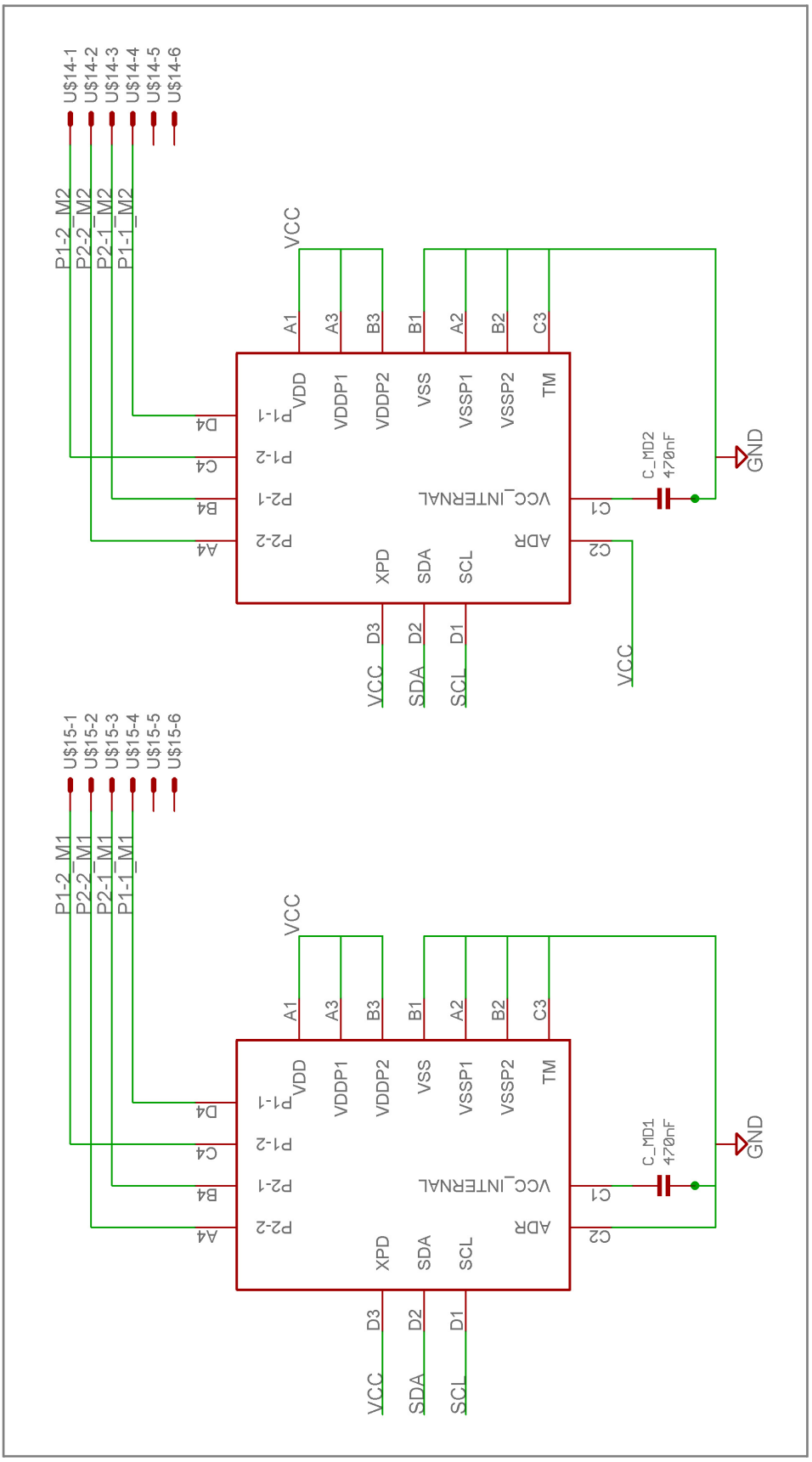

Figure C.5: Sensor board schematic (2 of 2)

C.3 Adaptor board

The adaptor board provides a means for connecting the orthodontic appliance to a computer via a USB port and also includes a circuit for charging the lithium-ion batteries used by the appliance. In contrast to the other two electronic subsystems, the adaptor board combines a commercially available Serial2USBLight converter (Arduino, Ivrea, Italy) with a custom built circuit. The Serial2USBLight board provides a USB interface and converts the $D+$ and $D-$ signals from the USB port to Rx and Tx serial communication signals. The physical specifications for the adaptor board are provided in Table C.5.

Table C.5: Adaptor board physical specifications

Description	Part No.	Qty	Dimensions [mm]
Outer dimensions			48 x 24 x 10
Arduino converter	Serial2USBLight	1	48 x 24 x 7
Battery charger IC	MCP73832	3	2.9 x 2.7
FPC connector	XF2L-0635-1A	1	6.9 x 3.5

Details regarding the electronic interfacing and connections required for the communication of the appliance with the GUI software are provided in Table C.6.

Table C.6: Adaptor board electronic specifications

Pin No.	Description	Symbol	Value	Unit
Adaptor/CPU port				
1	NC	-	-	-
2	Power supply	V_{IN}	5	V
3	Ground	GND	0	V
4	Serial transmit	TXD	5	V
5	Serial receive	RX	5	V
6	Reset	RST	5	V
USB port				
1	Power supply	V_{IN}	5	V
2	Data-	$D-$	5	V
3	Data-	$D+$	5	V
4	Ground	GND	0	V

Because the commercially available Serial2USBLight board was used, only the battery charging circuit and the circuit required for interfacing to the CPU board needed to be designed. The board layout for the battery charging circuit is presented in Figure C.6. Photographs of the physical adaptor board are shown in Figure C.7 thereafter. Figure C.7(a) shows the Serial2USBLight board which has been integrated with the custom built circuit shown in Figure C.7(b). The schematic for the electronic design of the adaptor board is finally presented in Figure C.8.

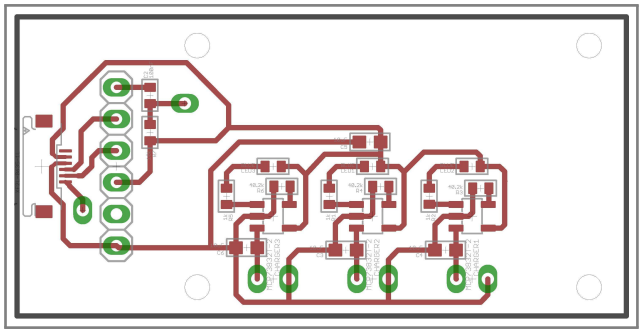

Figure C.6: Adaptor board circuit layout

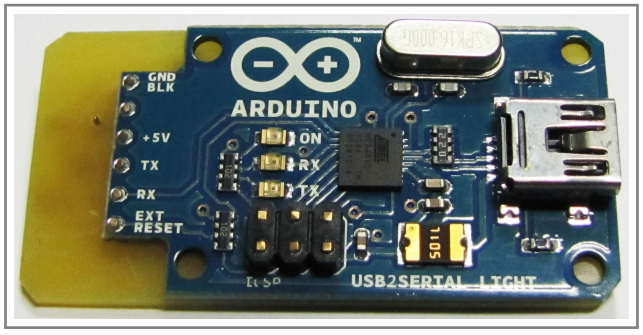

(a) Adaptor board USB-to-Serial converter circuit

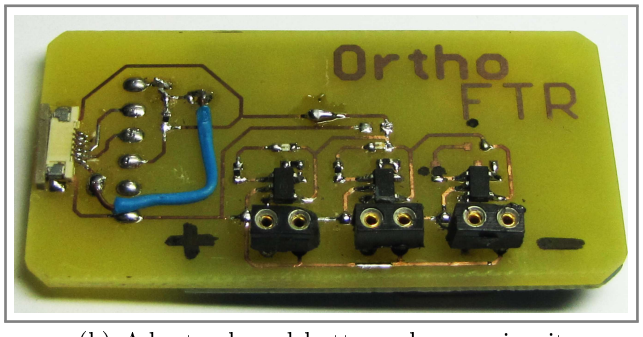

(b) Adaptor board battery charger circuit

Figure C.7: Adaptor board

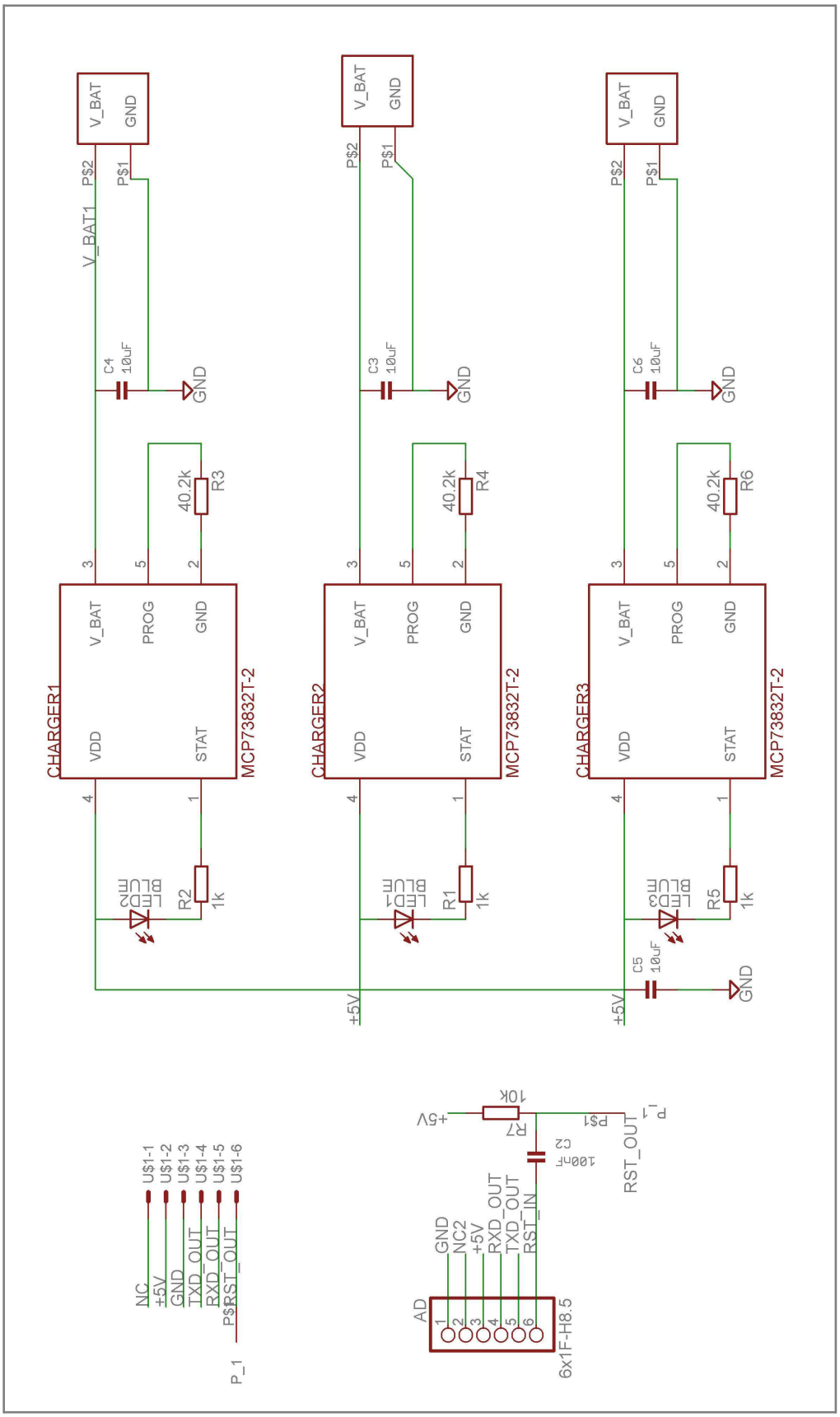

Figure C.8: Adaptor board schematic

Appendix D

Software communication protocol

A communication protocol was developed in order to optimize data exchange between the appliance CPU board and the GUI. Two factors kept paramount during the communication protocol design were speed and reliability. High speeds were required in order to allow for real-time viewing of the sensor data. When the CPU board is set to *Run* mode, five integers need to be sent to the GUI via the serial port several times every second. At the same time it must be possible to send commands to the CPU board to control the Squiggle motors. This process must be sufficiently reliable to prevent data loss or commands being missed.

To achieve this functionality the GUI which is run on a computer acts as a master, while the appliance software turns the CPU board into a slave device. Commands are sent from the GUI to the CPU board in the form of a command flag, according to which the appliance performs various functions. This process was illustrated in the flow diagram in Figure 4.12. The commands are received by the *Serial* function which sets the mode flag according to the received command or where necessary reads further data from the serial port. Table D.1 lists the command flags which can be interpreted by the *Serial* function along with the immediate task to be performed.

Table D.1: Serial function commands

Command	Function	Action
*	Measure	Read appliance sensors and send the measurements to the serial port immediately.
R	Run	Set the mode flag to *R*.
H	Halt	Reset the mode flag.
M	Move	Read further data from the serial port, describing the translation, the tipping angle, and the duration of movement. Then set the mode flag to *Move* to execute the defined movement.
F	Sweep forward	Set the mode flag to *F*.
B	Sweep backward	Set the mode flag to *B*.
P	Zero position	Measure the current effector positions, then calibrate the position sensors accordingly, so that a zero reading is obtained at the current positions.
Z	Zero force	Measure the current effector forces, then calibrate the FTS accordingly, so that a zero reading is obtained for the current forces.

Once all data has been read from the serial port and the mode flag has been set according to the command, the *Mode* function is used to evaluate the mode flag. The *Mode* function calls appropriate sub-functions either once, or repeatedly, until the mode flag is reset. The different modes are listed in Table D.2 as well as the actions performed for each mode.

The most important of the listed modes is likely the *Run* mode, which allows data to be sent to the GUI in real-time. Once the mode has been set to *Run*, the appliance measurements will be obtained during each iteration of the *Main* function and the acquired data will be sent to the computer via the serial port. The GUI program uses an interrupt to detect the availability of data on the serial port. As soon as data becomes available on the input buffer of the serial port, a function is called to read all of the data from the port. Depending on whether the *Record* function is active, data will either be written to an external file on the computer hard drive or displayed on the *Monitor* tab of the GUI.

Table D.2: Mode function commands

Flag	Mode	Action
R	Run mode	Read the appliance sensors during each iteration and send the measured data to the serial port.
F	Sweep forward	Move the effectors forward by a small step for each iteration. Reset the mode flag when the actuators stall.
B	Sweep backward	Move the effectors backward by a small step for each iteration. Reset the mode flag when the actuators stall.
M	Move mode	Call the *Move* function which measures the current effector positions and compare these to the reference position specified by the move command. Move the effectors to minimize the calculated error. Reset the mode flag when the movement is complete.

Using interrupts to detect data which has been sent from the CPU board allowed for high-speed data exchange. Their use resulted in the serial port being used for the shortest possible period of time, and further allowed commands to be sent while receiving appliance data. A sampling frequency of 20 Hz could be achieved without data loss, and commands could be sent reliably using this method.

Appendix E

Arduino implementation on an application specific circuit

The Arduino development environment offered a good solution for the electronic system design but the conventional Arduino hardware was not sufficiently small for the development of the orthodontic appliance. Therefore, a method needed to be devised which allowed the Arduino language to be implemented on the smallest possible circuit.

The CPU board was designed with the minimal hardware required to implement the Arduino language to reduce the appliance size. The CPU board design allows the microchip to be programmed using the serial interface and the Arduino IDE can be used to download sketches or programs that have been developed using the Arduino IDE to the microprocessor.

The implementation of the Arduino language on a application specific circuit requires a so-called 'bootloader' to be programmed to the microchip. The bootloader refers to a piece of code, which allows various ATmel microprocessors (Atmel, San Jose, California) to be used as an Arduino board in standalone mode. This method further enables application specific circuits to be developed and significantly reduces the circuit size as illustrated in Figure E.1.

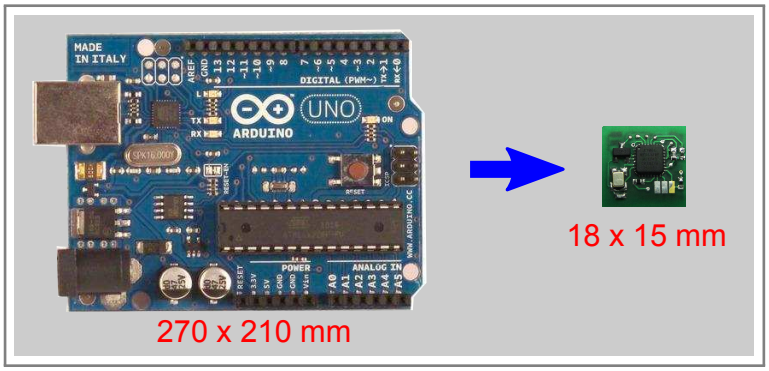

Figure E.1: Arduino implementation on an application-specific circuit

According to manufacturer of the Arduino boards, it is possible to program a microprocessor in stand-alone mode using a an Arduino board. However, this method could not be implemented successfully. Even though substantial effort was put toward realising this method, vague instructions and unreliable interfacing caused repeated errors and the bootloader could not be written to the ATmega microprocessor. A thorough study of on-line discussions regarding this method showed that this method frequently caused errors and was unreliable.

A special 'bootloader kit' was thus developed to write the Arduino bootloader to a ATmega microprocessor. The intention of this kit was to allow for an easy implementation of the Arduino language on application-specific hardware circuits instead of using the standard Arduino development boards. The bootloader kit is also intended to be used for future projects unrelated to this one.

The bootloader kit which is shown in Figure E.2 consists of the following components:

- **AVR pocket programmer:** The AVR pocket programmer provides a means for conveniently programming AVR microprocessors. It also works well with AVRDude, which is the low level command line interface used to communicate with the AVR chip.
- **Arduino UNO and shield:** The UNO and the shield are used mainly for interfacing purposes. The ATmega microprocessor has been removed from the UNO and only the ATmega16U2 chip is used as a USB-to-serial converter. The shield was designed to fit on top of the UNO board and combines the interfacing features on a single board.
- **6-pin in-system programming (ISP) cable and header:** The ISP cable and header transmit the programming signal to the target chip.
- **3-pin programming pen:** The programming pen is used to establish a temporary connection to the programming pads on the CPU board.

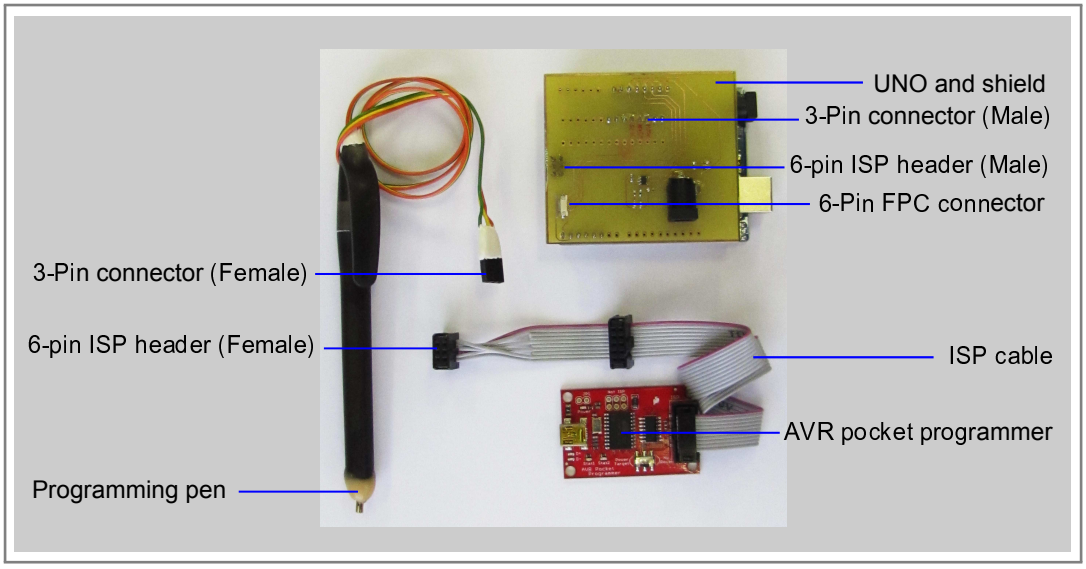

Figure E.2: Bootloader kit

For bootloading the ATmega microprocessor with the Arduino bootloader, the system is connected as illustrated in Figure E.3. Firstly, both the Arduino UNO board and shield as well as the AVR pocket programmer need to be connected to the USB ports of the computer. Secondly, the CPU board needs to be connected to the shield using the flexible printed circuit (FPC) connectors. This supplies power to the board and includes the reset pin which is required for bootloading the ATmega328P. Lastly, the 3-pin programming pen is connected to the shield and is used to establish a temporary connection programming pins on the CPU board.

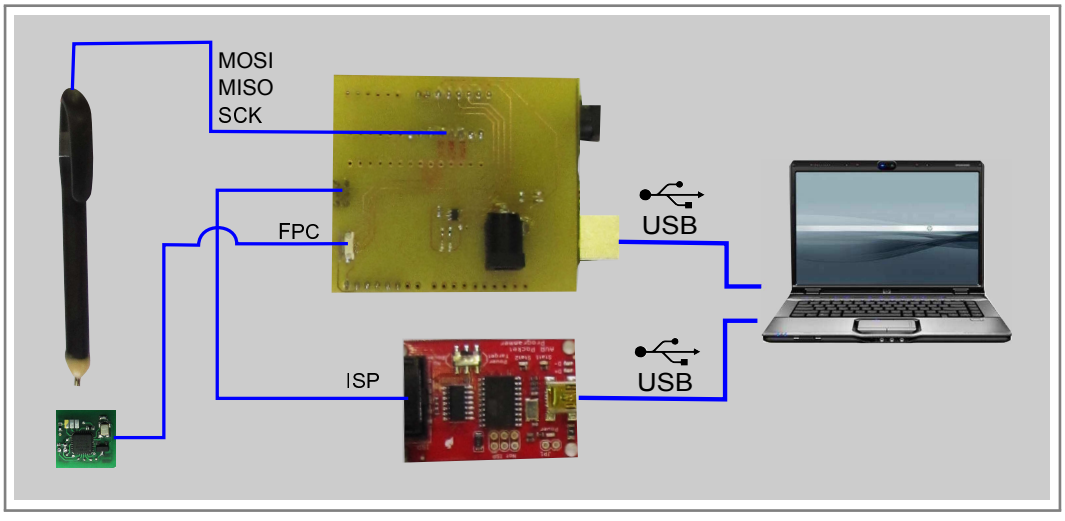

Figure E.3: Interfacing during bootloading procedure

The programming pen provides a temporary connection to the MOSI, MISO, SCK pins on the microprocessor. Because the bootloading procedure only needs to be performed once, using the copper pads in combination with the hand held pen to establish a temporary connection significantly reduces the circuit size. A photograph of the pads on the CPU board and the pen is provided in Figure E.4. The three pins are pressed onto the copper pads to establish a temporary connection.

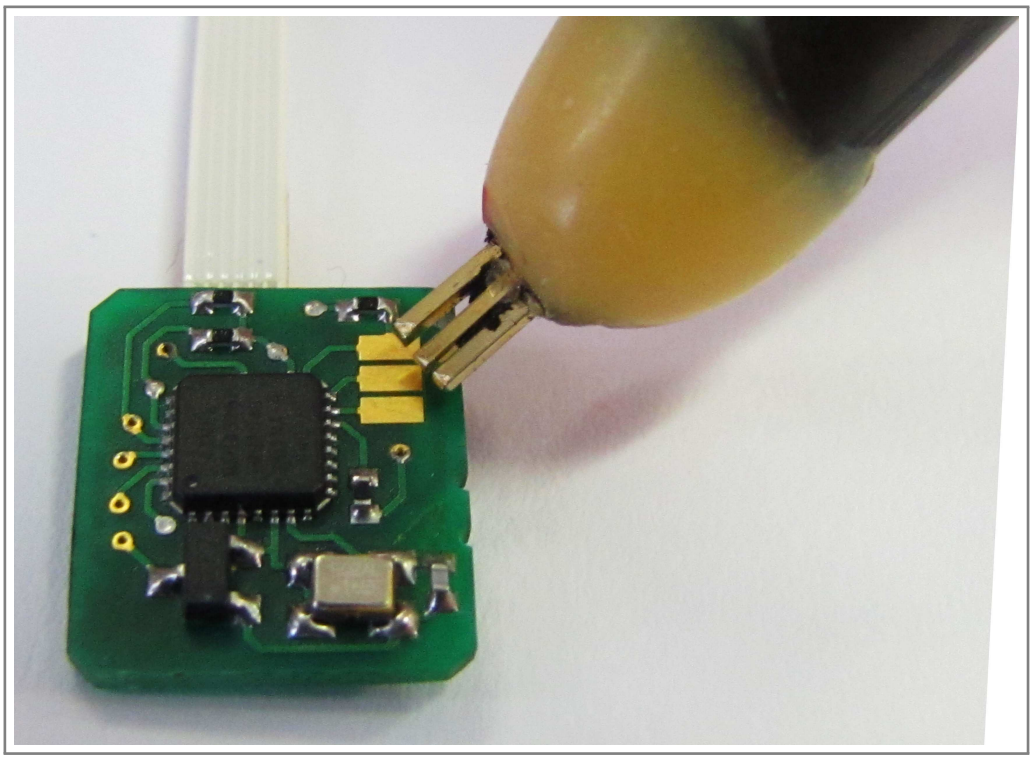

Figure E.4: Bootloader pen

Appendix F

Dental model analysis

The following information relates to the analysis of the dental models which was done using CT scans. Details specific to the scans done on the dental models are provided and the virtual models constructed from the scan data are subsequently presented.

F.1 Computed tomography scans

The scans were done using the VTomeX L240 CT scanner (General Electric, Fairfield, Connecticut, USA) shown in Figure F.1. Further technical specifications regarding the scans done on the dental models are listed in Table F.1.

Figure F.1: General Electric VTomeX L240 CT scanner

Table F.1: CT scan specifications

Description	Value	Unit
Equipment	General Electric VTomeX L240	-
Tube voltage	60	kV
Tube current	240	µA
Exposure	500	ms
Resolution	14	µm
Images per rotation	1500	-

F.2 Model examination

Molar model with 0.2 mm PDL

The PDL thickness of the molar model was measured and the results presented in Table 5.2 showed an average PDL thickness of 0.27 mm. The average value is close to the desired PDL thickness of 0.2 mm but localised thinning of the PDL was identified from the virtual models.

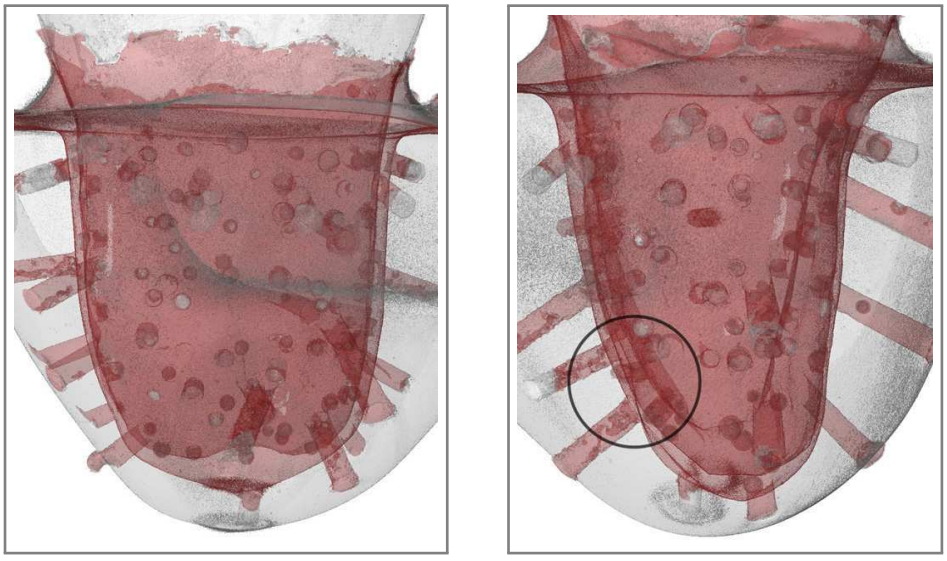

(a) Buccal view (b) Mesial view

Figure F.2: Localised thinning of molar PDL

Figure F.2 shows the buccal and mesial views of the molar model. On inspection of the buccal view a uniform PDL seems to exist for the mesial and distal surfaces. The mesial view in Figure F.2(b) however, shows localised thinning toward the buccal side of the root. When the virtual molar model is

viewed at an angle as in Figure F.3, significant thinning of the PDL along the linguo-distal surface of the root becomes apparent.

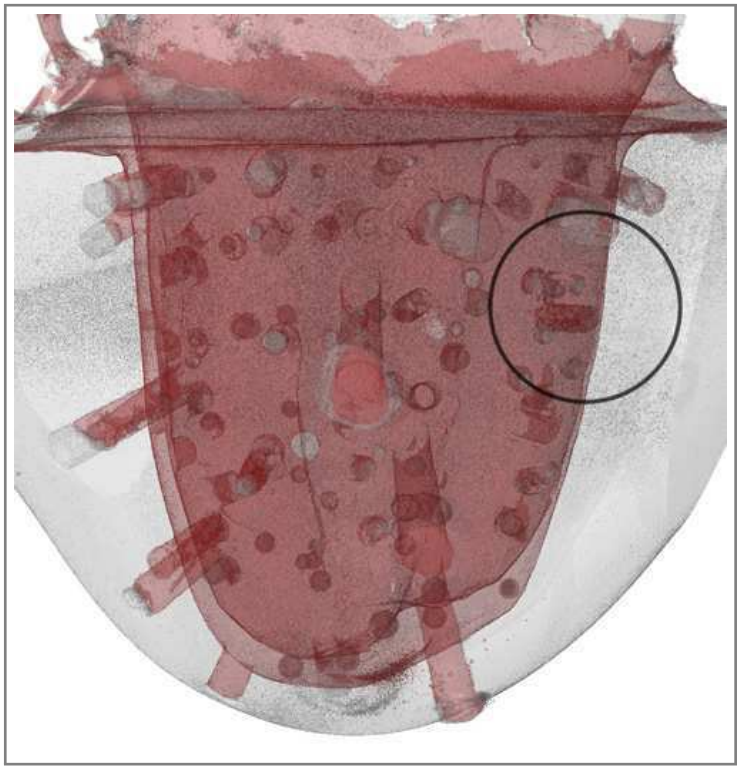

Figure F.3: Linguo-distal thinning of molar PDL

Premolar model with 0.2 mm PDL

The average thickness of the premolar PDL was also shown to correlate with the desired value of 0.2 mm, but significant localised thinning was again identified. Two points at which the PDL thickness is well below the desired value could be identified. Figure F.4(a) shows the labial view of the premolar model where the decreased PDL thickness on the distal side is apparent. Figure F.4(b) also seems to show the root apex touching the alveolar wall.

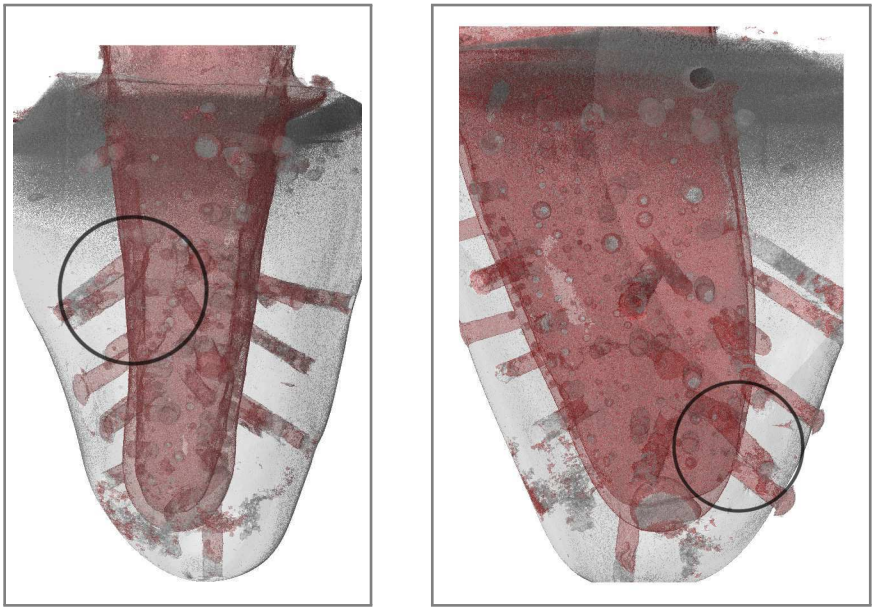

(a) Labial view (b) Mesial view

Figure F.4: Localised thinning of 0.2 mm premolar PDL

The distal thinning on the premolar model becomes more obvious when viewing the model from the labio-distal direction as presented in Figure F.5. The relatively large area of PDL thickness which can be seen from this angle was considered to inhibit the mesio-distal movement of the premolar model.

Figure F.5: Linguo-distal thinning of 0.2 mm premolar PDL

Premolar model with 0.5 mm PDL

Analysis of the premolar model featuring the 0.5 mm PDL revealed that the average thickness was close to the desired value of 0.5 mm and that no significant thinning of the PDL was present in this case. Figure F.6 shows the labial and the distal view of the virtual premolar model.

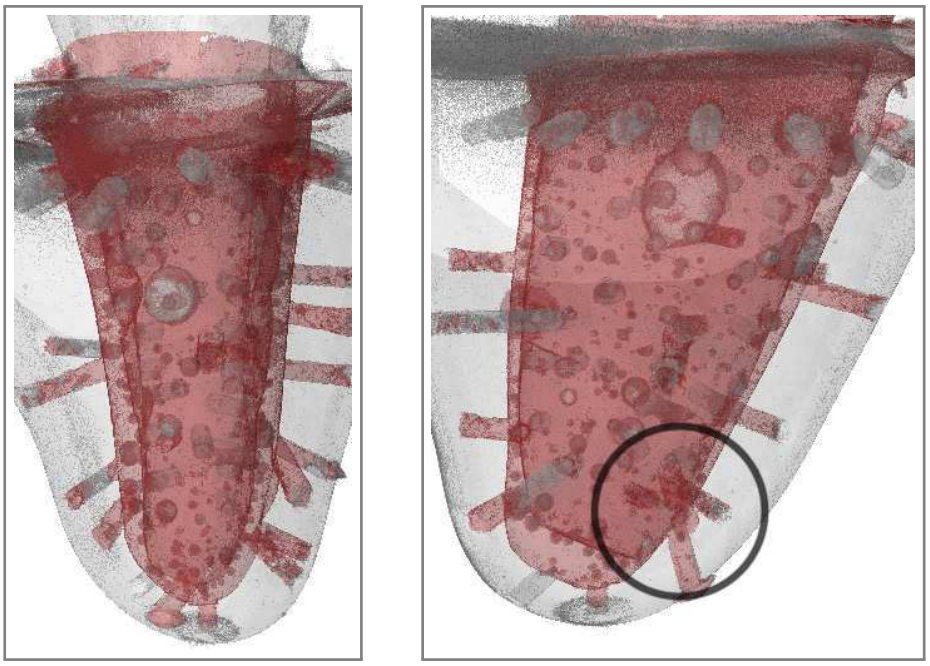

(a) Labial view (b) Distal view

Figure F.6: Thinning of 0.5 mm premolar PDL at root apex

Only a single point was identified at which the PDL thickness was less than 0.05 mm. This point is located labially at the root apex as indicated in Figure F.6(b). It was predicted that a thinner PDL at this location could potentially shift the CRes downward toward the apex, but that it would not significantly restrict the mesiodistal movement of the premolar.

Appendix G

Data processing for case characterisation experiments

Data processing was necessary to allow a direct comparison of the force vs. displacement relationship measured for the different orthodontic cases. The most important factor of the data processing done for the case characterisation experiments was to compensate for the hysteresis by calculating an average force at each tooth position. The data processing procedure will be explained with reference to Figures G.1 and G.2.

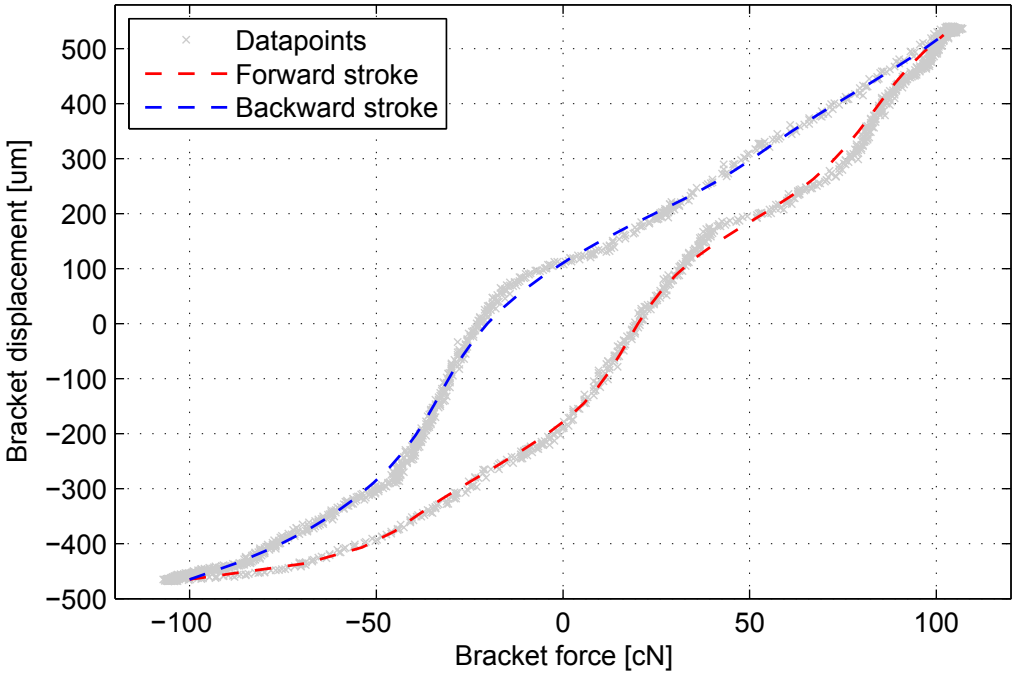

Figure G.1: Spline fitting for forward and backward strokes

First, the raw data was separated into two datasets. One being the forces recorded during a forward movement of the effectors and the second being the forces recorded during a backward movement of the effectors. A spline was then fitted to each of the two datasets as shown in Figure G.1 to smooth the raw data. A spline was specifically chosen to be fitted to the data instead of a polynomial in order to preserve the general shape of the data. This allowed a smooth curve to be fitted while preserving certain features or inconsistencies specific to each orthodontic case.

The method used to obtain an average force vs. displacement curve for each of the orthodontic cases is illustrated by Figure G.2. Three positions are indicated in the figure by green dotted lines passing through Point 1 at +300 µm, Point 2 at 0 µm, and Point 3 at −300 µm. At each of the three positions the force measured during the forward stroke is indicated by a red dot, while that recorded during a backward stroke is indicated by a blue dot. The average between these two forces was calculated, resulting in the average force indicated by the green dots. Finally, a spline was fitted through the average values to provide the black line plotted in Figure G.2. The black line was obtained and used as a basis for comparing each of the orthodontic cases. The algorithm which was executed in Matlab is presented on the following page.

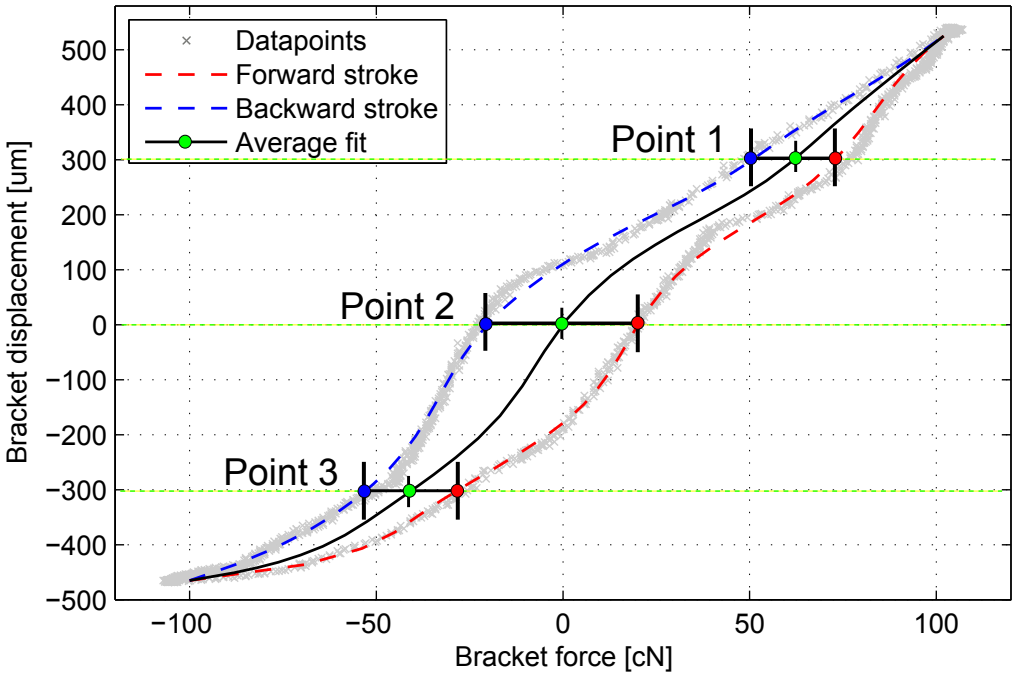

Figure G.2: Determination of average force vs. displacement relationship

```
function out = ortho_spline(d, N_points)
%This function fits a spline with N_points to the forward and backward
%movements as well as a spline for the average force at each position. The
%raw data as well as the fitted splines are also plotted%

%save variable. inca(:,1)=force, inca(:,2)=displacement
Fwd = d.inca;
%save variable. deca(:,1)=force, deca(:,2)=displacement
Bwd = d.deca;
%plot forward raw data in grey
plot(d.inc(:,1), d.inc(:,2), 'x', 'Color', [0.7 0.7 0.7])
hold on
%plot backward raw data in grey
plot(d.dec(:,1), d.dec(:,2), 'x', 'Color', [0.7 0.7 0.7])

%create N_points between the min and max displacement
yy = linspace(min(Fwd(:,2)),max(Fwd(:,2)),N_points);

%fit spline to Forward (force, displacement, at points yy)
force_fwd = spline(Fwd(:,2),Fwd(:,1),yy);
%plot the forward spline
plot(force_fwd,yy, 'k')

%fit spline to Backward (force, displacement, at points yy)
force_bwd = spline(Bwd(:,2),Bwd(:,1),yy);
%plot the backward spline
plot(force_bwd,yy, 'k')

%calculate the average force at each position
Avg_x = (force_fwd + force_bwd)/2;
%plot the average datapoints
plot(Avg_x,yy,'xk')

%create N_points between the min and max force
xx = linspace(min(Fwd(:,1)),max(Fwd(:,1)), N_points);
%fit the spline to average (force, displacement, at points yy)
Fit = spline(Avg_x, yy, xx);
%plot the average spline
plot(xx, Fit, 'r')
```